2015

Simplified population growth modeling for low earth orbit

Thomas Percy

SIMPLIFIED POPULATION GROWTH MODELING FOR LOW EARTH ORBIT

by

THOMAS PERCY

A DISSERTATION

Submitted in partial fulfillment of the requirements
for the degree of Doctor of Philosophy
in
The Department of Mechanical & Aerospace Engineering
to
The School of Graduate Studies
of
The University of Alabama in Huntsville

HUNTSVILLE, ALABAMA

2015

In presenting this dissertation in partial fulfillment of the requirements for a doctoral degree from The University of Alabama in Huntsville, I agree that the Library of this University shall make it freely available for inspection. I further agree that permission for extensive copying for scholarly purposes may be granted by my advisor or, in his/her absence, by the Chair of the Department or the Dean of the School of Graduate Studies. It is also understood that due recognition shall be given to me and to The University of Alabama in Huntsville in any scholarly use which may be made of any material in this dissertation.

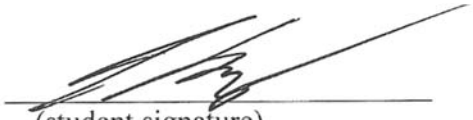

(student signature)

4/1/15

(date)

DISSERTATION APPROVAL FORM

Submitted by Thomas Percy in partial fulfillment of the requirements for the degree of Doctor of Philosophy in Aerospace Systems Engineering and accepted on behalf of the Faculty of the School of Graduate Studies by the dissertation committee.

We, the undersigned members of the Graduate Faculty of The University of Alabama in Huntsville, certify that we have advised and/or supervised the candidate on the work described in this dissertation. We further certify that we have reviewed the dissertation manuscript and approve it in partial fulfillment of the requirements for the degree of Doctor of Philosophy in Aerospace Systems Engineering.

4/1/15
Committee Chair
(Date)

Department Chair

College Dean

for S. Mahadevan

4/24/15
Graduate Dean

ABSTRACT
The School of Graduate Studies
The University of Alabama in Huntsville

Degree Doctor of Philosophy College/Dept. Mechanical & Aerospace Engineering

Name of Candidate Thomas Percy

Title Simplified Population Growth Modeling For Low Earth Orbit

The accumulation of 50 years' worth of man-made space objects has increased the risk of catastrophic collisions. Continuing to operate in a business-as-usual manner will one day render regions of LEO unusable. The landscape of future LEO satellite operations is complicated by the evolving nature of space policy and the emergence of the CubeSat which has the potential to radically shift the current LEO satellite market. Long-term population modeling is required to predict population growth, support policy decisions, and inform industry best practices. Many space agencies around the world have high-fidelity analysis codes to serve this function but they are complex and computationally expensive. The Simplified LEO Orbital Object Population (SLOOP) model has been developed to provide a broader user base a simplified, reasonably accurate prediction tool for rapidly evaluation future scenarios.

Expanding on previous simplified population models for LEO, new algorithms for evaluating fragment and intact object populations over time were developed. These algorithms add spatial fidelity and allow the evaluation of LEO as a series of layers rather than one large region of space. This addition enables more specific evaluations of LEO populations. Differential equations and coefficients that represent various contributors to

the orbital object populations were investigated and modified. To support this development, a new comprehensive orbital object database was created, integrating several data sources. A new model of atmospheric density was created to fill a gap in available data and help quantify natural orbit decay times at high LEO altitudes.

Comparisons of the SLOOP model with benchmark data from current high-fidelity models show only a +/- 5% error over a 100 year simulation. This level of agreement indicates that, for the first time, a simplified model can direct higher-fidelity studies by identifying trends with reasonably high accuracy in a fraction of the run time. A sample SLOOP analysis evaluating the impact of deploying large CubeSat constellations shows the power of the model to rapidly evaluate future operating scenarios. Overall, the data presented shows that with enhanced algorithms, improved use of demographic data, and faster simulations, the SLOOP model fills an important role in orbital debris analysis.

Abstract Approval: Committee Chair 4/1/15

Department Chair 4/2/15

Graduate Dean 4/24/15

ACKNOWLEDGEMENTS

The work described in this dissertation would not have been possible without the support of several people who deserve recognition for their contributions. First I would like to thank my advisor, Dr. D. Brian Landrum, for his guidance throughout this process and his support on my publications. Second, the other members of my committee have provided excellent suggestions through the course of my research. I must also thank my managers at Science Applications International Corporation not only for their financial contribution to my education but for their support and encouragement along the way. I would further like to recognize the engineers and scientists at NASA's Marshall Space Flight Center, and specifically those with whom I have the great pleasure of working at the Advanced Concepts Office, for their support and for initially involving me in the analysis work in orbital debris that inspired this research topic.

Finally, I would like to dedicate this work to my children, Abby Rose, Brady, and Colin and to my wife, Erin. Your immense patience and unwavering encouragement and support have carried me through this long journey. I will be forever indebted to you for allowing me the time and energy to pursue this work and I cannot wait to rejoin our regularly scheduled life, already in progress.

TABLE OF CONTENTS

LIST OF FIGURES

Page

LIST OF TABLES

Page

CHAPTER 1:

INTRODUCTION

The subject of orbital debris has become an increasing focus of concern over the last decade. National and international space policy makers recognize the growing risk of collisions in space, especially in the increasingly congested region between the upper atmosphere and 2000 km altitude known as Low Earth Orbit (LEO). Two major incidents, the destruction of the Fengyun-1C satellite by the Chinese government in 2007 and the collision of the Iridium 33 and Cosmos 2251 satellites in 2009, as well as increased debris population modeling, has led the space community to realize the seriousness of a phenomenon first addressed by Don Kessler in the 1970's.[1] The accumulation of 50 years' worth of man-made space objects has increased the risk of catastrophic collisions and many analysts believe continuing to operate in a "business-as-usual" manner will one day render regions of LEO unusable.[2]

In an attempt to mitigate the risks of orbital debris, the United States has published the U.S. Government Orbital Debris Mitigation Standard Practices[3]. Although non-binding and extremely short, this document developed jointly by the Department of Defense (DoD) and the National Aeronautics and Space Administration

(NASA) provides general guidance to all six agencies within the federal government that oversee space assets. Similar guidelines are being drafted in international forums such as the Inter-Agency Space Debris Coordination Committee (IADC)[4] and the UN Committee on the Peaceful Uses of Outer Space (COPUOS)[5]. All of these documents assert a basic principle that all orbiting assets should have post-mission lifetimes of no longer than 25 years. When this lifetime guideline was originally developed, 25 years was a reasonable compromise between the propellant required to lower a spacecraft's orbit and the impact it had on the long term orbital debris environment.

The main issue confronting today's space community in the area of LEO orbital debris is that compliance with the 25-year rule is too low and populations are steadily increasing. Compounding the issue is the current research and development focus on Active Debris Removal (ADR), an approach to dealing with the orbital debris problem that will be both technically and politically difficult to implement in the near term[6]. It is imperative that a policy structure be put into place to protect LEO from overpopulation, but to sustain this policy, it must be grounded in sound analysis. Current models for predicting population growth of both satellites and orbital debris are operated by a few subject-matter experts at national space agencies around the world. While several of these models have been shown to be in relatively good agreement, they are complex, computationally expensive, and are difficult for new analysts to acquire, especially if they are outside the community. Additionally, these models require new users to climb a steep learning curve prior to effectively executing analyses. By creating a simpler approach to the long-term projection of orbital object populations that is in reasonable agreement with the detailed models, a new paradigm can be created; one in

which general analysts can run many “what if” scenarios in a short period of time. This would open up the possibilities for broader trade studies to support the definition of effective and sustainable policies.

The objective of the work presented in this dissertation is to provide this simpler, flexible, yet accurate model. Through a combination of data mining, statistical analysis, and modeling and simulation, the Simplified LEO Orbital Object Population, or SLOOP, model has been developed. This effort leverages previous work done in the area of simplified modeling, but provides a more accurate and higher fidelity model than any previously developed. Chapter 2 is a review of previous work in this area of analysis. Data regarding the current state of populations in LEO is also presented. Chapter 3 dissects the Lafleur model[7], the most recent attempt to create a simplified model for orbital object population projection. This chapter also provides an overview of the SLOOP model’s overarching structure and component algorithms.

A new space object database has been created from multiple data sources that provides a more complete picture of man-made objects our sky than any single data source currently available. Chapter 4 discusses the detailed statistical mining of this database for relevant information and converting current data and historical data into accurate representations of the behavior of space object populations. New models were created to capture the natural decay of orbits from as high as 2000 km altitude by leveraging advanced environmental models maintained by NASA. Unlike previous attempts at simplified population modeling, the SLOOP model sub-divides LEO into layers, providing an unprecedented view of the sub-populations of LEO. The rapid analysis can predict orbital populations and collision probabilities over the next several

hundred years in less than 2 seconds of run time. A comparison of the results of the SLOOP model to current benchmark data in Chapter 5 confirms the relative accuracy of this model.

This dissertation further provides an example of the power of the SLOOP model to support data-driven policy. The model is used to determine the long-term impact of the newly emerging small satellite market. For the first time in human history, the emergence of CubeSats is enabling everyday people to fly real satellites in space at a fraction of the previous cost. These CubeSats can be launched in very large numbers on a single launch vehicle and represent a potential shift in the historical launch rates that have previously driven long-term population models.

This acceleration in the growth of satellite populations carries significant risk. To date, CubeSats have been launched in large numbers to lower altitude orbits with small populations which has minimized their contribution to collision probability. This will change as CubeSats increasingly fly as secondary payloads on commercial launches. In the 700 km to 900 km altitude region where most CubeSats are deployed when taking a ride share opportunity, the natural orbital life can easily exceed 1000 years. Coupling this with the increased population density at these altitudes, one can expect to see a significant increase in projected collisions in those higher orbital regions. In Chapter 6, the new SLOOP model is used to show the potential impacts of CubeSat launches over a range of potential orbital altitudes and launch frequencies. Based on model predictions of these scenarios, potential policy avenues are explored and evaluated for their general effectiveness.

It is time for simpler and straight forward satellite population modeling to be available to a broader space community. The data to support this type of modeling is available and waiting to be exploited. The computational power is available to support higher fidelity simple models of this complex problem. By bringing all of those components together, a new capability is now available to help steer the path of responsible space use for the next generation.

CHAPTER 2:

BACKGROUND AND LITERATURE REVIEW

Low Earth Orbit (LEO) is the region of space between 200 km and 2000 km altitude. Over the past 55 years, humanity has become increasingly dependent on LEO as a home for satellites that perform a myriad of functions affecting the daily lives of people across the globe. LEO satellites provide weather information and support natural resource monitoring. Communications satellites facilitate a global communications network. Scientists use specialized satellites to learn about the ever-changing climate of the Earth, the nature of gravity and relativity, and about our planet's place in space and time. National security interests operate spacecraft to gather intelligence and provide warfighters with critical battlefield information. All signs point to an increase in LEO operations with the emergence of the small satellite market and the initiation of serious efforts to mount human expeditions beyond LEO.

As many within the space community know, our successful use of this resource has been clouded by our lack of forethought and understanding of just how the current uses of LEO impact our future ability to make use of this resource. Debris from exploding rocket bodies and fragmented spacecraft already pose an increased threat to operational spacecraft throughout LEO. While technical measures such as the passivation of rocket bodies and conservation measures such as the 25-year rule have

reduced debris production over the past few decades, compliance with these guidelines has yet to be fully realized.[8] As a result, many studies have shown that a "business-as-usual" approach to orbital debris mitigation will allow the LEO debris population to continue to increase, thereby increasing the risk to operational satellites. Many within the community point to these dangerous trends and conclude that action must be taken to stem the growth of the debris population.

2.1 Populations and Collisions

The population of LEO objects is classified as either operational spacecraft or debris. Debris is typically categorized as small (<0.5 cm), medium (0.5 – 10 cm), or large (> 10 cm) objects. This classification captures both the observability and potential threat of a debris object. Small debris can typically be shielded against, presenting very little threat to operational spacecraft. Large debris, including spent rocket bodies and non-operational spacecraft, can be tracked and cataloged and currently makes up approximately 76% of the over 11,000 unclassified objects tracked in LEO by the Joint Space Operations Center (JSpOC).[9] A collision with a large debris object is typically catastrophic, destroying both objects. This was the case in the 2009 collision between the Iridium 33 and Cosmos 2251 satellites.[10] Medium sized debris is very difficult to track by ground assets but poses a lethal threat to operational satellites. Estimates for medium debris populations in LEO range from 300,000 to 500,000 unique objects. However, much of this data results from simulations due to very limited observational data sets.

Throughout the life of a spacecraft there are several opportunities to create debris of all shapes and sizes. Large debris is typically created at major events in a spacecraft's life. An upper stage can remain in orbit after it has delivered a satellite. Satellites only

operate for a finite period of time and once their mission is complete, they become space debris. Both of these categories of space debris are subject to guidelines for disposal. In LEO, the overarching guideline is the 25-year rule which states that, after their mission is complete, objects should be placed in orbits that will allow for them to naturally re-enter the Earth's atmosphere within 25 years of the end of their operations.

By far, the largest source of space debris is fragmentation, or the break-up of satellites and rocket bodies in orbit. To date, there have been 203 known breakups of orbiting objects.[11] The majority of these have occurred due to explosions. The fragmentation of a 5 to 10 ton satellite can produce 3,000 – 5,000 debris objects bigger than 10 cm and 150,000 – 250,000 debris objects between 1 and 10 cm.[12] There are several reasons for orbiting objects to explode. Propellant tanks and batteries can be heated by the sun in orbit. The remaining contents of these tanks will evaporate, increasing the pressure until they explode. These pressure vessels can also explode if struck by a small micrometeoroid or piece of debris. It is estimated that as much as 70% [11] of all fragmentations have been caused by explosions. Fragmentation can also be intentional, like the Chinese anti-satellite (ASAT) weapon test that destroyed the Fengyun-1C spacecraft in 2007. It is estimated that 29% of the fragmentation events in orbit were deliberate. The remaining 1% of fragmentation events were collisions between orbiting objects.[11]

While collisions make up a small percentage of fragmentation events today, several factors lead experts to predict that collision fragments will make up 50% of all objects in LEO within 50 years.[13] First, many spacecraft and rocket bodies now undergo a process known as passivation as part of their end-of-life operations. This

includes depressurizing all storage tanks to avoid explosions. Second, the space community expects a general decline in the number of intentional fragmentation events (ASAT tests) due to increased pressure to avoid the creation of orbital debris. Finally, it is expected that as the population of orbiting assets increases, so too will the probability of on-orbit collisions.

2.1.1 It's crowded up there

There are currently 22,000 objects being tracked in Earth orbit by JSpOC. Approximately 16,000 of these are publicly acknowledged; the remaining 6,000 are classified. In addition, there are an estimated 500,000 untracked objects in Earth orbit. These objects tend to be grouped into three orbit categories; Low Earth Orbit (LEO) extending from 200 km to 2000 km altitude, Geo-Synchronous Orbit (GEO) at approximately 35,800 km altitude and Medium Earth Orbit (MEO) which lies between LEO and GEO. Roughly 73% of all tracked objects in Earth orbit are located in LEO. While GEO is home to many communications satellites that have a high value, only about 5% of the tracked objects reside there. Additionally, relative velocities of objects in GEO are low and fragment populations are likewise projected to be low, reducing both the likelihood and consequence of collisions in the GEO region of space. For this reason, the primary focus for orbital debris is LEO.

Figure 2.1 shows that within LEO there are distinct regions of higher population. The number of active satellites is overlaid with the debris spatial density (the measure of number of debris objects per cubic kilometer) at those altitudes. This chart clearly shows the correlation of high satellite populations with large populations of orbital debris. The peak between 750 and 800 km is of particular interest as this orbit houses the Iridium

satellite constellation and contains most of the debris from the Iridium-Cosmos collision and the Fengyun-1C ASAT test.[14] For those working to mitigate the threat of orbital debris, these regions have become the focal point for research.

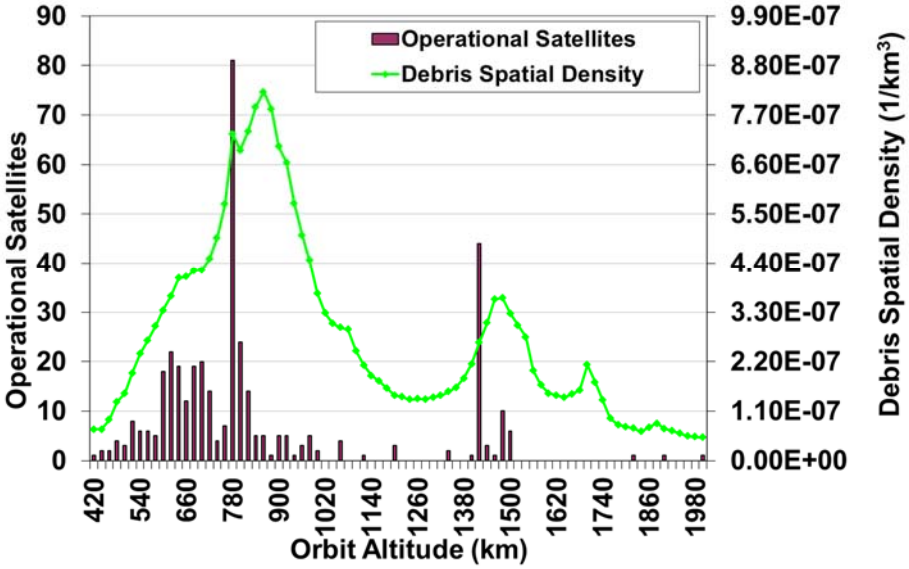

Figure 2.1: Operational Satellite Populations and Debris Spatial Density by Orbit

While large events such as the Iridium-Cosmos collision have brought new attention to the issue of orbital debris, the primary near-term threat to orbiting assets comes from the medium sized debris in Low Earth Orbit.[15] The reason is a combination of the aspects already discussed. LEO has the highest concentration of both active satellites and debris, thus increasing the probability of objects colliding. Due to the combination of velocity and mass, satellites cannot be effectively shielded against medium debris collisions like they can for small debris. Also, because the medium debris cannot be tracked from the ground, operators cannot perform collision avoidance maneuvers like they can when two large objects are predicted to collide. In short, medium debris is large enough to do significant damage but too small to be seen. Combining those characteristics with a convergence of high populations of both debris and active

satellites makes the medium orbital debris population in LEO the most threatening at this time.

2.1.2 And even more crowded in the future

Several agencies have performed studies to predict what the space environment will look like over the next 100 years and what strategies may be implemented to mitigate the threat of orbital debris. NASA's Orbital Debris Program Office (ODPO) at Johnson Space Center has taken a lead role in these efforts. Medium debris in LEO has been recognized, most recently by the Catcher's Mitt study, as the most significant threat to orbiting assets today.[15] However, it is also widely accepted that the removal or remediation of that debris is extremely technically challenging. As a result, the focus has been shifted to methods of reducing the production rate of medium and large orbital debris.

The *Kessler Syndrome* hypothesizes that debris populations can reach a certain magnitude where chain reactions of collisions will continue to produce debris even if no new objects are placed in that orbital region. These chain reactions are sustained by the production of medium and large orbital debris from collisions. Based on this theory and the technical challenges of removing medium orbital debris, many in the debris community have begun investigating methods to actively remove large debris objects from orbit. The theory is that by removing large debris, the probability of collisions will be reduced and less medium debris will be created.

J.C. Liou, of NASA's Orbital Debris Program Office, produced the plot shown in Figure 2.2 based on predictive modeling of the debris environment over the next 100 years using NASA's LEO-to-GEO Environment Debris (LEGEND) tool.[15] The

"business-as-usual" approach, labeled "A" in the figure, represents continuing to operate in LEO as the space community has historically operated. Two current approaches to mitigating the orbital debris threat are highlighted. The first approach, labeled "B" in the figure, is Post-Mission Disposal (PMD), which refers to adherence to the 25-year rule. The second approach, labeled "C", is Active Debris Removal (ADR), in which a spacecraft is sent to retrieve an inactive satellite or rocket body and deorbit it. Both approaches aim to reduce the large object population in order to slow or stop the growth of the debris population and thus reduce the operational threat to space assets.

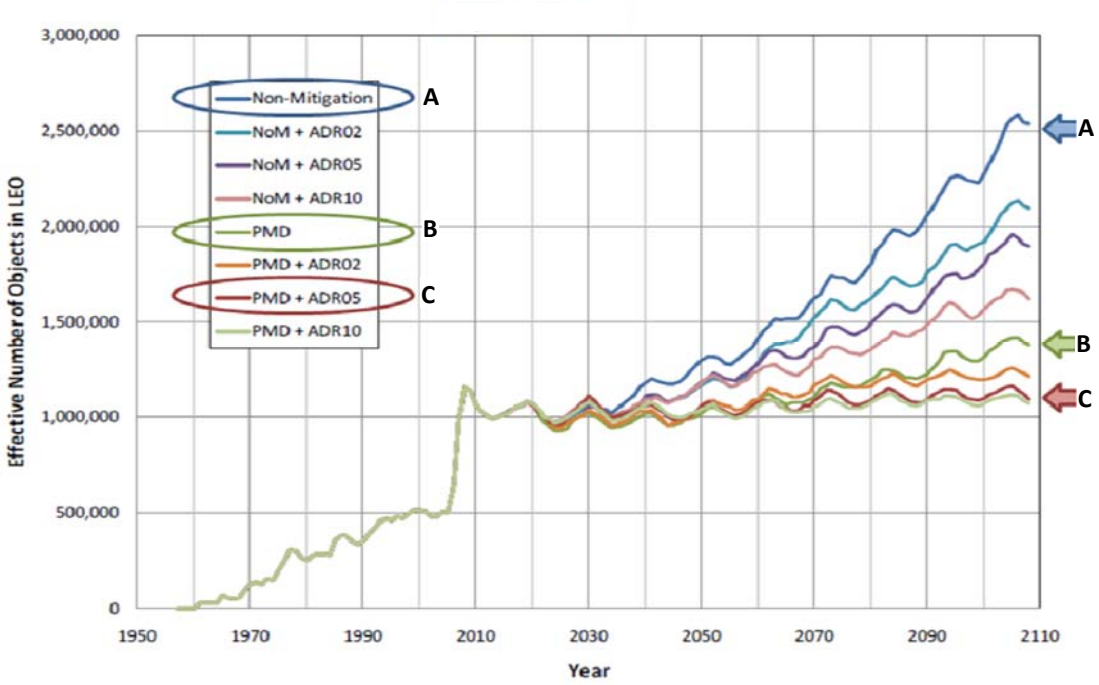

Figure 2.2: Population Growth of Objects >5mm under Various Scenarios [15]

The theory behind ADR is that, by specifically targeting large objects in LEO for removal, the production of debris through collisions will be reduced and the threat will diminish. However, ADR carries with it many technical and policy challenges that will make it difficult to enact. On the international policy front, advocates of ADR are faced with the questions of ownership of the offending space objects. To further complicate

matters, there are those within the national security community that see the same technologies that would enable ADR (specifically automated rendezvous and capture) as tools of war and point to ADR as a potential weaponization of space.[16] The challenge of making ADR a technical reality has spawned advances in deorbit technologies such as tethers, advanced drag augmentation devices, and other advanced propulsion technologies.[15] However, the technologies to support the rendezvous and capture of a passive, uncooperative, tumbling space object have yet to be fully realized.

While the data summarized in the chart in Figure 2.2 provide a picture of what LEO may look like in general over the next 100 years, a 2002 study performed in support of the ESA Space Debris Mitigation Handbook update provides a more complete picture.[17] In this study, analysts predicted orbital spatial density, or the number of objects per cubic kilometer of space, over both time and orbital altitude. A plot of this data is provided in Figure 2.3. This assessment assumes a business-as-usual approach to orbital debris mitigation and shows that peaks of maximum population in LEO tend to remain consistent as time progresses, especially in the higher altitudes where atmospheric drag is minimal. The regions of greatest concern are identified as the shell of interest from 800 – 1000 km and around 1400 km. While spatial density grows at all altitudes, these two regions exhibit accelerated growth due to the greater populations of debris.

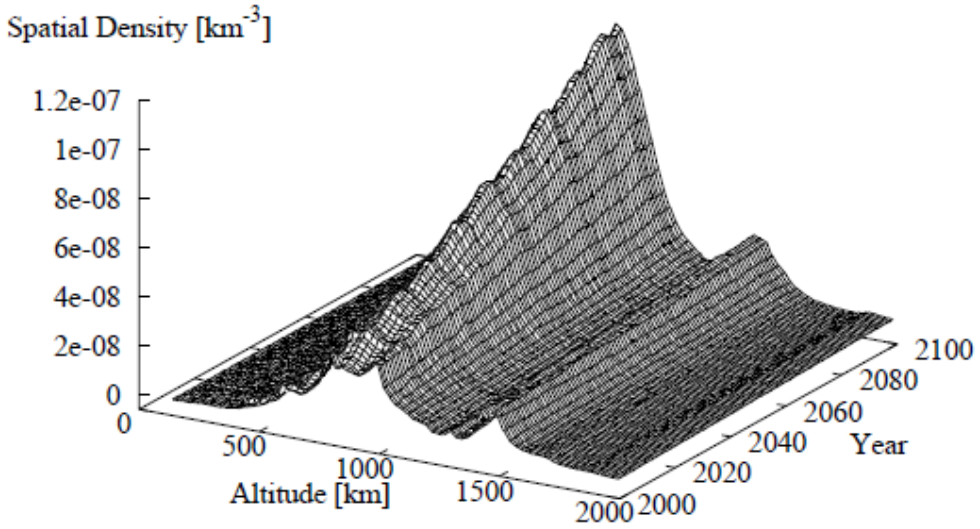

Figure 2.3: Spatial Density of Objects >1cm in LEO [17]

2.1.3 LEO crowd control

Several studies performed over the last 10 years suggest that regulation may significantly affect orbital debris. First, the results of J.C. Liou's 2009 investigation for DARPA (Figure 2.2) show that a stricter adherence to the current 25-year rule would significantly slow the growth rate of the debris population in LEO. This is evidenced by line "B", labeled PMD, which assumes a 90% adherence rate to the 25-year rule, up from the currently estimated 70% rate, represented by line "A".[15] Bradley and Wein deduced a similar trend noting that a compliance rate as high as 98% would cause the spacecraft risk levels to plateau for the next two centuries.[18]

The 2002 ESA study additionally investigated the impacts of shorter post-mission disposal times on LEO debris populations.[17] The data, provided in Figure 2.4, shows that with 100% compliance, any deorbit lifetime regulation would be effective in curbing the growth of the debris population. Further, it suggests that more strict guidelines that

require shorter post-mission disposal times may actually be able to reverse the debris population growth trends.

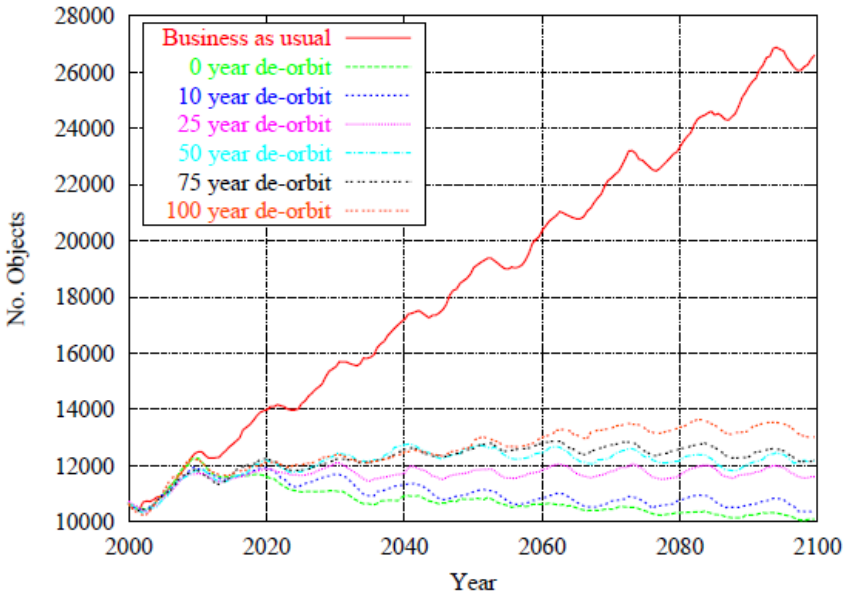

Figure 2.4: Sensitivity of Population Growth to Post-Mission Life Duration [17]

This reduction in the PMD duration carries with it several questions about its feasibility. The original 25-year rule was accepted because it balanced the conservation of LEO with the expenditures required to provide a liquid propulsion system capable of repositioning a satellite at the end of its life into an orbit compliant with the 25-year rule. To reduce this to some duration less than 25 years would levy higher energy requirements on propulsion systems. However, alternative deorbit technologies using advanced propulsion systems have been developed in the past few decades that may make shorter PMD durations more acceptable, leaving the possibility of reopening the duration discussion in light of this new information.

The technologies to enable PMD modifications must either be part of the original satellite bus design or readily integrated into a bus post-production. With satellite producers typically designing a bus for many different satellite applications and using

that design for an extended period of time, there are few opportunities to get fully integrated advanced deorbit technologies into the satellite market. Therefore, these changes are more likely to be phased into the industry over time as new spacecraft designs are developed and old designs are retired.

The 2002 ESA study provides us with a second piece of information to support regulation as a debris mitigation practice. The study team also projected the effects of higher compliance rates with post-mission disposal guidelines as a function of both time and orbit altitude. These results, provided in Figure 2.5, show that a stricter adherence to the 25-year rule brings the growth rate to nearly zero. This plot further shows the potential to conserve low-risk orbits through regulation now, thus avoiding growth in those orbits and leaving only two high risk shells of interest (at 900 km and 1400 km) for the next 100 years.[17] The third shell of increasing population at 2000 km is the disposal orbit for satellites in the higher regions of LEO where deorbit is not the most effective means of disposal.

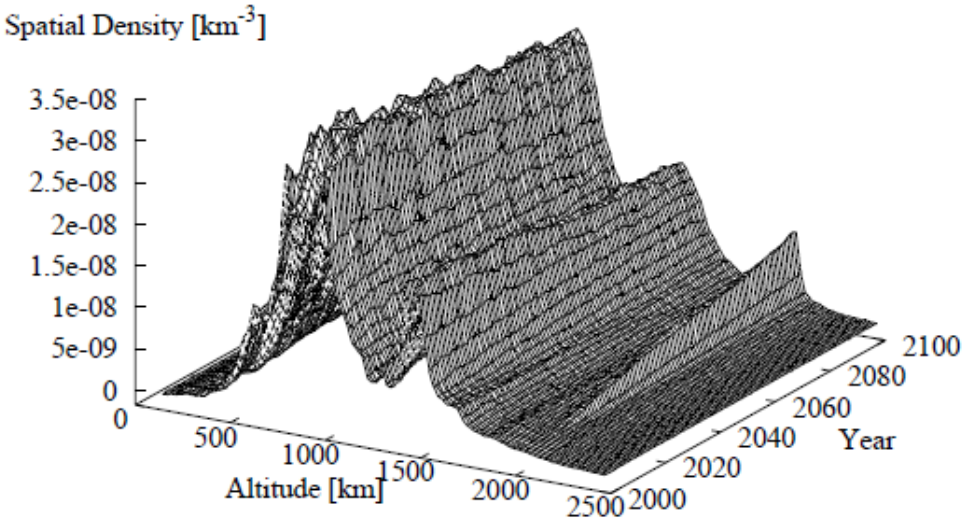

Figure 2.5: Spatial Density Growth under Strict Adherence to the 25-Year Rule [17]

Based on the results of this analysis, the ESA study team provided several key findings. Among them was the fact that "any post-mission de-orbit lifetime limitation policy between 0 and 100 years (in combination with passivation) would be effective in stabilizing the future collision rate and future LEO debris population levels."[17]

2.1.4 The Business of Space

The Department of Defense recognizes the strategic value of satellites in LEO, citing the congestion of space as a significant threat to important national assets.[19] NASA and other research entities such as the National Oceanic and Atmospheric Administration (NOAA) recognize the scientific value of Earth monitoring from LEO spacecraft. However, one must not overlook the economics of the commercial entities involved in LEO satellites. According to the Satellite Industry Association, the satellite industry in general saw $195.2 Billion in global revenues in 2013.[20] Satellite services, such as remote sensing and satellite communications, made up the majority of those revenues. While satellite television services like Direct TV and Dish Network made up the majority of those consumer services, LEO satellites providing satellite communications and satellite broadband internet saw 20% growth in 2013.[20] In fact, of the nearly 500 active satellites currently flying in LEO, nearly 25% of them belong to the satellite communications companies Orbcomm, Globalstar, and Iridium. Coupled with recent announcements by both SpaceX and Virgin [21] for new, massive satellite broadband internet constellations in LEO, it is clear that flying satellites in LEO is and will continue to be big business.

The business of building and getting satellites into LEO has also seen steady growth. Both the launch services and satellite manufacturing sectors saw 7% and 8%

growth, respectively, in 2013 and accounted for nearly $21.5 billion in global revenue.[20] In the United States, several new launch services providers have emerged in the last decade to rival the traditional powerhouse, United Launch Alliance (ULA). New launch vehicles such as SpaceX's Falcon series [22] and Orbital Sciences' Antares rockets [23] are catering to the LEO satellite market, offering reduced cost launches to lower altitudes. These rockets are less powerful than the Atlas V and Delta IV rockets but are more than capable of delivering substantial payloads to LEO.

The past two decades have also seen a large expansion in the number of countries operating satellites in LEO. With launch costs and satellite manufacturing costs dropping, even small countries are finding access to space a reasonable goal for national development. The result is that, since 1994 the number of countries operating satellites in LEO has grown from 16 to 46. These new space operators include Thailand, Nigeria, Luxembourg, Chile, and several other new comers to competitive aerospace markets.[24] While these nations do not have the resources to construct larger satellite operations, they have found an affordable home in LEO space.

Another emerging market in LEO satellites is the small satellite market. Of this new class of satellites, none has a greater potential to change the LEO landscape than CubeSats. Defined by their modular assembly of 10 cm cubes (or "U"s), a CubeSat is a fully operational spacecraft housed in a volume as small as one 10 cm cube or as large as a two by three array of 6Us. CubeSats offer a low cost alternative for groups looking to get into the satellite market. A 1U CubeSat kit can be purchased for $13,000 and a 6U configuration costs as little as $30,000.[20] These satellites are ideal for start-up companies such as Planet Labs, academic institutions, and low budget researchers.

With the emergence of this new class of satellite, launch providers are finding ways to use excess space on sold launches to provide ride-share opportunities to CubeSats as secondary payloads. Smaller launch providers are also offering dedicated CubeSat launches. Two such launches occurred over the span of two days in November of 2013. A Minotaur rocket was launched from the United States, sending 29 satellites to 450 km altitude.[14,25] A day later, a Dnepr-1 rocket launched 33 satellites from the Yasny Cosmodrome to an altitude of 580 km.[14,26] On these two days, the number of new satellites launched into orbit equaled the average annual number of satellites launched for the previous six years. The business case for LEO satellites is shifting and the launch market is taking note and preparing to support this revolution. The population of satellites in LEO is set for a sharp increase in the coming years.

2.2 A Brief History of Orbital Object Population Modeling

The cornerstone to any serious evaluation of orbital debris mitigation strategy is the long-term prediction of object populations. Typically, a prediction of object populations will span several hundred years in an attempt to quantify the long term effects of overpopulation and the relative efficacy of various proposed mitigation strategies. To gain an understanding of how the populations of satellites and debris objects grow and interact, analysts have drawn on analogies from the natural world, including collisions of asteroids in the asteroid belt and the theory of molecular collisions in gasses, to provide the physics-based context for the calculations.

2.2.1 Predicting Collisions

In 1978, Don Kessler first proposed his theory of space object interaction.[1] Based on a previous model developed to explain the interactions of objects in the asteroid

belt, Kessler's hypothesis came to be known as the *Kessler Syndrome* and Kessler himself is recognized as the grandfather of orbital debris analysis. The model that Kessler and his collaborators developed was based on calculations of object spatial density and flux, or impacts per unit area per unit time. The space around Earth was subdivided into differential volumes at specific increments of distance from the surface of the Earth, *R*, and geocentric latitude, β. Within any given volume, the impact rate on a particular spacecraft is represented by Equation 2.1,

$$\frac{dI}{dt} = S\overline{V_s}A_c \quad , \tag{2.1}$$

where *S* is the spatial density of objects in the volume, $\overline{V_s}$ is the average relative velocity, A_c is the cross-sectioned area of the spacecraft, and *I* is the total number of impacts with the spacecraft at time t. Integration of this equation over a full volume, for example a shell of orbital space, estimates the collision frequency of all objects in the space. This integral is shown as

$$\frac{dC}{dt} = \frac{1}{2}\int S^2 \overline{V_s}\overline{A_{cc}}dU \quad . \tag{2.2}$$

Kessler developed values for the spatial densities and average velocities of orbiting objects based on the cataloged population data of the time. The collisional cross-sectional area was taken as the area equivalent to an object that has a diameter that is the sum of the two colliding objects. Through hypervelocity impact testing, Kessler was also able to quantify the number of fragments that would be created by such a collision and was able to hypothesize that, if enough satellites were placed into a region of space,

collisions between satellites and satellite fragments would perpetuate in a cascading manner until a debris belt similar to the asteroid belt was created.

In a later paper published in 1981, Kessler continued to refine his methods and checked his general approach against similar work being done to predict the likelihood of collisions between the many outer moons of Jupiter.[27] Kessler reveals that the roots of his collision theory are based in general gas dynamics where collisions of molecules can be directly equated to the product of the spatial density of the molecules, relative velocity of the molecules, the collision cross-sectional area, and the time that the object in question resides in the volume being evaluated.[28] This is the same relationship represented in Equation 2.1 above.

Given that a satellite occupies a space that can be defined by its orbit and that other objects can be assumed to be randomly distributed within their own orbits, the potential for collisions can be related to orbital elements. Kessler again assumes a differential volume defined by both geocentric latitude, represented by orbital inclination, and altitude. Kessler further assumes that, over time, the objects in these orbits will appear to an individual orbital object to randomly occupy the entire space in the volume bounded by its inclination and altitude due to natural precession of the orbits in question. By integrating over all of the differential volumes in a given region, the number of collisions is calculated between objects. The relationship can be simplified to

$$\frac{C}{t} = N_1 N_2 \frac{\overline{v_{12}}\sigma}{V} \quad , \tag{2.3}$$

where C is the number of collisions in time t, N is the number of objects of type *1* and *2*, $\overline{v_{12}}$ is the relative velocity of objects *1* and *2*, σ is the collisional cross-sectional area and

V is the total volume of the region under investigation. Numerous applications of this general theory of collision probability have proven to be very good predictors and it is the basis of many of the highly complex population prediction models that are used today. Kessler would go on to become the first head of the NASA Orbital Debris Program Office and the theory of differential volume based collision prediction would become the basis for the LEGEND tool used by NASA today to make long term population and collision frequency predictions.[29]

In 2010, Kessler published a paper with several analysts who are operators of the LEGEND model.[2] They re-evaluated the validity of Kessler's original approach by using LEGEND to predict the collision probabilities through the 1990s and early 2000s based on known population data. What they found was that LEGEND, using the differential volume collision model, showed strong predictive capability when compared to observed instances of collisions. The predicted collision rate very closely resembled the observed collision rate over the period of time from 1990 to 2005.

2.2.2 Simplified Approaches to Population Analysis

While Kessler's approach to collision prediction and population growth is effective, the complex nature of the equations and the execution of the analysis through systematic evaluation of individual collision rates over differential volumes is computationally intensive. In 1991, Paolo Farinella and Alessandro Cordelli of the Universita di Pisa published a paper outlining their "simple mathematical model for the future proliferation in low earth orbit of space debris that is created by high-velocity destructive collisions of small objects with artificial satellites".[30] They developed two coupled, non-linear, first order differential equations that treated object populations like

ecological populations, tracking the creation and destruction of objects in space in much the same way as births and deaths within a biological population. These two equations tracked the change over time of a population of large objects (N), which included both active and inactive satellites and rocket bodies, and a population of debris fragments (n).

$$\frac{dN}{dt} = A - xnN \tag{2.4}$$

$$\frac{dn}{dt} = \beta A + \alpha xnN \tag{2.5}$$

In these equations, A represents the rate of insertion of big objects into orbit; essentially the birth rate of large objects. The estimated collision rate between big objects and small objects is represented by the "xnN" term, which uses simple particle-in-a-box theory to classify a collision probability represented by x. The "x" term is calculated much the same way as Kessler's collision probability, relating to the collisional cross-sectional area, relative velocities and the volume investigated. The "xnN" term is essentially the death rate of large objects. The corresponding increase in small objects is quantified by multiplying this collision rate by α, the estimated number of small objects created by such a collision. A second small object birth rate is quantified by multiplying the number of objects inserted into LEO by an estimated number of small objects created during deployment operations, β. By adding these two small object birth rates, the change in the small object population is quantified.

At the time Farinella and Cordelli published this work, simplified mathematical models were a virtual necessity. Given the limitations of computing power, long term projections of LEO object populations would require significant resources if not

evaluated under simplified terms. The authors identified several areas for potential improvement given their simplifying assumptions. On a gross level, the results of their modeling effort supported the general hypothesis that at some future time, over-population would lead to cascading collisions that could render whole regions of space virtually unusable. The simplified nature of the model allowed Farinella and Cordelli to evaluate several alternate future scenarios to show the impact of shifts in behaviors, providing analytical support for proposed operational guidelines aimed at reducing the growth rate of debris populations and extending the useful life of Low Earth Orbit.

Over the years, what Farinella and Cordelli referred to as the discipline of modeling "future proliferation in low earth orbit of space debris", evolved. Shortcomings of the original model were resolved by expanding the set of differential equations to account for more variables and the continuous nature of the populations. These populations were subdivided to account for the varying contributions of collisions of large objects of different sizes. At one point, an unwieldy 150-equation model was developed to attempt to capture the various nuances of the problem.[31] As computing power increased, focus turned to more physics-based modeling techniques and models became much more complex.

2.2.3 The High-Fidelity Approach

Space agencies around the world employ various high-fidelity codes in an attempt to accurately project orbital object populations. These models account for population interactions, collisions, launch rates, deorbit rates, and natural lifetimes of space objects across a wide range of sizes. Many predictions are deterministic or semi-deterministic, relying on high fidelity orbital data and orbit propagation models to evaluate collision

probabilities on individual representative satellites. Table 2.1 provides a short summary of these models by agency.

Table 2.1: Collision & Population Models from Space Agencies Around the World [32]

Model Name	Agency	Brief Description
SDM	ASI	Full 3-dimensional LEO-to-GEO simulation code using extremely detailed traffic models
DELTA	ESA	3-dimensional semi-deterministic model using representative objects to stochastically predict impacts
KSCPROP	ISRO	Filtered, sub-population collision assessments will fully propagated revolution by revolution simulation of any two objects in orbit
LEODEEM	JAXA	All-on-all collision prediction tool modeling all tracked objects with propagated orbits
LEGEND	NASA	Deterministic model mimics historical populations using pair-wide comparison algorithm for collision prediction based on differential volume collision modeling
DAMAGE	UKSA	Semi-deterministic model using fast, pair-wise algorithm based on differential volume approach to determine collision probabilities for all orbiting objects

A paper published by the Inter-Agency Space Debris Coordination Committee (IADC) in 2013 compared the results of these six population prediction models.[32] The paper shows very similar results from all of the models in both the prediction of the number of collisions and the overall prediction of the intact object and fragment populations over time. To account for variability in several of the inputs and settings, the models were executed using Monte Carlo analysis with distributions around many of the inputs. The published results show similar results and trends from all models and show an ever increasing margin of error as the prediction period is extended, as would be expected. All of these models are similar in their execution approach and are extremely complex.

The general analysis approach employed by NASA's LEGEND tool provides a good point of reference for how many of these complex models operate. The LEGEND tool is a full-scale three-dimensional debris evolutionary model. The model covers near-Earth space from 200 km to 38,000 km, divided into regions of LEO, MEO (Medium Earth Orbit) and GEO. The model is capable of providing a wide array of debris characteristics as a function of time and spatial position. The tool draws from several historical data sources for both active and large intact debris objects, as well as fragments. LEGEND relies on two orbit propagation codes, one for GEO and one for all other orbits, which account for atmospheric interactions, radiation pressure, and various Earth gravity model effects.[29]

LEGEND uses NASA's standard break up model to characterize the debris field resulting from a collision.[33] Monte Carlo techniques support the random selection of velocity and area-to-mass ratios for fragments based on probabilistic distributions of these characteristics. Debris fields can be created and tracked specifically to determine future interactions between those debris objects created by a collision and other orbiting objects. LEGEND has a large number of potential user inputs and settings which allows users to very specifically investigate different potential future scenarios.

While the utility of tools such as LEGEND is understood within the community, these high-fidelity models have several drawbacks. First, these models tend to have very complex user interfaces. Multiple settings and input variables make them difficult for a casual user to operate. The high fidelity nature of the tools also requires computational power that limits use and extends run times for longer simulations. The unpredictable nature of key input parameters, such as launch rate, make random sampling and

averaging using Monte Carlo analysis techniques a requirement to drive out sensitivities and determine average predicted values in an attempt to "cover the waterfront" of potential future scenarios.

The utility of a simplified model for long term orbital object population predictions has been recognized for some time. A simplified model offers several advantages over its higher-fidelity counterpart if it can provide comparable results. By reducing the population projection to very basic terms, the computing power required is greatly reduced. This in turn supports expanded sensitivity and trade analyses which can better isolate and characterize the main drivers in the population growth. Simplified input interfaces also make the modeling more accessible to analysts, allowing the model to reach a wider audience. With these characteristics, a simplified model can be a powerful tool to test the impacts of numerous future scenarios to a high enough level of fidelity to support broad evaluations of some of the more important drivers. In this way, the simplified model can provide a focusing function for more detailed evaluations using higher fidelity codes. Such a tool can also support informed policy decisions.

2.2.4 The Reemergence of the Simplified Model

In 2011, Jaret Lafleur, a graduate student at GeorgiaTech, revisited the concept of the simplified orbital population projection model by expanding on the original Farinella-Cordelli model.[7] Lafleur addressed several of the gaps in the Farinella-Cordelli model by expanding the Equations 2.4 and 2.5, adding terms to account for alternative means of population change. The Farinella-Cordelli model did not account for natural decay of object orbits, except by implicitly adjusting the "*A*" term to be a net rate of insertion. The Farinella-Cordelli model was also built under the "big sky" principle and did not,

therefore, account for the collision of two large objects, nor did it account for the collision of two small objects. To account for these missing factors, Lafleur added several terms to both the large object and small object population equations resulting in the following two equations:

$$\frac{dN}{dt} = (a + b\,sin(ct + d)) - \frac{N}{f + g\,sin(ht + k)} - xnN - 2yN^2 \tag{2.6}$$

$$\frac{dn}{dt} = \beta(a + b\,sin(ct + d)) - \frac{n}{p + q\,sin(ht + k)} + \alpha xnN + \gamma yN^2 - 2zn^2 \tag{2.7}$$

Through a survey of historical launch data, Lafleur noted the somewhat sinusoidal nature of the launch market. Especially over the last 20 years, the launch market has exhibited an ebb and flow that can be loosely modeled through the use of a sinusoidal function that Lafleur inserted as the first term in his equations. This change replaces the previous flat average rate approach taken by Farinella and Cordelli. Lafleur retains the "xnN" term that Farinella and Cordelli had employed as the death rate of satellites due to collisions with fragments. However, Lafleur also expanded the death rate of satellites to include two very important aspects overlooked by the original Farinella-Cordelli mode. A collision rate between satellites, represented as $2yN^2$, was added to account for the potential for collisions between two large objects in space. This potential was overlooked in the original model because the adopted theory at the time was that the likelihood of such a collision was so low as to be discounted. With the Iridium-Cosmos collision, we have now seen that collisions between large intact objects must be accounted for regardless of how remote they seem.

Lafleur also added a term to account for the natural decay of objects in orbit. All objects in LEO are subject to some level of atmospheric drag. Over time, sometimes on the scale of hundreds or even thousands of years, the altitude of their orbits will be reduced by this drag force. Just as Lafleur had expanded the original *"A"* term through the use of a sinusoidal function to more accurately account for the cyclical nature of launches, he also added a decay term to explicitly separate the inherent birth rate and death rate. In general, this orbit decay time can be translated into a number of objects that re-enter the atmosphere per unit of time by dividing the number of objects by their typical orbital life time. Lafleur chose to use the sinusoidal functions [$p + q\ sin(ht+k)$] and [$f + g\ sin(ht+k)$] to represent this orbital life because the drag force on a given object is directly tied to solar activity, which fluctuates cyclically over time.

Lafleur similarly expanded the equation that tracks the population of fragments in orbit. Using the same *"β"* term approach, Lafleur accounts for fragments caused by deployment operations in the second equation while coupling that with the launch rate term from the first equation. As with the first equation, Lafleur also accounts for the natural decay of the fragment orbits over time due to drag. The number of fragments resulting from a fragment-intact collision was retained from the original Farinella-Cordelli model using the *"α"* term. A corresponding fragment production term for intact-intact collisions, *"γ"*, was added as was a term for the loss of fragments due to fragment-fragment collisions, *"z"*.

To calculate his coefficients, Lafleur surveyed available data and determined average values for relative velocity, collisional cross-sectional area, and object lifetime. Lafleur chose to retain the values used by Farinella and Cordelli and used source material

related to the Iridium-Cosmos collision to classify his new variable, γ, to quantify the number of fragments resulting from a collision between two intact objects. Similarly to Farinella and Cordelli, Lafleur also chose to model LEO as one large volume of space from 200 km to 2000 km altitude.

Lafleur demonstrated relative agreement between his model and the original Farinella-Cordelli model in terms of general shape of the population profiles. Figure 2.6, taken from Lafleur's 2011 paper, shows that both models exhibit a general growth trend followed by a drop in the population. Both models attributed this drop in population to the cascading collisions of the *Kessler Syndrome*. Without the additional removal terms, the Farinella-Cordelli model shows a rapidly rising fragment population. However, with Lafleur's new data set for calculating coefficients for his model, the magnitude of both the intact satellite and fragment populations is significantly reduced. Also, the sinusoidal nature of both the launch rate and decay rate of the satellites manifests in a noticeable fluctuation in the population values when compared to the relatively smooth lines of the original model.

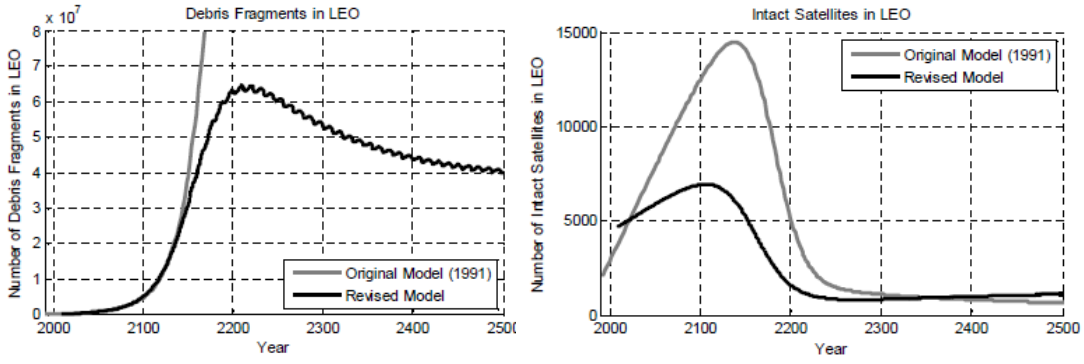

Figure 2.6: Comparison of Lafleur and Farinella-Cordelli Model Results [7]

There is value in the high-fidelity LEO population and collision prediction modeling but value also exists in a simplified approach that is rapidly executed and more user-friendly. However, refinement and recalibration of the simple approach to population modeling is an important step in supporting broader LEO environment studies. While Lafleur continued the legacy of simplified modeling, there are several areas where his model runs into trouble. In Chapter 3, the shortfalls of the previous attempts to provide this simplified modeling approach are investigated. A new model with significantly improved accuracy will be presented that provides a better representation of the higher-fidelity codes and will open the door to new trade analyses to support a wider evaluation of the LEO population growth problem.

CHAPTER 3:

DEVELOPMENT OF THE SLOOP MODEL

The continued growth of orbiting object populations represents a threat to the future useability of LEO. The ability to accurately predict the growth of these populations improves projections of collision probability and can support evaluations of emerging operational trends to isolate potential threats to current and future LEO spacecraft. The complex, high-fidelity models discussed in Chapter 2 provide an avenue to perform detailed population analyses but their complexity make them difficult and computationally taxing to operate.

The future is a difficult thing to predict, especially in the world of satellite operations. Launch rates fluctuate with markets and the ebb and flow of government funding compounds this variability. Paradigm shifts in the market can also significantly impact the predicted number of satellite collisions and are often difficult to predict. The recent explosion in the CubeSat market is a prime example of a significant change in the historical launch cadence that could adversely affect the safety of orbiting assets. Changes in operational policy can also have impacts to the projection of potential collisions. A renewed interest in the efficacy of post mission disposal may lead to

changes in regulations that can drive collision probabilities by impacting the residence time of orbiting objects.

The impacts of all of these potential changes in the standard operating scenarios of LEO can be evaluated with models designed to project collision probabilities and population growth. A simplified modeling approach that produces reasonably accurate representations of the results of more details tools can be a valuable resource in rapidly evaluating these changes to understand the first order impacts to the LEO environment. Rapidly executed "what-if" analyses can support evaluations of future scenarios much more readily with simple models than with large, complex models. Additionally, a user friendly platform will be accessible to more users supporting a broader expanse of potential analyses. Previous attempts at the simplified modeling approach have produced mixed results but there is great potential in this paradigm of modeling. Through a systematic approach to update previous methods using current analysis techniques and reflecting current populations and operational trends, the SLOOP model has been produced to fit this application. The development and performance of the SLOOP model is discussed in this chapter.

3.1 Establishing a Baseline for Comparison

In the course of developing a simplified modeling technique that provides reasonably good approximations of more complex tools, we must first establish the baseline for comparison. Two current models are used to provide baselines for the populations to be modeled. For the fragment population, the ESA tool MASTER2009 [34] was used to project the population of objects greater than 1 cm in diameter. MASTER2009 uses an assortment of data sources to probabilistically determine the

spatial density of particles of various sizes in orbit. By setting the size threshold of the model to 1 cm or greater, it can generate a spatial density distribution of particles over a 50 year timeframe. This data was then converted to a number of particles by multiplying by the volume of space extending from 200 km altitude to 2000 km altitude, $1.27e^{12}$ km^3. The converted data was then plotted and fit with a trend line in Excel, shown in Figure 3.1. The resulting equation used to represent the fragment population benchmark in all analyses presented in this document is

$$y = 6681t + 279652 \quad , \tag{3.1}$$

where y is the number of fragments greater than 1 cm in diameter and t is the time in years.

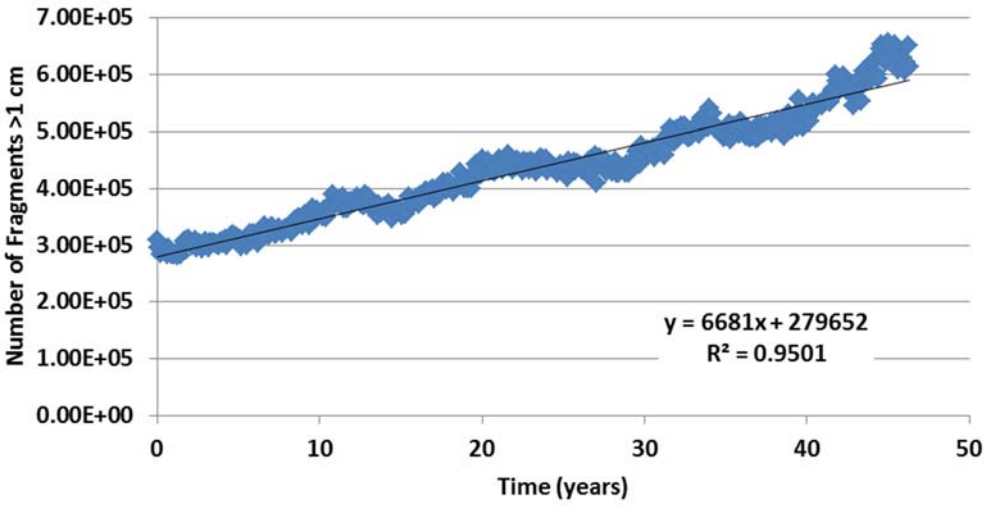

Figure 3.1: Curve Fit for MASTER2009 Fragment Population Projection

For large orbital objects, published data from the LEGEND tool were used. In a 2010 paper, J.C. Liou published 200 year projection data produced by the LEGEND tool.[35] The plot was recreated in Excel and an exponential curve fit was applied to the data and an equation was developed to represent the number of objects larger than 10 cm

in LEO as a function of time in years. The original data plot is provided in Figure 3.2 and the recreated Excel plot with curve fit is provided in Figure 3.3. The resulting equation used to represent the LEGEND benchmark in all analyses presented in this document is

$$y = 10096e^{0.0095t} \quad , \tag{3.2}$$

where y is the number of objects greater than 10 cm in diameter and t is again the time in years.

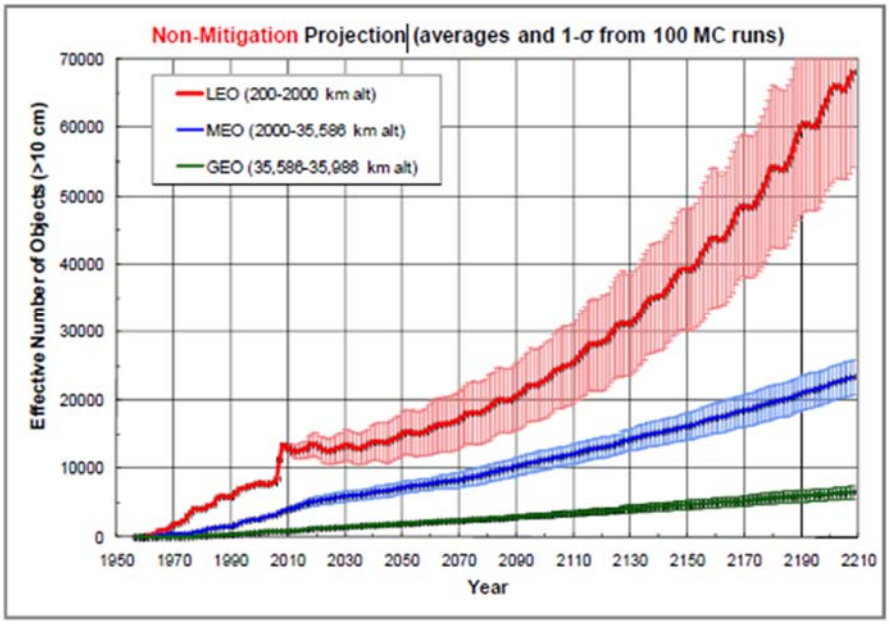

Figure 3.2: Various LEGEND Model Projections for Populations of Objects >10cm [35]

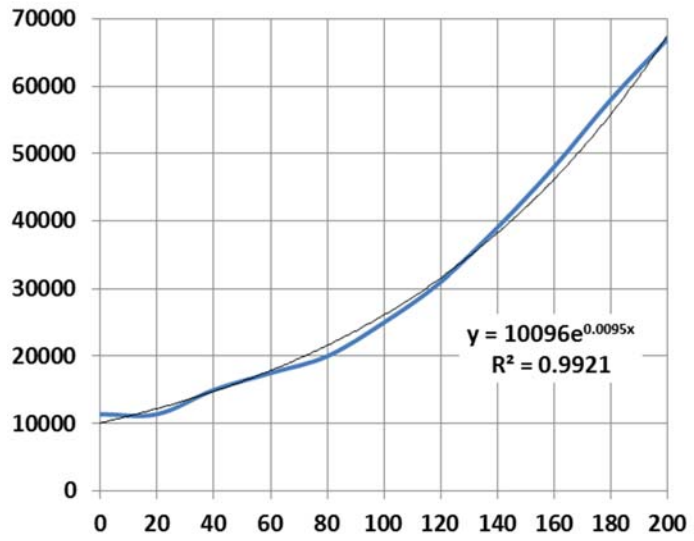

Figure 3.3: Curve-Fit of LEGEND Population Projections

To accurately compare the model results discussed in the rest of this document to the LEGEND and MASTER2009 benchmarks, it is important to understand what populations are actually being projected by both models. The MASTER2009 model projects the populations of debris fragments over time. The model allows the user to specify the range of diameters of fragments to be considered and the benchmark used in these analyses projects the population for a range of fragment diameters greater than or equal to 1 cm. The LEGEND tool projects the effective number of objects in orbit greater than 10 cm, a size threshold that mirrors the current observational capabilities of the ground-based radar systems from which JSpOC generates their catalog. This population includes both intact objects and fragments greater than 10 cm. By running the MASTER2009 model with lower size thresholds of 10 cm and 1 cm, the percentage of fragments greater than 10 cm out of the entire fragment population greater than 1 cm is shown to be 2.72%. This value is used to more accurately compare the results of the simplified modeling approaches with the published LEGEND results.

3.2 An Evaluation of the Lafleur Simplified LEO Population Model

The first step in building the SLOOP model was to code and evaluate Lafleur's population model. An overview of the general operating principles of the Lafleur model was provided in Chapter 2. To evaluate the model's operation, it was coded in MATLAB and different techniques for integration were investigated. The full MATLAB code for the Lafleur model is provided in Appendix A. A quick comparison of integration techniques shows that using a difference method and a reasonably small time step produces nearly identical results compared to using the ODE evaluation functions within MATLAB. A typical long term projection of population spans 100 to 200 years. Using a step size of 0.1 years produces the same results as the ODE45 function available in MATLAB. After coding the coupled differential equations using a difference method, the model was run using Lafleur's original coefficients. Figures 3.4 and 3.5 show plots of the results of the MATLAB model overlaid on the results provided in Lafleur's AAS paper for Intact Object and Fragment populations.[7] These results show a perfect match between the MATLAB code and the original data indicating that the model was coded correctly.

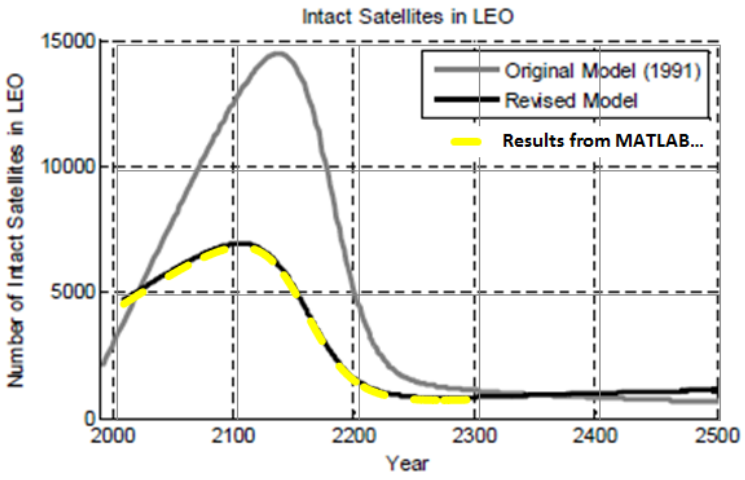

Figure 3.4: Comparison of MATLAB Code Results with Original Lafleur Intact Satellite Predictions

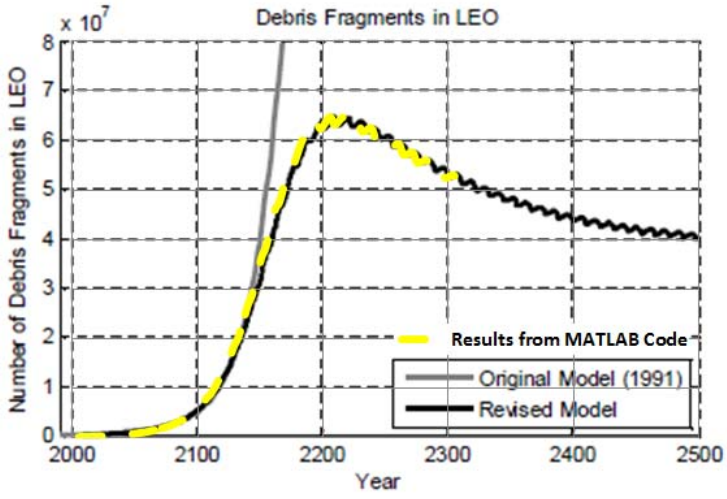

Figure 3.5: Comparison of MATLAB Code Results with Original Lafleur Fragment Predictions

Once the general operation of the Lafleur model MATLAB code was confirmed, the results of the model were compared to the LEGEND and MASTER20009 benchmark analyses. Figures 3.6 and 3.7 show the results of this comparison. When compared to the benchmark models, Lafleur's model significantly over-predicts the population of fragments and, due to this over-prediction, the number of objects >10 cm is also over

predicted. These results indicated a need to revisit the coefficients used in the original Lafleur model.

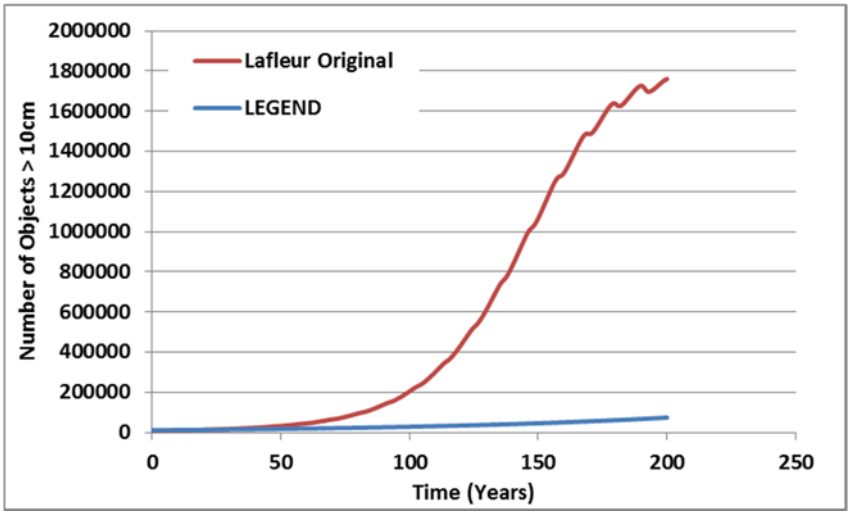

Figure 3.6: Comparison of Lafleur Model Projections and the LEGEND Model

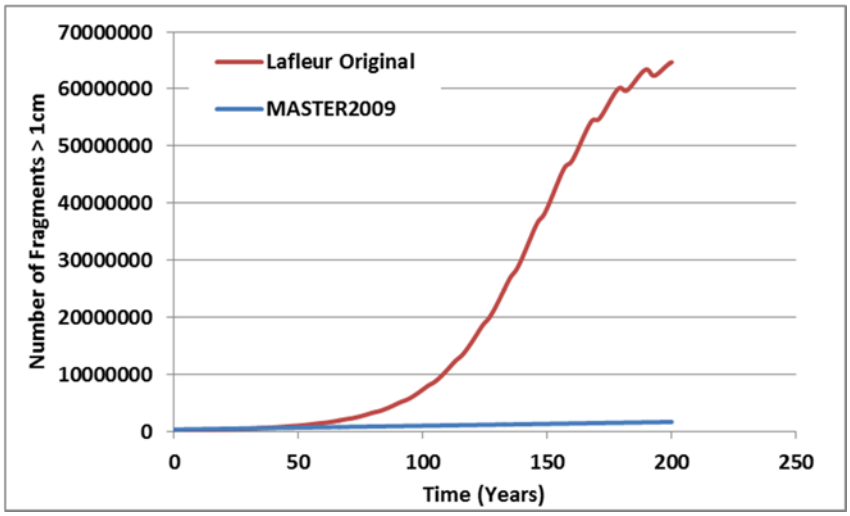

Figure 3.7: Comparison of Lafleur Model Projections and the MASTER2009 Model

An analysis of variance (ANOVA) was also performed on the Lafleur model to gain a better understanding of the relative importance of the 16 coefficients used in Equations 2.6 and 2.7. A range of values for each of the 16 coefficients was provided and randomly sampled using a Latin Hypercube space filling design of experiments in the

statistical analysis software JMP.[36] This produced a set of 160 unique input cases that were loaded into the input matrix of the Lafleur MATLAB program. The execution of the model generated a time-dependent data set of results for the intact object population, *N*, and the fragment population, *n*. These results were sampled at 50, 100, 200, and 275 years of simulated time and evaluated for correlation using a multivariate correlation technique in JMP. The resulting correlation values for *N* and *n* are shown in Figure 3.8.

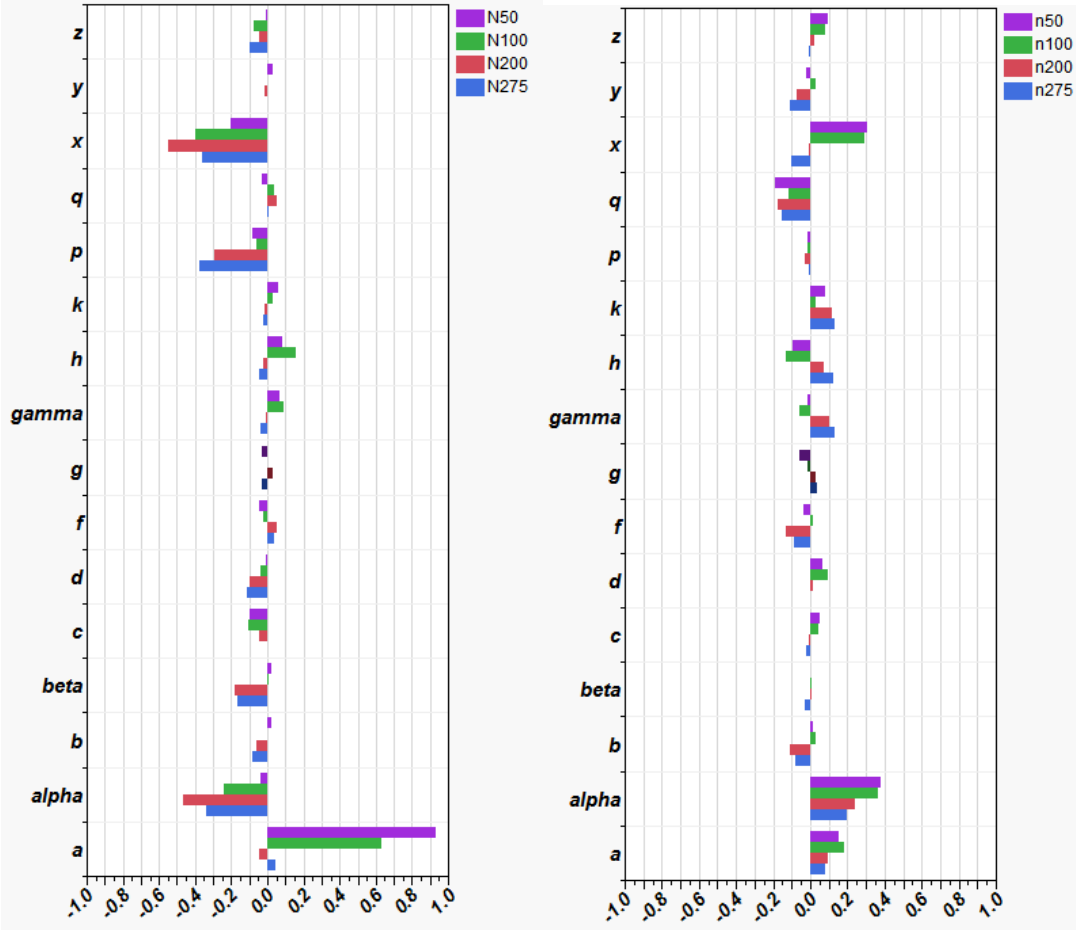

Figure 3.8: Lafleur ANOVA Sensitivity Results for Intact Objects (*N*) and Fragments (*n*)

In each plot, the length of the bar indicates the strength of the correlation between the coefficient, listed on the y-axis, and the parameter in question. Coefficients *a*, *α*, *p*, and *x* clearly have significantly greater impacts on the projection of the population of

intact objects. Similarly, a, α, and x play a significant role in the growth of the fragment population. Positive correlation indicates that values trend in the same direction. For example, larger values of the coefficient a result in increases in the populations of both N and n while p and x correlate to reductions in the population of intact objects. While α shows a negative correlation to intact object population, it also shows a positive correlation to the fragment population.

Several conclusions can be drawn about the nature of this model through these results. Coefficient a can be thought of as the average insertion rate of intact objects. While Lafleur attempts to capture the sinusoidal nature of launch markets, the low correlation of coefficients b, c, and d indicates that this may have little impact on the overall population projections. Coefficient a also has a positive correlation with fragment populations because, as more intact objects are inserted into orbit, there are more objects available for collisions, which is the most significant source of fragments.

The collision dynamic also explains the correlations of α and x. Coefficient α is the multiplier that indicates how many fragments result from an intact-fragment collision. Therefore, it has a significant positive correlation with the fragment population. Coefficient x is the collision probability term that indicates the likelihood of a collision between an intact object and a fragment. The greater the likelihood, the more intact objects will be lost to collisions and the more fragments will be created. The collision interaction is also seen in the negative correlation between the intact object population and the coefficients p and α. The longer a fragment spends in orbit, indicated by the orbital life coefficient of fragments, p, the more likely it will cause a collision with an

intact object. Likewise, the larger the fragment population grows, as driven by the coefficient α, the more likely the collisions will be.

Similar conclusions to those drawn about the sinusoidal launch rate can be drawn about the sinusoidal modeling of the natural decay life. Low correlation in both population sets with the g, h, k, and q coefficients indicates that the sinusoidal nature of the solar cycles has little impact on the population calculation. This correlation makes physical sense when considering the frequency of the solar cycles compared to the average natural orbit life of the objects being evaluated. The sun's activity fluctuates over an 11 year average cycle. The average natural orbital life of an object in LEO can range from tens of years to tens of thousands of years with an overall average life of approximately 7500 years for all of the objects in LEO. This means that objects in LEO will observe and be affected by many solar cycles during their orbital life, with the effects of those cycles being averaged out over time. This would support the observation that coefficients used to capture the solar cycle are of very little significance to the projected population. While the average residence time of fragments, indicated by p, does correlate with the intact object population, the sinusoidal function has very little impact on the results of the model.

Several things are clear from the evaluation of the Lafleur model. First, there is very clearly a strongly coupled nature between the intact population and the fragment population. This supports the general theory first applied by Farinella and Cordelli and later leveraged by Lafleur that the LEO orbiting object system must be modeled as a coupled set of differential equations. By comparing the results of the Lafleur model to the benchmark data sets, it is shown that, while the general approach may be valid, the

coefficients used by Lafleur must be refined. Third, the ANOVA revealed that refinement of the modeling technique and the coefficients themselves should focus on a sub-set of Lafleur's 16 coefficients. While launch rate, fragment residence time, and intact-fragment collision properties are strong drivers of the model results, the other coefficients play secondary and, in some cases, extremely minor roles in the model.

Based on these preliminary findings, a set of development goals was defined for the SLOOP model. The first goal was to develop a more accurate set of coefficients based on current and historical data available in the public domain. The second goal was to simplify the coefficient set where possible. This can be accomplished by eliminating the sinusoidal orbital life functions and replacing them with a simpler classification of the orbital life that will be discussed in a subsequent section. The structure of the other coefficients was retained. The third goal was to modify the model to support the evaluation of various post-mission disposal strategies. In Lafleur's version of the model, the orbital life term had to be adjusted outside of the model to account for a sub-set of the intact object population following the post-mission disposal guidelines for limiting orbital life. The SLOOP model is capable of explicitly evaluating post-mission disposal by segmenting the population into intact objects whose orbits naturally decay and those that have an accelerated orbital decay time to comply with the 25-year rule.

The final goal was to improve the fidelity of the model by taking the simplified, coupled ODE approach to modeling the population and applying it to orbital shells. Lafleur's model evaluated populations in a single LEO region stretching from 200 km to 2000 km altitude. By coding the SLOOP model in MATLAB, the general approach to modeling the problem can be applied to any volume of space and can be iteratively

executed to account for interactions between volumes. In this way, evaluations of shells of interest can be executed. The general simplified approach is retained, along with the resulting computational time benefits, but a better understanding of the LEO populations is achieved by adding spatial fidelity to the model. The remainder of this chapter is dedicated to explaining the general structure and execution of the SLOOP model. Chapter 4 provides an in depth discussion of the development of the SLOOP model coefficients.

3.3 The SLOOP Model Structure

The SLOOP model consists of a set of three ordinary differential equations (Equations 3.3, 3.4, and 3.5) coded in MATLAB. These three equations are based on the two-equation set developed by Lafleur, however, they split the population of intact objects into two sub-populations. The first sub-population, denoted as *NN*, is the set of intact objects whose orbits naturally decay due to atmospheric drag. The second sub-population, denoted as *ND*, are intact objects that are disposed of as part of PMD-compliant end of life operations. The third ODE tracks the population of fragments larger than 1 cm in diameter, denoted as *n*.

$$\frac{d(NN)}{dt} = (1-p)(a + b\,sin(ct+d)) + (NN)_{in} - \frac{(NN)}{f} - xn(NN) - 2y(NN)^2 \quad (3.3)$$

$$\frac{d(ND)}{dt} = (p)(a + b\,sin(ct+d)) - \frac{(ND)}{g} - xn(ND) - 2y(ND)^2 \quad (3.4)$$

$$\frac{dn}{dt} = \beta(a + b\,sin(ct+d)) + n_{in} - \frac{n}{h} + \alpha x\big(n(NN) + n(ND)\big) + \gamma y((NN)^2 + (ND)^2) - 2zn^2 \quad (3.5)$$

Table 3.1 provides the definitions of each coefficient in both the Lafleur model and the SLOOP model.

Table 3.1: Comparison of Coefficients for the Lafleur and SLOOP Models

Symbol	*Lafleur Model*	*SLOOP Model*
a	Launch Term 1: Vertical Shift	
b	Launch Term 2: Amplitude	
c	Launch Term 3: Period	
d	Launch Term 4: Phase Shift	
f	Intact Object Decay Rate: Vertical Shift	Intact object orbit decay time constant
g	Intact Object Decay Rate: Amplitude	PMD-compliant object time constant
h	Intact & Fragment Decay Rate: Period	Fragment orbit decay time constant
k	Intact & Fragment Decay Rate: Phase Shift	
x	Intact-Fragment collision likelihood	
y	Intact-Intact collision likelihood	
β	Fragments produced per satellite deployment	
p	Fragment Decay Rate: Vertical Shift	% of intact object that are PMD compliant
q	Fragment Object Decay Rate: Amplitude	
α	Fragments produced in Intact-Fragment collisions	
γ	Fragments produced in Intact-Intact collisions	
z	Fragment-Fragment collision likelihood	

Several of the coefficients and terms were retained from the original Lafleur model. However, some significant changes were made to accommodate the new modeling goals. First was the addition of a third equation. One of the drawbacks of the original Lafleur model was the difficult process for evaluating impacts from post-mission disposal compliance rates. This is a key area of investigation in the evaluation of collision likelihood and the efficacy of shifts in orbital debris policy. By sub-dividing the population of intact objects into those objects that decay naturally (*NN*) and those objects that are deorbited in compliance with PMD guidelines (*ND*), the PMD guidelines can be more readily evaluated. The equation for the *ND* population includes the same terms for determining collision probability but uses a different orbital life time constant than the *NN* population. This time constant is designed to reflect the significantly shorter orbit

lifetime that objects have if they are in compliance with PMD guidelines. Simply by adjusting the coefficient *p*, the split in the intact population between PMD-compliant objects and non-PMD-compliant objects can be adjusted to investigate sensitivities to compliance rates.

Another significant change is the simplification of the deorbit term in each of the three equations. As previously discussed, Lafleur tried to capture the solar cycle effects in the deorbit terms for his equations. The analysis of variance confirmed that this was an unnecessary complication to the model due to the long time scales of natural orbital life and the relatively short time scale of solar activity. The SLOOP model takes a simplified approach that more closely represents typical biological population models.[37] In simple biological models, the population growth is modeled as the sum of a birth rate and a death rate. Death rate can be reasonably approximated as the population divided by the life expectancy. Therefore, instead of a sinusoidal orbital decay rate, the SLOOP model divides the population by its orbit decay time constant.

The third significant change to the equations is the inclusion of an inheritance term for both the naturally decaying intact population (*NN*) and the fragment population (*n*). These two terms, denoted by the subscript "in", enable the subdivision of LEO into shells of interest. The fundamental concepts behind all of the other terms in the equations can be applied to any spatial volume of interest provided that the coefficients and initial populations are calculated appropriately to correspond to that volume. This means that whether the volume investigated is all of LEO or just the shell from 900 km to 1000 km altitude, the same equations will apply. The exception to this assertion is that there is now one additional source of objects in the populations. As an object's orbit decays, it

will eventually exit the volume of interest and enter the volume immediately below. If the volume of interest is LEO in general, this is equivalent to the object deorbiting. However, if we are investigating subsets of LEO, the object that deorbits the shell above enters the shell below. The inheritance terms account for these objects that enter on their natural journey from orbit to reentry.

The application of this inheritance term slightly alters the calculations for the coefficients that support the analysis. For layered models of LEO, the decay time constant is calculated as the time for an object's orbit to decay a distance equivalent to the differential altitude of the LEO subdivision. For the purposes of the analyses in this discussion, LEO was subdivided into 18 orbital shells, each 100 km in differential altitude. Therefore, the time constants are calculated based on the time it takes an object's orbit to decay 100 km. After that time, the object is assume to be inherited by the orbital shell below and the time constant for that orbital shell is then applied. This inheritance term is not applied to the PMD-compliant object population because the typical time constant for PMD-compliant objects is significantly lower than the natural time constant. To achieve PMD-compliance an object must deorbit within 25 years of its operational life. This is typically done propulsively where the resident time in any one shell is significantly shorter than the natural residence time and thus has a significantly reduced opportunity to interact with objects in that shell. Therefore, no inheritance term is necessary and the objects are assumed to be removed completely from LEO after their PMD-compliant life is over.

The execution of the model is performed via a MATLAB code that consists of two nested do-loops. The MATLAB code for the SLOOP model is provided in Appendix

B. Just as with the original Lafleur code, the SLOOP model evaluates the ODE through a difference method of integration with a time step size of 0.1 years. The matrix data management scheme of MATLAB is leveraged to maintain inputs, population values, and collision values over time for each shell of interest in the analysis. Each column of data corresponds to a different altitude shell and each row of data is a step in time. When the model is executed over LEO as a complete volume it is referred to as "bulk" mode and there is only a single column of data. When evaluated using distinct shells of interest it is referred to as "layered" mode and each column represents an individual layer in the overall volume of LEO.

Users initiate the code by creating four input matrices in MATLAB. The "c" matrix is the matrix of coefficient values. Each column holds the 16 coefficient values for a given shell of interest. These coefficient values are calculated through an Excel spreadsheet that takes average number of objects launched, additional number of small secondary payloads launched, post mission disposal rate, and maximum post mission disposal life limit and converts those user inputs into the matrix of coefficient values required for the SLOOP code. Those values are copied and pasted into the "c" matrix. Users also create an *NN*, *ND*, and *n* matrix and populate the first row of each matrix with the initial population values for the corresponding population sets. These three matrices are then used by the model to capture the population output values of each of these three populations.

The code itself consists of two main do-loops. The internal loop calculates values across each individual shell of interest for a given time step, moving across the data matrix columns from left to right. The number of iterations through the inner do-loop is

determined by the number of shells of interest, which is read in based on the size of the coefficient matrix "c". Once the inner loop has completed a set of iterations, the time is increased by the time step and the inner loop is completed again. The inheritance term is taken in from the column of data directly to the right, representing the shell of interest directly above the shell being calculated. In this way, the dual iteration loop is working its way across and down the matrix, incrementally calculating all of the parameters in the three differential equations at each time step. When the outer do-loop reaches the user-specified end time for the analysis, the model ends its run. Typical model runs with 18 shells of interest (100 km altitude increments) execute in less than 2 seconds of run time.

Within each iteration loop several other values are calculated. During the execution of the inner do-loop, a value for the number of objects greater than 10 cm is calculated to facilitate comparisons with the LEGEND benchmark data. A cumulative number of collisions is also calculated. The xnN and yN^2 terms in the model equations are actually the number of collisions of each type expected in a given year. By multiplying them by the time step and adding them on each iteration of the outer loop, a cumulative number of collisions is calculated. This value is the true value of interest in a population model because satellite operators are primarily concerned about collisions that are the consequence of over-population. While the SLOOP model cannot pinpoint the time and place of a collision like some of the higher fidelity codes can, the cumulative number of collisions gives insight into the relative risk posture of the various scenarios investigated with the tool.

Values such as the cumulative collisions and population totals are captured for each shell of interest. During the execution of the outer iteration loop, before the next

time step is applied, the sum of these values is calculated across all shells of interest to calculate a total number for each value in all of LEO. This allows users to quantify the effects of the scenarios investigated in terms of total impact to LEO, the way that these types of results are typically reported, while taking advantage of the added fidelity of a layered analysis. An example of the utility of this capability is provided in Chapter 5. The benchmark data from LEGEND and MASTER2009 are also calculated for each time step during the outer loop execution as well as an error function comparing the model population results to these benchmark values. This capability is useful in calibrating and evaluating the baseline coefficient values and in comparing alternative scenario results to the currently published community projections. A flow chart of the general code structure is provided in Figure 3.9. Chapter 4 provides a detailed discussion of the development of the coefficient values used to align with the benchmark data.

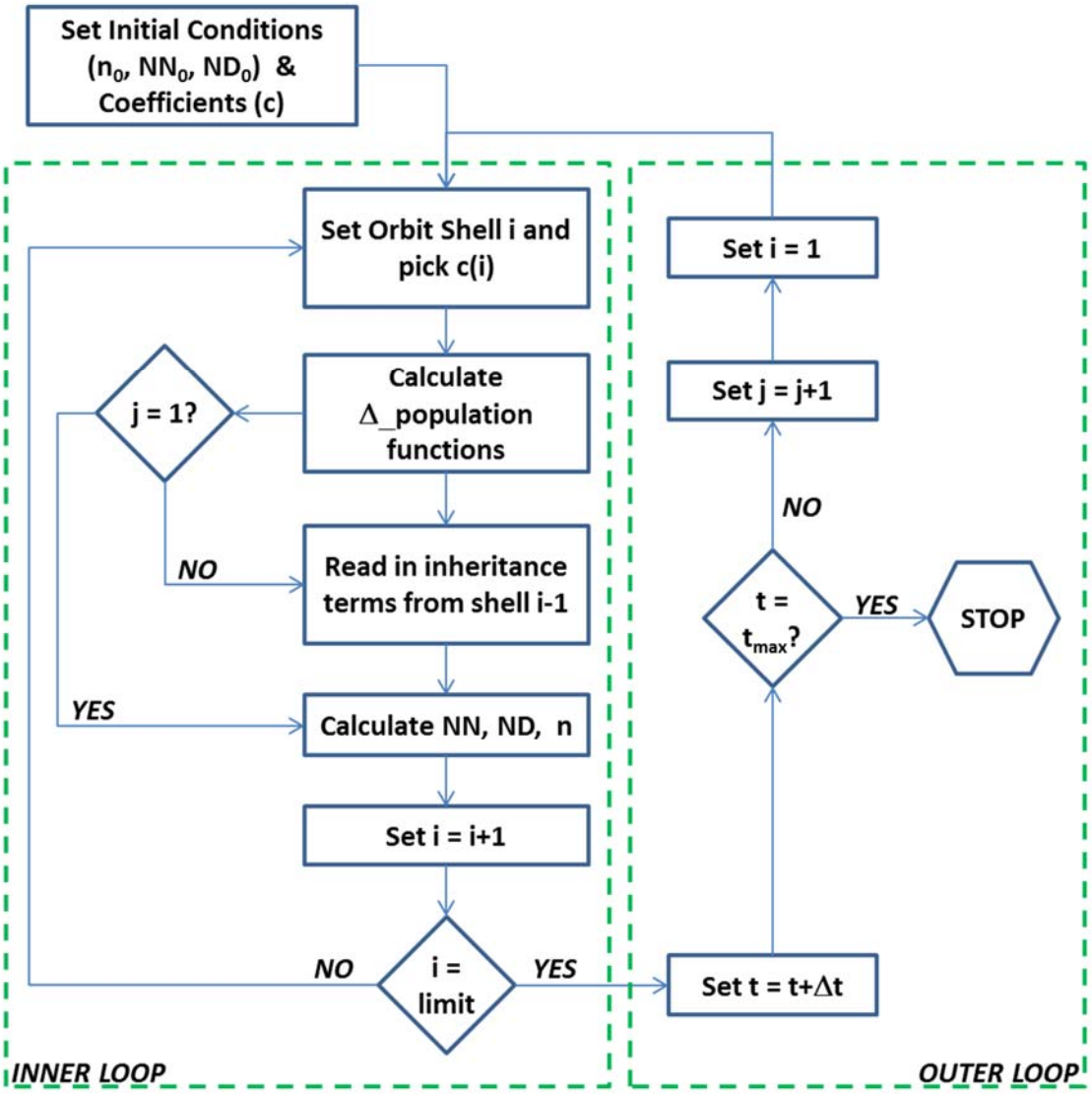

Figure 3.9: SLOOP Model Flow Chart

CHAPTER 4:

CALCULATION OF COEFFICIENT VALUES FOR THE SLOOP MODEL

The key to executing useful and accurate analysis with the SLOOP model is the coefficients used to characterize the physical environment and characteristics of orbital objects. Executing Lafleur's model and comparing it to the benchmark data revealed a significant error when compared to the higher fidelity codes. The value of a simplified approach to population modeling is that it provides a reasonably accurate representation of the data that would be produced by a higher fidelity code while being more user-friendly and executing in a fraction of the time. If the simplified modeling approach produces results that do not match the higher fidelity codes, the analysis is of little value. This chapter outlines the calculation of each of the coefficients used in the SLOOP model including the data used to perform the calculations.

4.1 Combining Data Sources

A significant amount of physical data is required to calculate the coefficients for the SLOOP model. Over the course of this investigation, several data sources were identified but no one data source provided all of the information necessary to support the SLOOP analyses. The work done combining data sources for this dissertation is being converted into a relational database known as the Space Asset Management Database, or SAM-D, at NASA's Marshall Space Flight Center. This combinatory database will be

available to the community at large to support analyses related to satellite populations, including those performed by the SLOOP model. A brief summary of each of the six major data sources is provided in the following sections.

4.1.1 The Joint Space Operations Center Catalog

The Joint Space Operations Center (JSpOC) maintains the most up-to-date catalog of tracked objects in orbit around Earth. Each tracked object is provided a NORAD number, a unique sequential number that is given after the first sighting of the object by ground-based tracking resources. NORAD, or the North American Air Defense Command, was the predecessor to the JSpOC. The catalog maintains a two-line element (TLE) data set for each object in orbit which includes general information about the launch date and origin of the object as well as orbital parameters that can be used to determine the object's position in space. The current JSpOC catalog is maintained at two levels. The unclassified catalog is publically available through several free web sites including Space-Track.org.[14] The classified catalog is only available to a limited number of users and contains positional data on classified orbital assets such as those belonging to the Department of Defense or the National Reconnaissance Office. There are currently over 14,800 entries in the publically available JSpOC catalog, covering all regions of space around Earth. Of these, over 11,000 objects reside in LEO.

Using standard orbital mechanics equations, the TLE data can be converted into several useful orbital parameters. The TLE provides the inclination, eccentricity, and mean motion of the object's orbit. The mean motion can be used to calculate the semi-major axis of the orbit. The semi-major axis can be used in conjunction with the

eccentricity to calculate the perigee and apogee altitudes of the orbit. These values can also be used to calculate the object's velocity at any point along its orbit.

The primary data used from the JSpOC catalog is the derived perigee, apogee, and velocity. A survey of the eccentricity of the intact objects within the catalog shows that approximately 89% of the objects are in obits where there is less than 100 km difference between perigee and apogee. Figure 4.1 provides a histogram of this data, with the darker bars representing objects with eccentricities greater than 0.0075. The velocity and altitude of the orbit of an object are used throughout the calculations for the various SLOOP model coefficients and many of these calculations are simplified by assuming a circular orbit. Additionally, the layered version of the SLOOP model does not account for eccentric orbits that allow objects to cross between shells of interest. The eccentricity data derived from the JSpOC catalog shows that an assumption of circular orbits will only inaccurately represent 11% of the current population. Therefore, all objects are characterized by their equivalent circular orbit altitude (ECA), or the semi-major axis of the orbit minus the radius of the Earth, and it is this altitude which is used to bin the objects into orbital shells of interest, and to calculate orbital parameters such as velocity and orbital life.

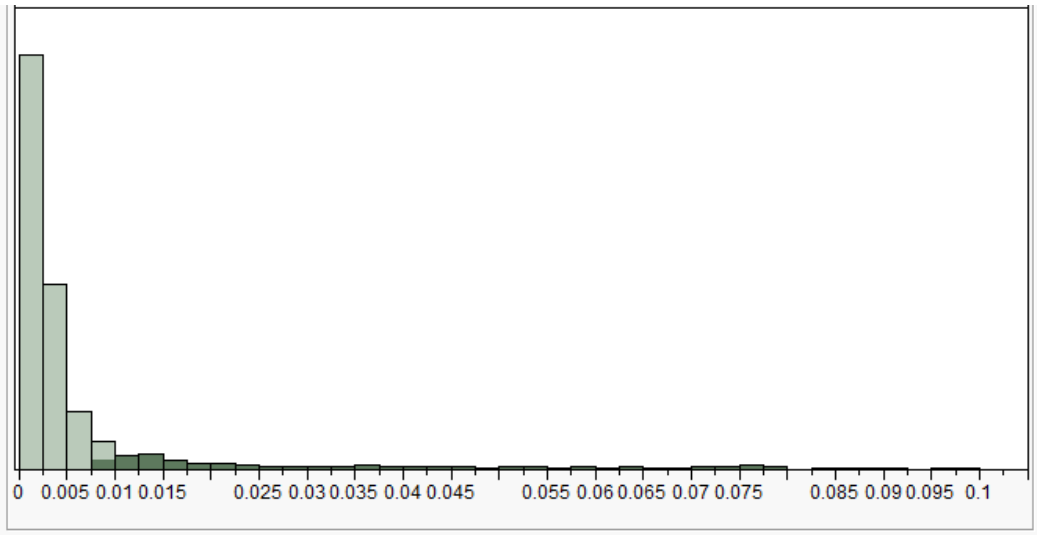

Figure 4.1: Histogram of Orbit Eccentricity of Cataloged LEO Objects

4.1.2 The SATCAT Database

The JSpOC catalog only provides a small set of the overall data required for coefficient determination. The Satellite Catalog (SATCAT) Database [24] provides a significant amount of supplemental information that is useful in the calculation of SLOOP coefficients. The SATCAT database is a historical database of Earth satellite information maintained by the Center for Space Standards and Innovation (CSSI) at Analytical Graphics, Inc., makers of Satellite Tool Kit (STK).[38] Historical data about orbital objects found in the SATCAT database include launch site, country of origin, and operational status. These items support historical analysis of metadata concerning satellite ownership that can be useful in policy analyses.

For the purposes of developing a set of coefficients for the SLOOP model, relevant SATCAT items include the radar cross section of the orbital assets and their launch date. One unique aspect of the SATCAT database is that it holds a record of all assets launched since the beginning of space flight, over 39,000 entries. This information

becomes extremely useful in establishing historical launch rates and separates the SATCAT database from the JSpOC catalog, the latter of which only keeps a running record of objects currently in orbit.

The radar cross sectional area is used in orbit lifetime calculations. Orbital decay is dependent on the drag force applied to a spacecraft by the very thin but still existent atmosphere. By coupling the area and mass of a satellite with a sufficiently accurate atmospheric density model, the orbital lifetime can be calculated. The tumbling frontal area is typically used in these calculations as the orientation of disabled satellites and rocket bodies is rarely maintained. The tumbling frontal area of a three-dimensional solid was shown by Cauchy to be 0.25 times the surface area of the solid.[39] In 2012, Zachary Slepian published a paper outlining the calculation of average projected area for objects of several dimensions. He showed that the average projected area of a two-dimensional surface is 0.318 of the total surface area.[39] For the purpose of calculating the average projected area of a satellite, the three-dimensional calculation can be coupled with the two-dimensional calculation for deployed surfaces such as antenna and solar arrays.

Using this information, the average projected area can be calculated for a few known satellites. The Iridium satellites consist of a rectangular main body and two deployed solar arrays. The area of the main body of the satellite is 8.09 m^2 with an average projected area of 2.02 m^2. The solar arrays have a total surface area of 5.76 m^2 with an average projected area of 1.83 m^2. The total average projected area is calculated as 3.85 m^2 as compared to the SATCAT radar cross section of 3.87 m^2. The Tiros satellite is a cylindrical body satellite with an approximate height of 0.5 m and a diameter

of 1.1 m. The total surface area of the satellite is 3.4 m^2 with an average projected area of 0.85 m^2. Comparing this with the SATCAT radar cross section of 0.84 m^2, it can be seen that the radar cross section of the satellites in the SATCAT database can be used as a replacement for the average projected area of the tumbling spacecraft. The Iridium and Tiros satellites are shown in Figure 4.2. This data from the SATCAT database is used to support the orbital life calculations for the objects in LEO.

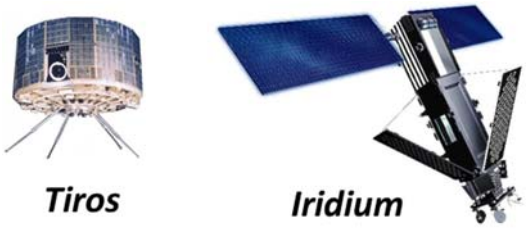

Figure 4.2: Tiros and Iridium Satellites

4.1.3 The Union of Concerned Scientists Database

Union of Concerned Scientists maintains a spreadsheet database of operational satellites as part of their effort to support secure space.[40] According to their web site, the UCS operates with the mission of "putting rigorous, independent science to work to solve our planet's most pressing problems." As an organization, they support research and advocacy in many areas including space security. The UCS database was created "as a research tool that collects open-source information on operational satellites and presents it in a format that is easily manipulated for research and analysis". Updated quarterly, the UCS Satellite Database provides important reference material and metadata about satellites in the JSpOC catalog and is used in conjunction with the other resources mentioned to provide a complete database of tracked objects.

4.1.4 The Satellite Tool Kit Database and Other Spacecraft References

AGI's STK software provides a full suite of satellite simulation tools for use in mission planning, operations analysis, and mission execution.[38] Among the many features of STK is the ability to perform conjunction analysis, evaluating the likelihood of two objects colliding in space. This software is used extensively among government and commercial operators of space assets. STK also has the ability to calculate orbital life and maintains a catalog of many of the objects currently in orbit. This orbit life calculation requires some knowledge of the mass of the spacecraft and STK maintains a small database of mass values associated with a subset of objects from the JSpOC catalog. Mass data for the objects in space is the most difficult parameter to find as no one database maintains a complete set of this information. The STK database provides the mass data for 1430 of the 2643 intact objects in LEO. Web resources such as Gunter's Space Page[41], Encyclopedia Astronautica[42], and the NASA Space Science Data Center (NSSDC)[43] are also excellent public sources of mass data for satellites. Over time, through many searches of these resources, the mass data for another 959 intact objects was gathered.

4.1.5 MASTER2009

The European Space Agency's MASTER model was designed to provide "a realistic description of the natural and the man-made particulate environment of the Earth."[34] MASTER2009 is a semi-deterministic model used to classify future orbital environmental conditions based on a myriad of historical data and external models. MASTER2009 characterizes a wide range of debris sources, from explosion and collision fragments to solid rocket motor slag particles, and historical debris sources such as NaK

particles from defunct Russian nuclear reactors. Using a differential volume approach, the model combines these various debris sources and quantifies the spatial density of regions of interest as well as debris flux on a user specified spacecraft area. The user can specify a lower and upper threshold for fragment size as well as the classes of fragments to be considered.

MASTER2009 employs several models for quantifying the physical characteristics of fragments produced by collisions and explosions. Historical data related to past fragmentation events helps the model determine the number of collisions and explosions that can be expected over the time and space investigated. Data from hypervelocity impact experiments supplies a general understanding of the distribution of size, mass, and velocity of the fragments produced in these fragmentation events. As the simulation moves forward in time, these characteristics are folded into the population being simulated and their impacts on future states of the environment are accounted for.

MASTER2009 provides a wide range of output values that can be used to approximate the growth of the LEO fragment environment and the statistical distributions of the physical characteristics of those fragments. For the purposes of generating coefficients for the SLOOP model, the analysis was focused on the resulting distributions of mass, velocity, and quantity of fragments with a size greater than 1 cm in diameter. The fragment population in general is extremely large when considering particles of this size. While some accuracy is sacrificed by using mean values for these physical characteristics, the overall use of these statistical distributions is accurate enough to provide a general probability-based view of the fragment environment.

While there are many fragments classified in the JSpOC catalog as debris, there are very little physical data available about these fragments. Based on a general knowledge of the catalog, it is known that the lower threshold for the size of these fragments is 10 cm but very little additional information is provided. The population of debris fragments in the catalog is orders of magnitude smaller than the overall population of fragments provided by the MASTER model. Therefore, the general trends in physical characteristic, including size and mass, were applied to the cataloged objects and the two data sources were merged to provide a baseline for the current population of fragments in LEO. This specific data is provided in the respective coefficient calculation sections later in this document.

4.2 Calculating Coefficients

The three equations that provide the backbone of the SLOOP model (Equations 3.3, 3.4, and 3.5) depend on the accurate calculation of 14 coefficient values (see Table 3.1). These coefficients combine various physical characteristics of the orbital objects to represent collision probabilities, fragmentation characteristics, and orbital life. While the general approach to Lafleur's two-equation model appears reasonable, the calculation of coefficients appears to be one reason why the results from his model do not align with the current benchmark data. Surveying the various data sources described in previous sections, a new set of coefficient values has been determined to align the SLOOP model results with the benchmarks. The following sections describe in detail the physical origins and calculations for each coefficient and provide insight into the specific data gathered and applied to each calculation, both for the bulk representation of LEO and the layered.

Two general comments apply across all calculations. The first relates to the assumed orbital altitude. The vast majority of the intact objects in LEO are in circular or near circular orbits. While 11% of the objects are in elliptical orbits, many of the coefficient calculations are greatly simplified by assuming that objects are in circular orbits. Therefore, the Equivalent Circular Altitude (ECA) has been used for all objects. This value is the difference between the orbit's semi-major axis and the radius of the Earth. The ECA is a very accurate representation of most objects in LEO and is an accurate means of performing calculations for characteristics such as average orbital velocity and orbit life. In order to maintain consistency across all calculations, the ECA was used in each aspect of the coefficient development where altitude was required including the generation of initial population values for the layered model.

The second general comment is that, when discussing the layered approach to modeling LEO, the layers have been set at 100 km intervals from 200 km to 2000 km altitude. In the various graphs and plots provided, the bins are characterized by the altitude of their lower boundary. For example, a 2 represents the orbital shell from 200 km to 300 km altitude while an 11 represents the shell from 1100 km to 1200 km. Higher fidelity models can be developed simply by decomposing the available data by narrower bands of altitude but this must be balanced with the time it takes to classify all of the coefficients for each shell. For the initial runs of the model, 100 km was selected to provide sufficient granularity without overburdening the process of developing the coefficients.

4.2.1 The Launch Term

The launch rate, or more specifically the object insertion rate, is a key term in determining the population growth over time. Launching objects into space is the only source of new objects in the population model. This periodic influx of satellites and rocket bodies drives the fragment production rate by increasing the large object population, thus increasing the odds of the collisions that feed the fragment population. The object insertion rate has been generally modeled as a sinusoidal function to try to capture the typical fluctuation in launches over time. The SLOOP model continues this approach and uses historical launch data from the SATCAT database to develop the coefficients in the launch term represented by

$$(a + b\,sin(ct + d)). \tag{4.1}$$

The coefficient a essentially represents the average number of launched objects while the coefficients b, c, and d supplement that average with a sinusoidal surge and regression function that captures the cyclical nature of the launch market.

A survey of market analyses related to the space launch industry indicates that, while there is steady financial growth in the industry, analysts expect that the number of launches will remain true to the recent historical trends. Launches are driven by the satellite market, which consists of scientific, defense, and commercial sectors. All of these sectors expect to see business-as-usual operations for the foreseeable future.

One significant aspect of the business as usual model for LEO satellites is the idea of satellite replacements. The Iridium constellation of communications satellites consists of 72 satellites deployed at 775 km altitude.[44] These satellites service a wide array of communications customers including maritime, military, and civilian end users.

Originally launched between 1997 and 1998, these satellites are in need of replacement. Between 2014 and 2017, the Iridium NEXT constellation will be launched to replace the original fleet of satellites.[44] This trend should continue over an approximately 20 year cycle. Similar constellations exist in other orbits that must also be replenished and replaced as the satellites age. This replacement cycle is not unique to satellite constellations but is also required for Earth observing scientific satellites. While this is generally considered business-as-usual operations for satellite operators, it is the primary driver behind the cyclical nature of LEO satellite launches.

One potentially significant exception to the business-as-usual projections for LEO satellites is the emergence of CubeSats. A CubeSat is a fully operational satellite that is a cube 10 cm on a side. The 10 cm cubes, called units or "U"s within the industry, can be combined to form various sizes of satellites from 1U to 6U or larger. Figure 4.3 provides an example of CubeSat scaling, showing four different configurations of CubeSats ranging from 1U to 3U.

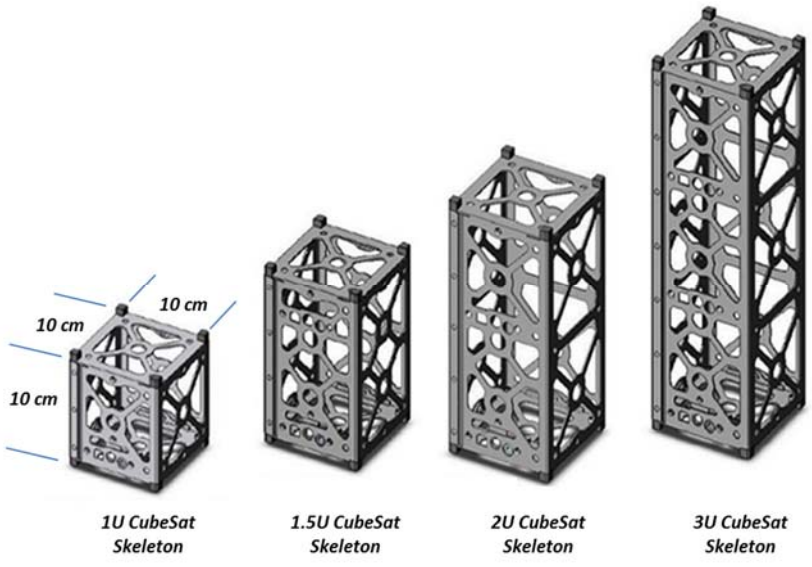

Figure 4.3: CubeSat Configurations [45]

The small nature of these satellites provides two significant advantages over traditional satellites. First, the CubeSats are extremely low cost compared to full sized LEO satellites. According to the Satellite Industry Association, a 1U CubeSat kit can be purchased for as low as $13,000 while a 6U configuration can cost $30,000.[20] This cost, coupled with the miniaturization of cameras and other sensor payloads, opens an extremely wide-reaching market that was previously much more difficult to enter due to the high initial start-up cost. Universities have leveraged this low cost into academics where students can learn satellite design and operations while also having the opportunity to fabricate and fly real satellites in space. NASA provides launch opportunities for these university payloads through their successful CubeSat Launch Initiative (CSLI) which has launched 44 CubeSats since 2011.[46] The low initial start-up cost has also shown benefits in the commercial sector. One prime example is the relatively new start-up company, Planet Labs. Started out of a Cupertino, CA garage in 2012, Planet Labs is developing a constellation of 3U CubeSats they call “Doves” that provide 3-5 meter resolution, real-time observations of Earth.[47] Their goal is to provide real-time constant observation of the entire Earth as open source data to anyone who would like to use it. CubeSats enable an entirely new sector of the space industry and many industry experts foresee a surge in CubeSat flights in the coming years.

The second significant advantage of CubeSats is related to the other large financial limiter in the satellite industry; launch costs. Launching satellites into space is a very expensive undertaking. However, with small physical size and low mass, CubeSats present an opportunity to fly as secondary payloads. Launch providers, such as the United Launch Alliance (ULA), have developed special payload adapters for their launch

vehicles that support the launch and deployment of secondary payloads, including CubeSats. On any given launch, the launch vehicle typically has some performance margin, meaning that the primary satellite weighs a little less than what the launch vehicle can send into orbit. This margin in launch capability presents a potential business opportunity for the launch provider if they can find a way to fill that space. ULA has worked with Moog to develop the ESPA ring, a specially designed payload adapter that supports the primary payload on the top but also provides deployment mechanisms for a range of payloads from SmallSats (30 to 50 cm on a side) to CubeSats.[48,49] Owners of smaller secondary payloads can fly on these launches at a significantly reduced price that makes the launch affordable. This, in turn, creates a high-profit secondary business model for the launch provider. An example of the SpaceX Falcon launch vehicle version of this capability is shown in Figure 4.4.[50]

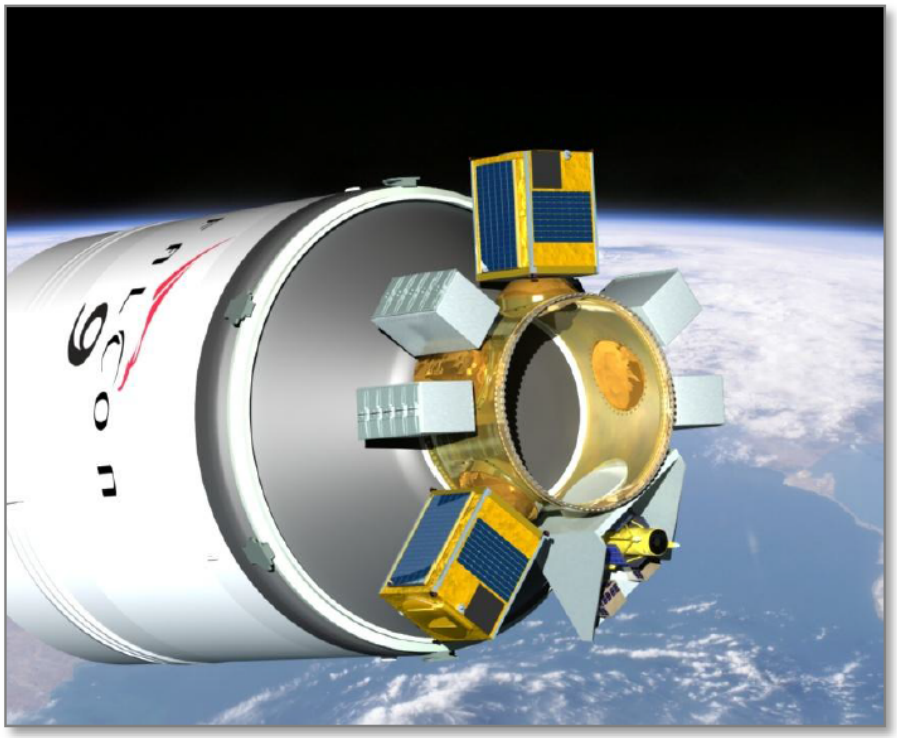

Figure 4.4: SpaceX Secondary Payload Concept [50]

These two advantages of the SmallSat market represent potentially significant ramifications to the world of satellite population modeling and collision prediction. SmallSats and CubeSats can be co-manifested as secondary payloads on many launches. This shifts the paradigm of launches contributing to intact object populations from one or two satellites per launch to tens of satellites per launch. From a population modeling standpoint, this induces a significantly more rapid increase in population over time. In biological terms, this would be equivalent to human reproduction producing one baby or the occasional set of twins to suddenly resulting in a steady rate of octuplets. Examples of the multi-manifested launch have already been seen. As previously mentioned, over a two day period in late November of 2013, two launches occurred launching a total of 62 satellites into LEO.[25,26] This number is equal to the average number of satellites launched annually in each of the previous six years. This population explosion has the potential to accelerate the *Kessler Syndrome* and represents a wild card in the business of attempting to predict future launch rates.

Population growth can lead to an increase in the number of collisions but this growth rate is also a function of the orbits where these new satellites are deployed. First, there is the issue of orbital life. Many of these CubeSats do not currently have the ability to actively deorbit at the end of their mission. This leaves their compliance with the 25-year rule for post-mission disposal entirely dependent on the natural decay rate of their orbits. The 62 satellites launched in late 2013 were all placed in orbits lower than 500 km, ensuring that they would naturally de-orbit within just a few years. However, as large launch providers such as ULA begin to offer ride-share options, there will be a potential increase in the number of CubeSats launched to higher and more populated

orbits because these are the destinations of choice for ULA's primary customers. This will result in significantly longer residence times for these CubeSats and further compound the collision risk problem because they are placed into orbits with higher populations.

These two major issues present a unique challenge for population models. The SLOOP model was developed specifically with these challenges in mind. First, the user interface that generates the coefficients used in the SLOOP model provides a place for the user to specify the number of small satellites they expect to be launched in addition to the business-as-usual primary payloads. Therefore, the user can specify not only the average number of primary payload launches in the "*a*" coefficient of Equation 4.1, but also the number of secondary payloads they expect to see launched annually. The coefficient generator combines the user's primary payload and secondary payload count inputs and makes the sum total of those two values the "*a*" coefficient in the launch term. The *b*, *c*, and *d* coefficients are built from historical data and cannot be edited from the user interface, therefore maintaining the cyclical fluctuations in the primary payload launch market that the industry expects will continue.

By providing a layered approach to LEO population analysis, the SLOOP model also captures the varied impacts of significant increases in secondary payload launches to specific regions of LEO. The risk presented by this influx of new satellites into orbits of higher population can be evaluated relative to that same influx to orbits of lower population. This increase in spatial fidelity can help determine the impacts of the CubeSat market more specifically.

To determine the launch rate coefficients, historical launch data was pulled from the SATCAT database. The launch data from 1991 to 2011 was extracted and the number of objects launched annually over that time span was determined. This 20 year time span represents typical day-to-day operations expected over the years to come. During this time frame, new nations have joined the LEO satellite community and the larger satellite owners found a steady state operating cadence. This time span also includes the initial fielding of both the Iridium and Orbcomm satellite constellations meaning that any functional representation of this data would include the periodic replenishment and replacement of these assets. Finally, the cutoff date of 2012 was chosen in order to match the assumptions used to run the models that produced the benchmark data being used as a comparison point. This is significant because it does not include the two multi-manifested CubeSat launches of 2013. This makes this data set a better representation of the general business-as-usual operating scenario and leaves the CubeSat market surge entirely up to the SLOOP model user to take into account through user inputs.

Using a simple regression analysis, the coefficients were found that provided the highest coefficient of determination, or R^2. Regression analysis determines the relative goodness of fit of a function that is intended to represent a set of discrete data points. The coefficient of determination relates the variance of the data itself to the error of the function that represents the data. The total sum of squares of the data, y_i, proportional to the data variance, $\bar{y}$, and is calculated using

$$SS_{tot} = \sum_i (y_i - \bar{y})^2. \quad (4.2)$$

The residual sum of squares classifies the delta between the data points and the results of the function being used to represent that data, f_i , and is calculated using

$$SS_{res} = \sum_i (y_i - f_i)^2. \quad (4.3)$$

The coefficient of determination is then calculated by

$$R^2 = 1 - \frac{SS_{res}}{SS_{tot}}. \quad (4.4)$$

A coefficient of determination value of 1 indicates a perfect fit of the data and the goal in fitting equations to data is to drive the R^2 value as close to 1 as possible. This is difficult to achieve if there is significant variance in the source data and is also difficult to do with data sets that have extreme outlier points. However, if the goal of the fit is to provide a general representation of the data, averaged over time, a visual check of the representative function along with a positive coefficient of determination value near 0.5 indicates a generally acceptable fit. This approach and general rule of thumb were used in the determination of both the bulk and layered launch rate coefficients.

4.2.1.1 Launch Rate Coefficients: Layered LEO Representation

The number of objects launched into LEO each year between 1991 and 2011 was found using the SATCAT database. This data was then subdivided by Equivalent Circular Altitude (ECA) of each object's orbit to provide a launch rate for each shell of interest in the SLOOP layered LEO model. As previously stated, the ECA is the circular orbit altitude equivalent to the semi-major axis of the orbit, thus reducing elliptical orbits to a simpler circular representation for the purposes of calculations. A complete set of data plots is provided in the Figure 4.5. Inspection of these plots reveals that while some of these data sets appear sinusoidal in nature, several have very flat and steady launch rates over the 20 year period in question. This set of plots also reveals that some orbital

shells are more popular than others. Relatively few satellites reside in the region of LEO above 1000 km with the exception of the band from 1400 km to 1500 km. The 1400 km shell is home to the Globalstar satellite constellation. Similarly, the Iridium and Orbcomm constellations reside between 700 and 800 km altitude and are responsible for the sharp surge in launches to the 700 km shell in the period from 1997 to 1999.

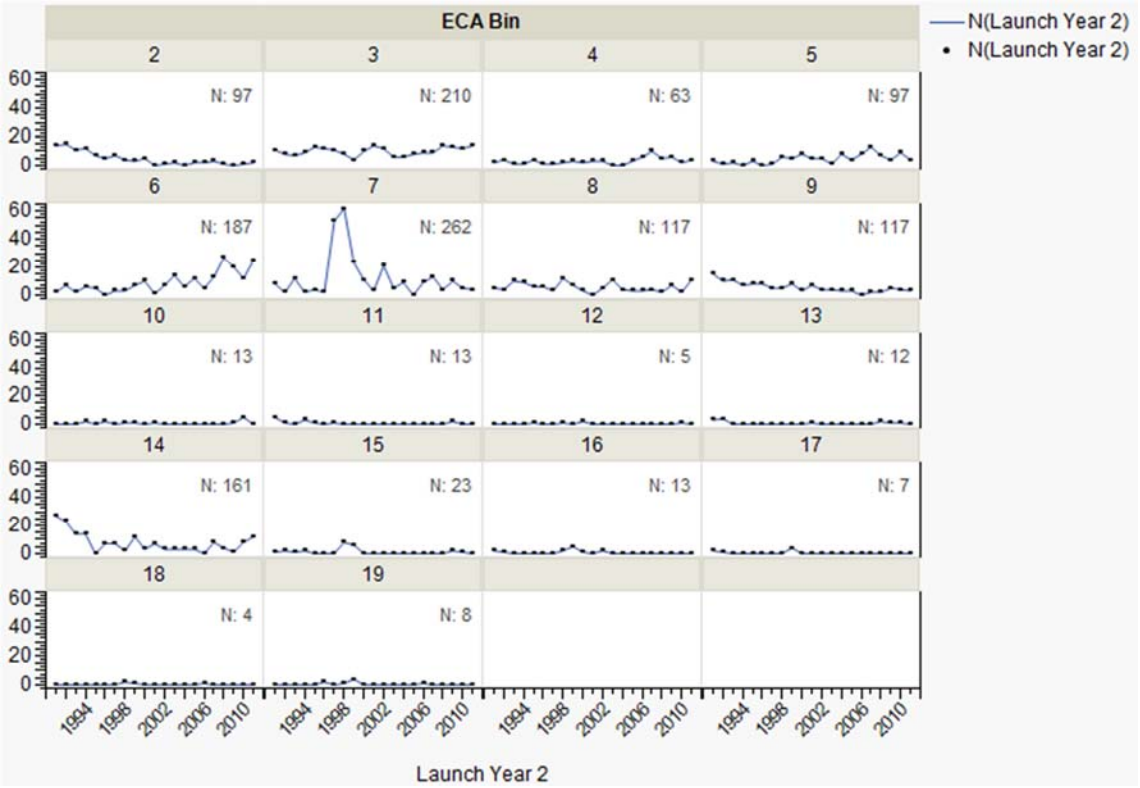

Figure 4.5: Historical Launch Data by Equivalent Circular Altitude Bin

For orbital shells that exhibit a flat launch rate over time, the *b*, *c*, and *d* coefficients were set to 0, leaving only the "*a*" coefficient to represent the average number of objects launched per year. These curve fits do not produce a value for the coefficient of determination. The coefficients for the launch term for each orbital shell are provided in the Table 4.1 along with the coefficient of determination for those orbits that are represented by a sinusoidal function. The negative coefficient of determination

values in the 300 km and 700 km shells are the result of significant outlier data. The curve fit was made to reflect the total number of objects delivered over the span of time reviewed while maintaining the general sinusoidal shape essentially smoothing the data set to an averaged sine function.

Table 4.1: Launch Rate Coefficients by ECA Bin

	Coefficient Values				
Orbital Shell	a	b	c	d	R^2
200-300	7	6	-0	1.3	0.839
300-400	10	3	0.9	-2	-0.192
400-500	3.02	1.65	0.7	-4	0.239
500-600	4.43	-2.87	0.2	0.8	0.443
600-700	13	8.52	0.2	-3	0.577
700-800	20	14	0.3	-0	-0.167
800-900	5.7	2.85	1.4	2.4	0.367
900-1000	7	6	-0	1.3	0.673
1000-1100	0.62	0	0	0	
1100-1200	0.62	0	0	0	
1200-1300	0.24	0	0	0	
1300-1400	0.57	0	0	0	
1400-1500	17	13.3	-0	0.5	0.567
1500-1600	0.38	0	0	0	
1600-1700	0.33	0	0	0	
1700-1800	0.19	0	0	0	
1800-1900	0.14	0	0	0	
1900-2000	0.19	0	0	0	

4.2.1.2 Launch Rate Coefficients: Bulk LEO Representation

Two approaches were used to determine the coefficients for the bulk representation of LEO. First, the general number of objects launched into LEO each year between 1991 and 2011 was found using the SATCAT database. A sinusoidal function was developed to fit the data and a coefficient of determination was calculated. The data and representative function are shown in Figure 4.6. This approach to fitting the data

resulted in a 0.229 coefficient of determination. At this level, it is difficult to capture the outlier points that represent the Iridium, Globalstar and Orbcomm constellation launches in the late 1990s, throwing off the fit of this function.

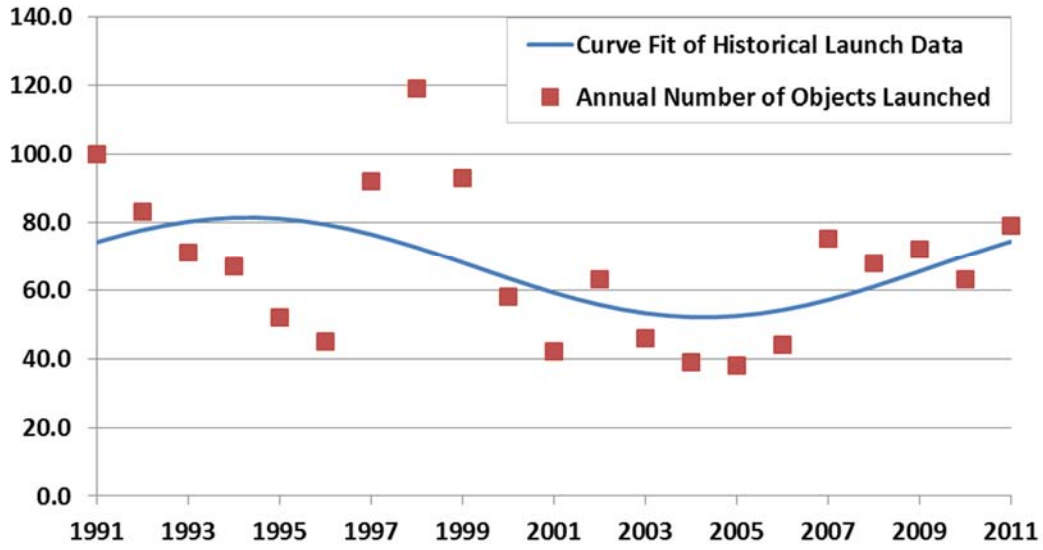

Figure 4.6: Bulk Mode Historical Launch Data and Curve Fit Using Actual Historical Launch Data

By subdividing LEO, a better fit can be determined for each individual orbital shell. While the difficulty in capturing the surge launches of constellations is still a challenge, it is applied only to those orbital shells in question, while the other shells can achieve better correlation. This can be seen in Table 4.1. Therefore, by using the layered models to calculate equivalent launches per year, summing those launches across all layers, and developing a bulk LEO model from those values, a better fit can be achieved. This also ensures that the launch rate used in the bulk model will better represent the layered model, thus carrying the higher fidelity of the layered model into the bulk model. This approach resulted in a coefficient of determination of 0.992. The resulting bulk model launch rate coefficients are provided in Table 4.2. The associated data and representative function are shown in Figure 4.7.

Table 4.2: Bulk Model Launch Coefficients

Coefficient Values				
a	b	c	d	R^2
70.9	22.3	0.3	0.4	0.992

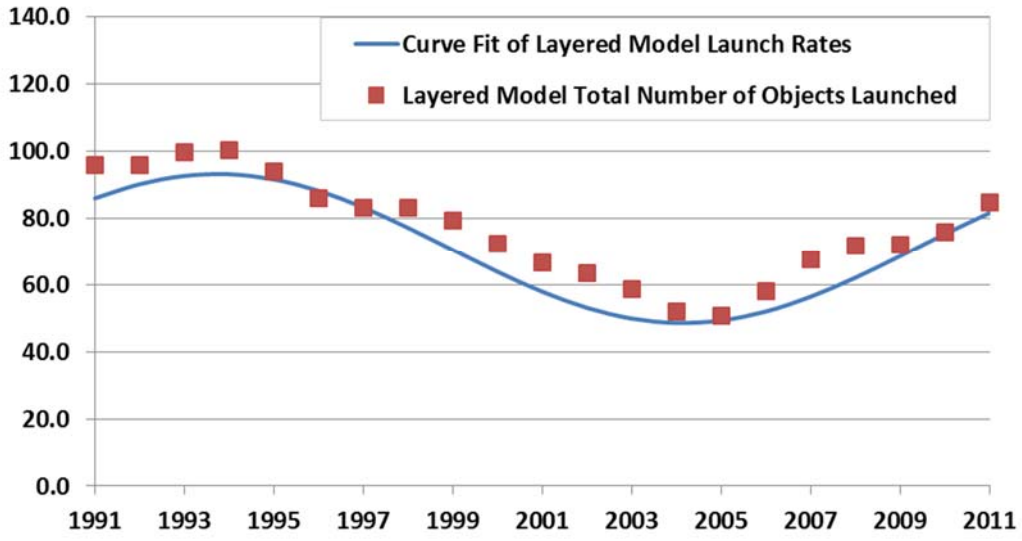

Figure 4.7: Historical Launch Curve Fit Using Layered Model Representations

4.2.2 The Orbit Decay Terms

In each of the three equations in the SLOOP model, the orbit decay coefficients, *f*, *g*, and *h*, tell the model how long an object will remain resident in the volume of interest. This combines the operational life of the object with the post-mission life for a total residence time. The longer an object remains in orbit, the more likely it is that it will collide with another object. In a bulk representation of LEO, orbit decay time is

equivalent to the time it takes for the object to de-orbit. An object will reside in LEO until its orbit decays, either naturally due to drag forces or in combination with propulsive maneuvers. As discussed previously, in the layered representation of LEO, the orbit decay term determines how long an object remains in the shell of interest before passing into the shell below it. This drives the inheritance terms that are the key to the layered representation of LEO in the SLOOP model.

In all cases, the orbit decay term is simply the total number of objects in a layer divided by the expected lifetime of an object in that population. This is the same way that life expectancy is accounted for in biological population models. The difference in this application is that the life expectancy can be calculated for any given object if the mass, area, and atmospheric conditions are known. Therefore a general life-expectancy for a subset of the population with similar physical characteristics can be determined and, if enough data points are available, these life-expectances can be averaged and applied to any future members of that population. This is the general method used to determine the orbit decay coefficients for each of the three populations tracked by the SLOOP model.

The model assumes a standard satellite lifetime and then adds the orbit decay time constant to that value. For the objects that are compliant with the post-mission disposal guidelines, the orbit decay time constant (g) is set as a fixed value. This value is determined by user input and the user has the ability to use either the current standard best practice value of 25 years or they can use the SLOOP model to investigate changes in that standard best practice. This population is tracked separately from the other intact objects, providing the SLOOP model with two different populations of intact objects; one having an accelerated end of life through some designed de-orbit system that speeds up

the decay of the orbit to comply with current guidelines, and one with a natural decay. Assuming an average operational life of 15 years, the orbit decay time constant for PMD-compliant objects is taken to be the smaller of either the natural decay time constant or 40 years depending on the orbital shell of interest.

The orbit decay time constant for naturally decaying intact objects (f) and fragments (h) are entirely dependent on the object's altitude and physical characteristics. It is therefore necessary to determine the average expected decay time for these objects in order to determine a value for f and h. In the Lafleur model, this orbit decay time constant was assumed to be sinusoidal in nature. As previously discussed, this was to account for the cyclical nature of solar activity. Solar activity has a significant effect on the atmospheric density at orbital altitudes. At times of peak solar activity, the Earth's atmosphere is inflated by its interaction with solar particles, thus creating a higher-density atmosphere in LEO. The opposite is true during times of low solar activity. However, the solar cycle itself is typically 11 years while the natural orbital life of almost all LEO objects is hundreds or even thousands of years. This difference in timescale indicates that the LEO orbital objects will experience many solar cycles and the effects of these fluctuations in activity will be averaged over the life of the objects. For this reason, the SLOOP orbital decay time constant is simply represented as the average life of the orbit in question. The solar cycle is taken into account during the process of determining the orbit life of the object, a process that is outlined next.

Orbit decay rate can be determined by a host of orbit simulation tools including AGI's STK software and the Aerospace Corporation's Satellite Orbit Analysis Program (SOAP). There are also several orbit life models for evaluating very low orbits using

curve fits of historical data. NASA's orbital debris program office also maintains the Debris Assessment Software (DAS) [51] tool which has an engineering toolbox capable of calculating orbital life. Originally, the approach to calculating the orbit decay time constant was to input the average physical characteristics for a population or sub-population into the DAS tool and calculate an orbit life. Two major issues arose with this approach. First, the DAS tool is designed as a resource for evaluating a satellite's compliance with NASA's orbital debris guidelines. These guidelines use the 25-year rule and thus, the DAS tool will only calculate orbit life up to 100 years, or 4 times the current best practice guideline. While this number is valuable for compliance evaluation, this is insufficient for the task of determining average orbital lifetimes for the populations of interest in the SLOOP model.

The second major issue extends to all currently available orbit lifetime models. The physical calculations that provide the orbit decay time are non-linear in nature. This is because of the cyclical nature of solar activity that drives the fluctuation of atmospheric density and the fact that the atmospheric density itself varies exponentially with altitude. Therefore, as an object's orbit decays, it experiences a non-linear increase in density. The method chosen to evaluate the change in the orbit of an object relies on the calculation of the orbit's period and then relates the change in altitude to an incremental change in orbital period. The circular orbital period is related to altitude through the non-linear equation

$$P = 2\pi\sqrt{\frac{r^3}{\mu}}, \tag{4.5}$$

where P is the orbital period, r is the orbit radius, and μ is the Earth's gravitational constant.

Unlike linear relationships, non-linear functions will not produce an average output when using the average values for all of the inputs. Therefore, in order to calculate the average orbital life of a sub-set of objects, the life of each object must first be calculated and then those values averaged. To represent the average lifetime by inputting the average area, mass, and orbit altitude values would produce an inaccurate result. While high-end simulation software such as STK and SOAP can be used to evaluate orbit life, with thousands of objects to evaluate, using such high-end simulations would be computationally intensive and unwieldy. With no simplified model for orbital life available that spans the entirety of LEO from 200 km to 2000 km, a new model for orbital life had to be created to calculate the orbit decay time constants.

A simplified method for orbit shaping was used based on a paper published by the Australian Space Weather Agency.[52] Using the general equation for drag (Equation 4.6) and the equation for circular orbit period (Equation 4.5), the agency developed a method to determine the differential change in orbit period resulting from drag forces on an orbiting body (Equation 4.7).

$$D = 0.5\rho v^2 A C_d \tag{4.6}$$

$$\frac{dP}{dt} = -3\pi a \rho \left(\frac{AC_d}{m}\right) \tag{4.7}$$

In these equations, ρ is the atmospheric density, v is the object velocity, A is the object average frontal area, C_d is the drag coefficient, a is the semi-major axis of the orbit, and m is the object mass. This equation was coded in MATLAB and the code is provided

in Appendix C. By using a difference method for integration, the differential period of the orbit with respect to time was calculated and translated into an orbital altitude. This calculation was iteratively executed until a specified end condition was met. For full orbital life, the code iterates until the orbital altitude reaches 180 km, which was assumed to be the nominal atmospheric entry altitude. For orbit decay times, the overall orbital altitude reduction can be set by the user. For the purposes of calculating the SLOOP coefficients, this differential was set to 100 km, meaning that the code produces the time it takes for the object's orbit to decay 100 km. This is taken to be the time to transition from one orbital shell to the next.

This orbit life model requires an accurate representation of the atmospheric density over the altitude range from 200 km to 2000 km. Standard atmospheres, such as the COSPAR International Reference Atmosphere[53], only provide density values up to 900 km altitude. Extrapolation of this data proves to be inadequate for predicting densities at higher altitudes. Working with the Space Environments group at NASA's Marshall Space Flight Center, a surrogate model was developed for the Marshall Engineering Thermosphere (MET) 2.0 model.[54] Using MET 2.0, a database of density values was generated. Using advanced modeling techniques, a response surface model was generated to create a single equation to represent the MET model for use in orbit lifetime calculations.

The MET 2.0 model is an executable code that uses simple text input to generate text file outputs. Taking in information about the time, orbit size, and solar activity, the model returns values for various physical parameters of the thermosphere, including the mass density. The model can be used to calculate atmosphere parameters between 90 and

2500 km altitude, making it ideal for calculating the densities over the altitude range of interest for use in the SLOOP model.

The process of generating multi-dimensional response surfaces requires a significant number of data points. Variability of the atmospheric density in the upper thermosphere is an inherently multi-dimensional problem. Looking at the problem purely in terms of the altitude dimension, it is widely known that density decreases with increases in altitude. What is not commonly known is that, even at extremely high LEO altitudes (i.e. up to 2000 km), satellites still encounter drag forces due to interactions with the atmosphere. The densities are extremely low (on the order of 10^{-16} kg/m^3), but over the span of tens of thousands of years this density is still sufficient to slowly reduce the velocity and altitude of a satellite. The multi-dimensional aspect of atmospheric density has to do with the thermosphere's interaction with particles from the Sun, which presents as a density dependence on both time and geocentric location.

Over the course of the approximately 11 year solar activity cycle, the atmospheric density can increase or decrease depending on solar activity. This density fluctuation is also dependent on the latitude and longitude of the satellite's location in orbit around the Earth as the orientation of the Earth to the sun will affect the localized atmospheric interaction with the solar particles. This results in a local density fluctuation that is seasonal in nature, meaning that different regions over the Earth will have different atmospheric properties during the equinox and solstice periods throughout a given year. In generating the data set to support the response surface development, input parameters to the MET model were evaluated over the following ranges:

Latitude: -90° to 90° in steps of 18°

Longitude: -180° to 180° in steps of 36°

Altitude: 200 km to 2000 km in steps of 50 km

The time step used in the model was 1 second, which ensured that each data point in the full factorial expansion of latitude, longitude, and altitude was evaluated on the same day of the year. This was repeated 44 times over the time period from January 2020 to September 2030 with runs on March 1st, June 1st, September 1st, and December 1st of each year. This time step is sufficient to capture the seasonal variation and the time span is long enough to capture a full solar cycle.

To capture the solar cycle information, the model asks for the 13-month-averaged 10.7-cm solar flux (*F10.7_avg*) as well as the 10.7-cm solar flux (*F10.7*) and geomagnetic activity index (*ap*) for the date specified. Historical data is collected for each of these parameters and is available on a number of web sites including the OMNIWeb site maintained by NASA's Goddard Space Flight Center. A table of projected values for *F10.7* and *ap* over the time range from January 2020 to October 2030 was provided by the Space Environments at NASA MSFC. This data was extrapolated and compared to the historical data from the OMNIWeb site and it was determined that the 50th Percentile data set most closely matched the historical data, shown in Figure 4.8.

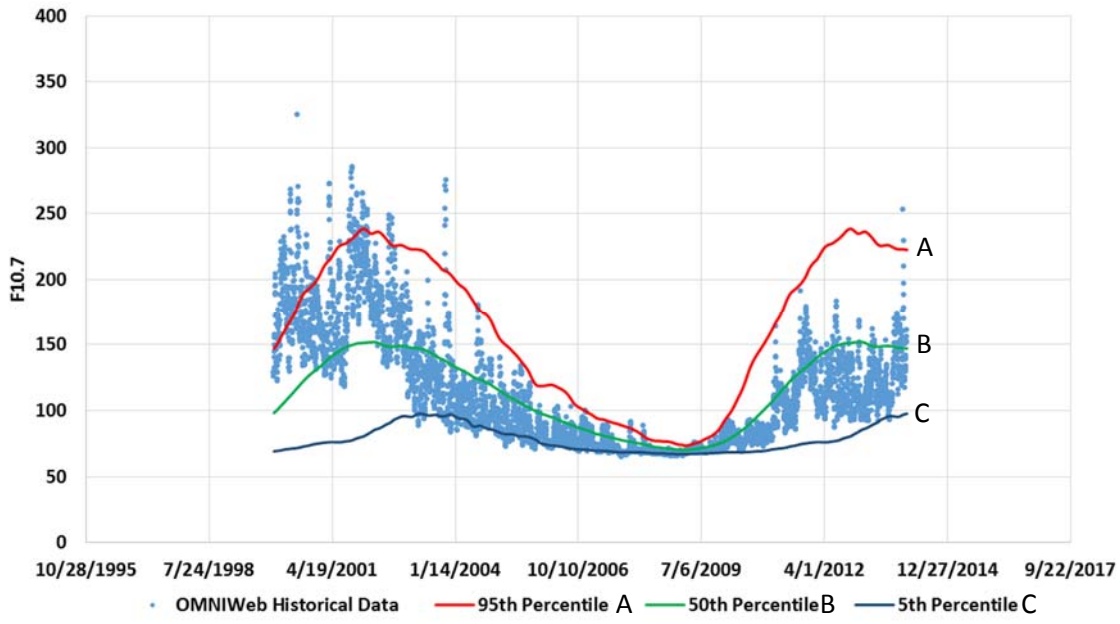

Figure 4.8: Predicted F10.7 Value Compared to Historical Data

The model runs for each of the 44 dates generated 4477 data points. These data sets were post processed to calculate the average orbit density for an individual orbit altitude resulting in 37 average atmospheric density values for each of the 44 dates. These 1628 data points were then used to produce the time and altitude dependent response surface. The full data set could be used in the future to generate a response surface that also accounts for orbit position by using the latitude and longitude values in each orbit. However, this level of granularity was not required for the current application.

The set of altitude-average density values was imported into the JMP software program for post processing. The date values were converted into a number of days from the first data run setting January 1, 2020 as time = 0 and converting each subsequent date into a number of days since time = 0. This represents the time function generically and allows the data set to repeat cyclically for dates beyond December 2030. Because the

atmospheric density drops orders of magnitude from 200 km altitude to 2000 km altitude, the density values were converted into natural log values before fitting.

JMP [36] was used to develop a neural-net response surface fit of density as a function of time and altitude. The resulting response surface has a 0.996 coefficient of determination, implying an extremely accurate fit. The final equation for the response surface is

$$\begin{gathered}\rho = e^{\left(-24.960481+(11.76373*\mathrm{C1})+(3.81465*\mathrm{C2})-(7.667977*\mathrm{C3})\right)} \\ C1 = \tanh(0.5 * (0.4658 + (0.000065 * \mathrm{T}) - (0.004212 * \mathrm{H}))) \\ C2 = \tanh(0.5 * (3.3367 - (0.001422 * \mathrm{T}) + (0.0000548 * \mathrm{H}))) \\ C3 = \tanh(0.5 * (-0.26232 - (0.0004975 * \mathrm{T}) + (0.000722 * \mathrm{H})))\end{gathered} \tag{4.8}$$

Here, T is the time since the beginning of the model run in days and H is the orbit altitude in kilometers. The time variable T used in this model has a very specific definition. Since the solar cycle repeats over an 11 year period, the density model is also set to repeat over the same 11 year cycle. With an evaluation period beginning on January 1, 2020, the density function above represents the density as a function of time over the 4018 day period starting on January 1, 2020. Therefore, the time value, T, must be a number between 0 and 4018. In order to generate this value, simply calculate the number of days between the date being evaluated and January 1, 2020, divide by 4018, remove the integer value, and use the remaining decimal as a multiplier to calculate the time position within the repeating 11 year cycle. The MATLAB code for the entire density calculation, including the time evaluation, can be found as part of the orbit life code provided in Appendix C. Figure 4.9 shows a comparison of the newly developed density model with the various published COSPAR density models. The plot shows the

MET 2.0 surrogate model closely matches the COSPAR Moderate Solar Activity model up to the 900 km altitude limit of the COSPAR model.

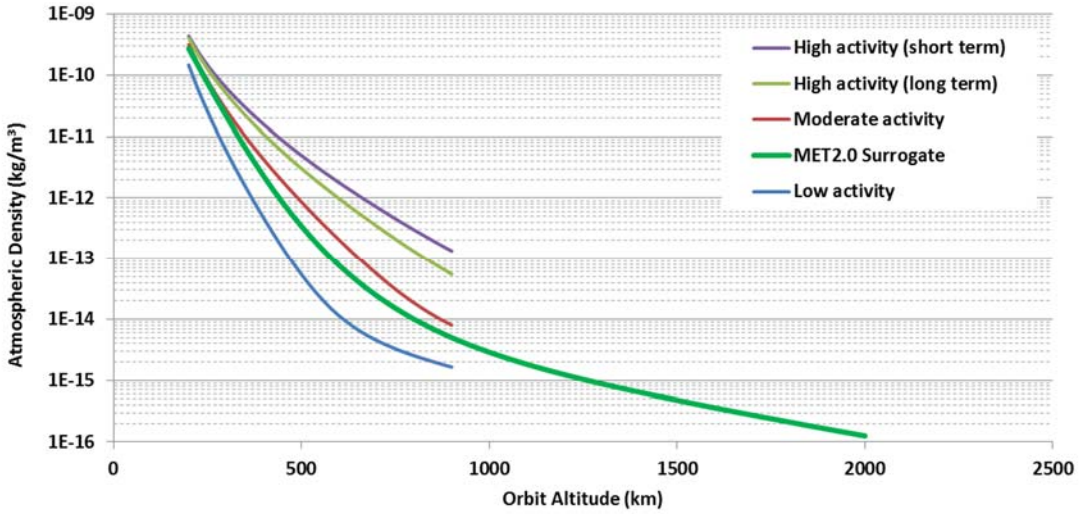

Figure 4.9: MET Surrogate Density Model Compared to the COSPAR Standard Reference Model

Once the code was developed with the appropriate representation for the atmospheric density with altitude, the model was used to generate a specific orbit life time for each object. These orbit life values were then averaged to provide a mean orbit life value that was set as the orbital decay time constant for the naturally decaying intact objects (f) and the fragment populations (h) tracked by the SLOOP equations.

4.2.2.1 Orbit Life Time Constants: Layered LEO Representation

The orbit life time constants for naturally decaying intact objects was calculated using data from the SATCAT database [24], JSpOC catalog [14], the STK database [38] and the orbit life model discussed above. In the layered LEO representation, the orbit life time constant was set to the time for the orbit to decay 100 km, thus taking the object out of its original shell and into the one below. This object then adds to the population of the

lower shell where it is subject to the orbital time constant of that shell. The orbit life mode requires three main inputs for each calculation; the mass and area of the object, and the starting altitude of the object's orbit.

To avoid skewing the results of the analysis due to the non-linearity of the problem, the orbital decay time was calculated for each intact object for which all three of the required inputs is known. Once complete, the objects were binned by their equivalent circular altitude and the orbit decay time was averaged to provide a time constant for intact objects for each of the 18 shells in the layered model. There were 2389 objects available from the various data sources that met the minimum data requirements for orbit lifetime calculations. Radar cross section taken from the SATCAT database was used for the average projected frontal area. The mass of the objects was gathered from various web sources and the STK database. The equivalent circular altitude was determined using orbital parameters provided in the JSpOC catalog. The resulting mean values from the orbit life model are provided in Figure 4.10.

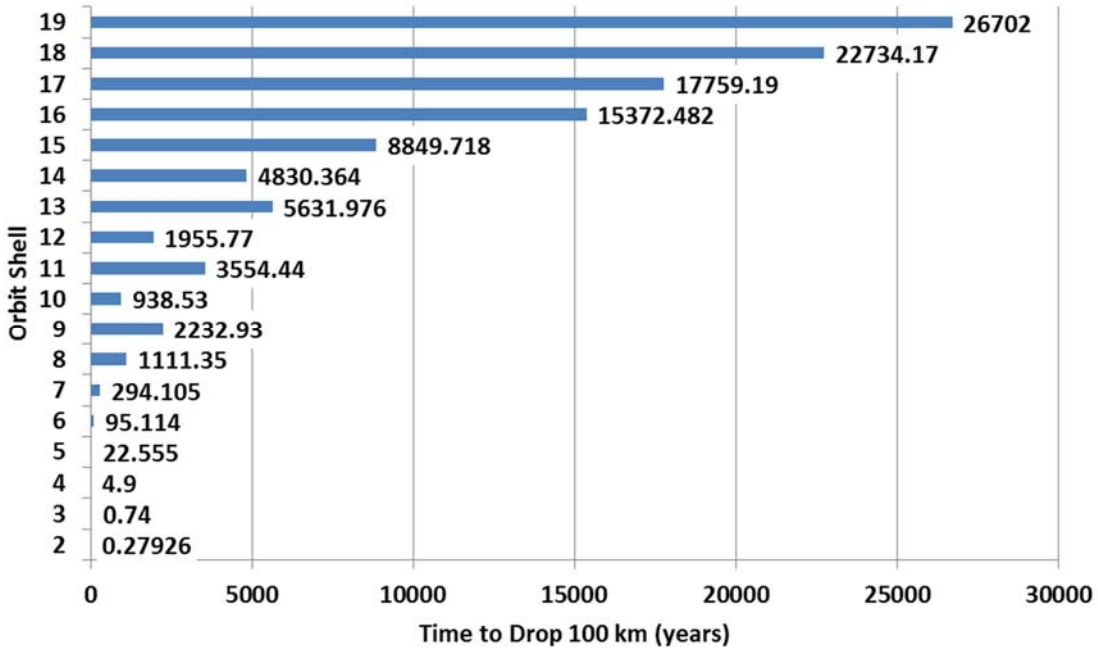

Figure 4.10: Average Time to Drop 100 km for Intact Objects by Orbital Shell

The orbit decay time does not fully characterize the full time an object spends in a particular orbit. In order to fully account for the possibility of a collision, the satellite's operational time must also be considered. For this purpose an average operational life value was added to the decay time to generate the time constant used in the SLOOP model. Based on historical data, a 10 year operational life was assumed for the lower orbit shells while a 20 year operation life was assumed for the higher orbital shells. The final values used as the orbital time constants in the layered LEO model are provided in Figure 4.11.

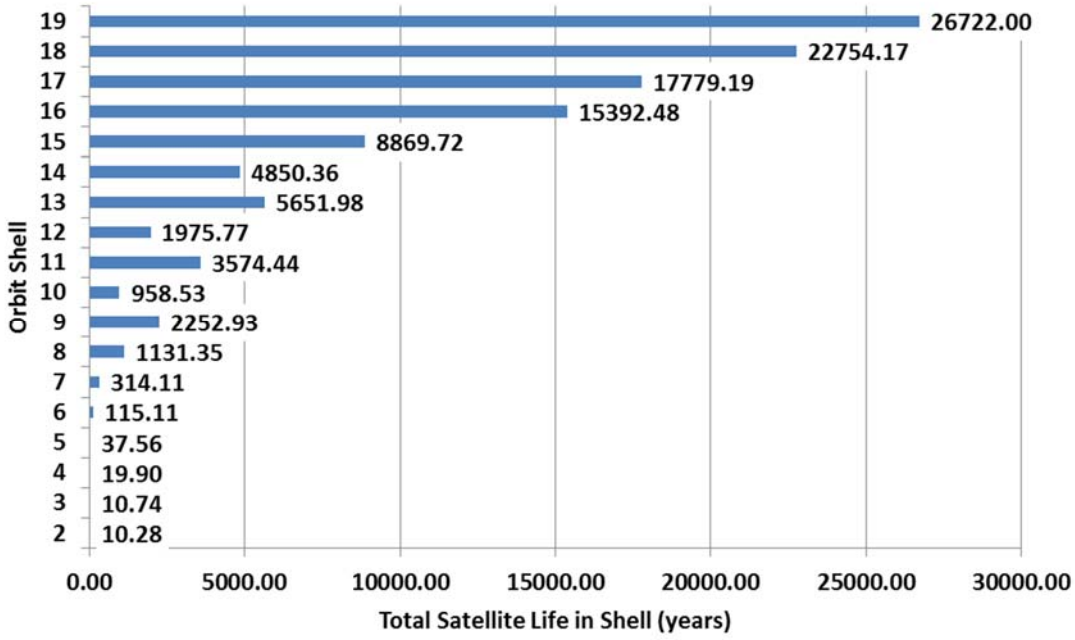

Figure 4.11: Total Intact Object Residence Time in Shell

The method for calculating the orbital decay time constants for fragments was slightly different. Due to the very large number of fragments in orbit and the format of the results provided from the MASTER2009 model, the fragments were analyzed based on a weighted average of their characteristics rather than on an individual life calculation for each fragment. The MASTER2009 model provides outputs of spatial density (number of objects per cubic kilometer) of objects of a certain characteristic size in a certain orbit. These data distributions are binned into histograms. The binned MASTER2009 data were converted into object counts for each characteristic size in each of the orbital shells of interest. A correlation between fragment characteristic size and fragment mass was developed based on the MASTER2009 results and used to provide a corresponding average mass for each size-orbit bin of data. The mass correlation is

$$y = 30.766\text{x} - 0.0016 \quad , \tag{4.9}$$

Where y is the average mass and x is the object's radar cross section (m^2). The correlation and data are plotted in Figure 4.12.

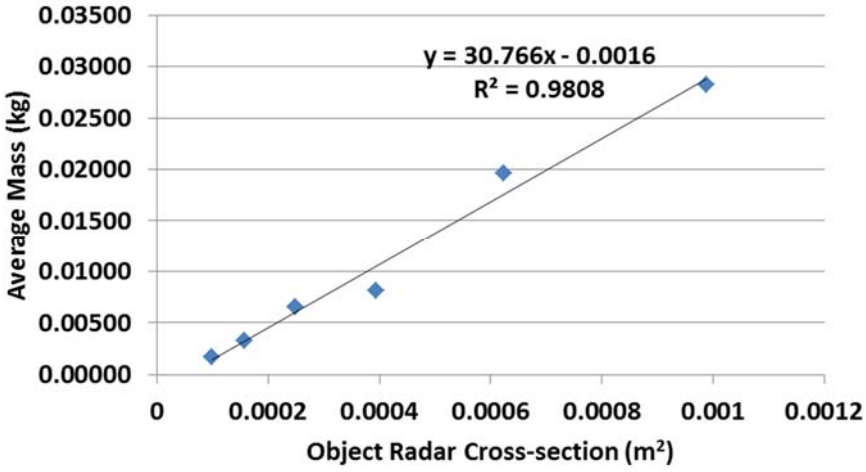

Figure 4.12: Relationship Between Object Radar Cross-Section and Object Mass Based on MASTER2009 Data

The resulting set of 162 object count bins were merged with the 8500 SATCAT database entries identified as debris fragments with corresponding radar cross-sectional area data. Using the MASTER2009-derived mass-area relationship, a corresponding mass was assigned to each binned group of SATCAT debris fragments. The orbit life model was then run for each size-orbit bin data set, resulting in an average orbit decay rate for each set of objects. Some loss of fidelity was unavoidable due to the non-linearity of the orbit life problem and the format of the source data. By subdividing the population into size-orbit bins, some accuracy was regained. A weighted mean orbit decay time value was then calculated based on the number of objects corresponding to each size-orbit bin and the orbit decay time constant for each orbital shell was determined. The resulting orbit decay time constants are shown in Figure 4.13. Table 4.3 provides the value for the orbit decay time constants by orbital shell for the layered LEO

representation in the SLOOP model for the naturally decaying intact objects, the PMD-compliant intact objects, and the fragments.

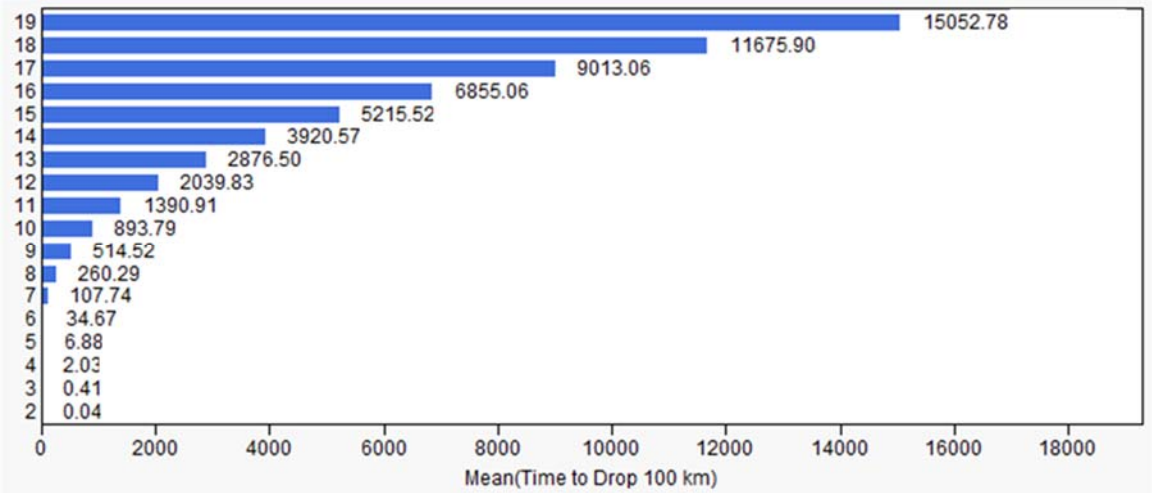

Figure 4.13: Average Time to Drop 100 km for Fragments by Orbital Shell

Table 4.3: Orbital Decay Coefficients by Orbital Shell

Orbital Shell	Coefficient Values		
	f	g	h
200-300	10.3	10.3	0.04
300-400	10.7	10.7	0.42
400-500	19.9	19.9	2.0
500-600	37.6	37.6	6.9
600-700	115.1	40	34.7
700-800	314.1	40	107.7
800-900	1131.4	40	260.3
900-1000	2252.9	40	514.5
1000-1100	958.5	40	893.8
1100-1200	3574.4	40	1390.9
1200-1300	1975.8	40	2039.8
1300-1400	5651.9	40	2876.5
1400-1500	4850.4	40	3920.6
1500-1600	8869.7	40	5215.5
1600-1700	15392.5	40	6855.1
1700-1800	17779.2	40	9013.1
1800-1900	22754.2	40	11675.9
1900-2000	26722	40	15052.8

4.2.2.2 Orbit Life Time Constants: Bulk LEO Representation

To generate the orbital decay time constants for the bulk LEO representation, the same calculations were performed as for the layered representation with one notable exception. When considering the orbital decay of objects in the entire region of LEO, the only time an object exits this region is when it re-enters Earth's atmosphere. Therefore, the orbit life model was executed using the same input parameters as in the layered model. However, the time to drop 100 km was replaced with the time for the object's orbit to reach an altitude of 180 km. Once this value was calculated for the individual objects in the database, the distribution of deorbit times was plotted and the mean value was taken to represent the objects in LEO in the bulk representation of LEO in the SLOOP model. The distribution and summary statistics for the intact object population are provided in Figure 4.14.

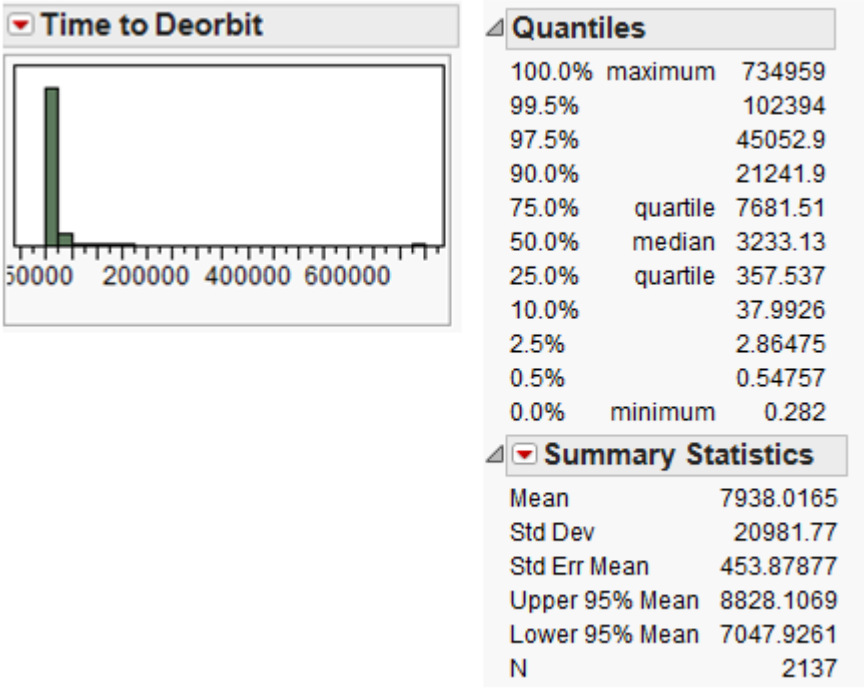

Figure 4.14: Histogram of Deorbit Time for Intact Objects

The fragment population was treated in a similar manner. The size-orbit bins used in the development of the orbit decay time constants for the layered representation of LEO were again used for the bulk representation but the orbit life model was run to deorbit conditions and not the 100 km drop conditions. Again, a weighted average of the data was taken and this mean value was applied to all fragments in the bulk LEO model. The distribution and summary statistics for the fragment population are provided in Figure 4.15. Table 4.4 provides the value for the orbit decay time constants for the bulk LEO representation in the SLOOP model for the naturally decaying intact objects, the PMD-compliant intact objects, and the fragments.

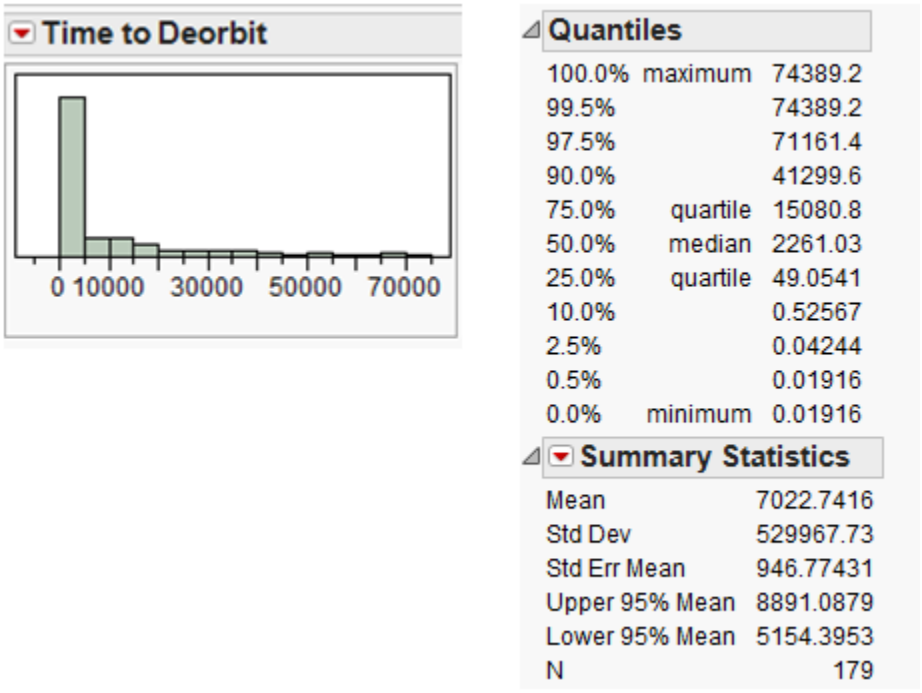

Figure 4.15: Histogram of Deorbit Time for Fragments

Table 4.4: Deorbit Time Coefficients for Bulk LEO Representation

Coefficient Values		
f	g	h
7938.0165	40	7022.742

4.2.3 The Object Collision Terms

One main objective in developing a population growth model for LEO objects is to enable the estimation of collision probabilities. The size of the population only becomes a concern when it increases to the point that operational satellites are at risk of being lost due to collisions. These collisions can happen between two large, intact objects, such as the collision between the Iridium 33 and Cosmos 2251 satellites in 2009. However, even collisions between an intact object and an object as small as 1 cm in diameter can produce some fragments and cause the intact object to lose functionality. The consequence of a collision is entirely dependent on the energy of that collision, which is a function of the mass of the two objects and their relative velocity. Each collision increases the population of fragments which are then more likely to collide with other objects in the future, potentially leading to the cascading collision scenario outlined by Kessler in 1978.[1]

The SLOOP model uses an approach similar to Lafleur and Kessler to calculate the collision probability and account for collisions in the population analysis process. The collision terms in each equation are based on the theory of gas dynamics as applied to the interaction of molecules. There are thee collision terms in the equations that form the analytical backbone of the SLOOP model.

$$Collision_{Nn} = xnN \tag{4.10}$$

$$Collision_{NN} = yN^2 \tag{4.11}$$

$$Collision_{nn} = zn^2 \tag{4.12}$$

In these equations, n represents the population of fragments and N represents the population of intact objects. In Equations 3.3 and 3.4, intact object collisions are specified for both the naturally decaying intact objects and the PMD-compliant intact objects, using NN and ND respectively, in place of the generic N. However, the coefficients and structure of the collision terms are the same as the generic terms provided above.

Another item of note in the application of these collision terms is the use of a factor of 2 in Equations 3.3, 3.4, and 3.5. In the three equations that drive the SLOOP model, the collision terms are used as loss terms in the representation of the populations of intact objects and fragments. When a collision occurs between a large object and a small object, as represented by Equation 4.10, only one intact object is removed from the intact object population. However, when two like objects collide, as represented by Equations 4.11 and 4.12, two objects are lost from the populations being evaluated. In these cases, a factor of 2 is added to indicate the loss of two objects and this factor can be seen in Equations 3.3, 3.4, and 3.5.

The physical basis for modeling orbital object collisions using an analogy of molecular collisions in gas dynamics has its roots in the original research of Kessler. As mentioned in Chapter 2, Kessler and subsequent researchers have characterized collisions using a differential volume application of the molecular collision models of gasses,

assuming that collisional cross-section can be represented by object cross section. Due to orbit precession and integrating over time, it can be reasonably assumed that objects can occupy all differential volumes of a region of space over time.

This approach is more appropriately applied for the populations of small debris. Simulations and observations of the fragment clouds produced by recent fragmentation events such as the Iridium-Cosmos collision of 2009 and the Fengyun-1 ASAT test show that debris fragments tend to disburse over time facilitated by differential orbital velocities and orbit precession rates. These fragment clouds become fairly evenly distributed in an orbit shell over time. This same phenomenon contributes to the probabilistic evaluation of fragment proliferation in models such as the MASTER2009 model. This would indicate that interactions with small debris fragments will reasonably resemble random molecular motion in a gas. Application of the gas dynamics analogy to intact object interactions is an accepted practice in the community that performs these population and collision simulations.

Recalling Equations 2.2 and 2.3, repeated here for convenience

$$\frac{dC}{dt} = \frac{1}{2}\int S^2 \overline{V_s} \overline{A_{cc}} dU \tag{2.2}$$

$$\frac{C}{t} = N_1 N_2 \frac{\overline{v_{12}}\sigma}{V} \tag{2.3}$$

the collision probability of two molecules is related to their spatial density, their relative velocity and their collisional cross section. Spatial density is defined as the ratio of the number of particles over a given reference volume. By integrating Equation 2.2 over the full volume of interest, the collisions per unit time can be represented with Equation 2.3 where the spatial density has been expanded to specifically show populations of particles 1 and 2 and the reference volume is specifically called out as V.

When applied to orbiting object populations, Equation 2.3 is a generic representation of Equations 4.10 – 4.12. The generic N variables in Equation 2.3 are replaced with the intact and fragment populations, N and n respectively. The ratio relating velocity, cross-section, and volume is represented in the SLOOP collision terms as the coefficients x, y, and z, which are specifically calculated by

$$x = \frac{\overline{v_{nN}}\sigma_{nN}}{V} \tag{4.13}$$

$$y = \frac{\overline{v_{NN}}\sigma_{NN}}{V} \tag{4.14}$$

$$z = \frac{\overline{v_{nn}}\sigma_{nn}}{V} \tag{4.15}$$

In the SLOOP model, the average relative velocity, in km/s, is calculated from the known velocities of two objects. The volume is taken as the full volume of space under evaluation. For the layered representation of LEO, this is the volume of the orbital shells being investigated. For the bulk representation of LEO, this is the full volume of LEO from 200 km to 2000 km. The collisional cross-section is uniquely calculated based on the gas dynamics definition. Generically, the collisional cross-section is defined by

$$\sigma_{12} = \pi(r_1 + r_2)^2. \tag{4.16}$$

The distinction to be made in this equation is that the collisional cross-section is not simply the sum of the cross-sectional areas of the two objects colliding. Rather, the cross-section is a composite area of a notional disk with a radius equal to the sum of the radii of the two colliding objects. This application requires a decomposition of the available data for fragments and intact objects to rebuild a composite collision cross-section. The available physical characteristic in the SATCAT database is the radar cross-section which is equivalent to the average frontal cross-sectional area. This number is

converted into a radius where it can then be recombined using Equation 4.16 into a collisional cross-section. For use in the SLOOP model, this cross-section is calculated in km^2.

To determine the average velocity for each collision type, the orbital data from the JSpOC catalog was used. Assuming the equivalent circular altitude for the orbits of the objects in the catalog, Equation 4.17 was used to determine the circular orbit velocity for each object,

$$v_{circ} = \sqrt{\frac{\mu}{(R_E + h)}} \quad , \tag{4.17}$$

where μ is the Earth's gravitational constant, R_E is the radius of the Earth, and h is the altitude of the orbit.

The same process was performed for the fragment data produced in the MASTER2009 runs mentioned in section 4.2.2. A weighted average value for velocity was then determined for each of the three collision coefficients based on the populations of interest and the region of LEO investigated. This was based on the size-orbit data binning that results from the statistical distribution outputs of the MASTER2009 model. The specific data and resulting coefficients for the layered and bulk representations of LEO are presented in sections 4.2.3.1 and 4.2.3.2 that follow. It is important to note that the time unit in the collision terms is years, requiring a conversion from seconds to years to make the time segment of the velocity term align with the general time unit of the SLOOP model.

In addition to supporting the tracking of populations over time, the collision terms in Equations 3.3 – 3.5 also support the generation of a running tally of projected

collisions as a secondary output of the SLOOP model. Many of the orbital object population models provide a count of collisions over the time period investigated in addition to the running count of populations that are typically plotted and published. This number of collisions provides the key information that translates the environmental information of population into the consequence of collisions. By tracking the total number of collisions expected, the population growth can be directly related to the risk estimation of flying a satellite in a particular region of space.

Equations 4.13 – 4.15 essentially provide a number of collisions per time over the duration of the simulation. These collisions are accounted for in Equations 3.3 – 3.5, where each term in the equation is multiplied by the time step of the simulation to support the difference method of integration. By also isolating the product of the collision term and the time step and then calculating a running summation of those values over the duration of the simulation, a cumulative number of collisions can be reported. This data can show the correlation between population growth and increasing collision risk. It can also provide insights such as a total number of collisions expected over the next 100 years in a given region of space based on the assumed future operational launch cadence. By tracking both the fragment population and the intact object population, the SLOOP model can not only account for the projected number of Iridium-Cosmos-class collisions, but also the projected number of potentially debilitating intact-fragment collisions that pose an additional threat to operational spacecraft. The power of these values will be demonstrated in the application example provided in Chapter 6.

4.2.3.1 Collision Coefficients: Layered LEO Representation

The collision coefficients *x*, *y*, and *z* were calculated for the layered LEO representation using the methods described in the previous section. The intact objects in the JSpOC catalog were surveyed and mean orbital velocities were calculated for each object. Using the SATCAT database, the radar cross-section was decomposed into a characteristic radius for the intact objects. The distribution of mean velocities and characteristic radii by orbital shell are provided in Figures 4.16 and 4.17. These values support the generation of the *y* coefficient for intact-on-intact collisions.

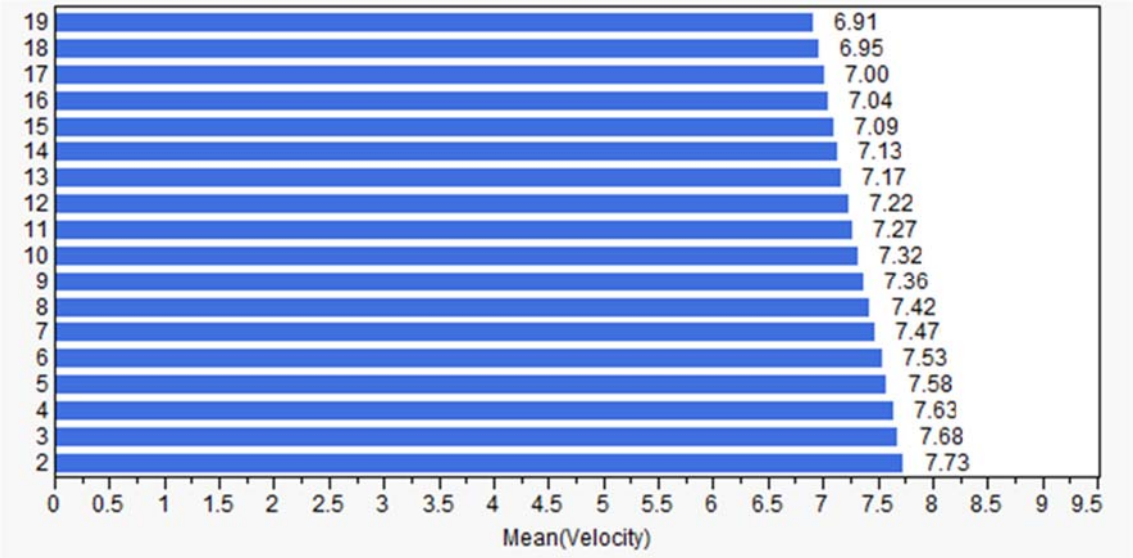

Figure 4.16: Mean Intact Object Velocity (km/s) by EAC Bin

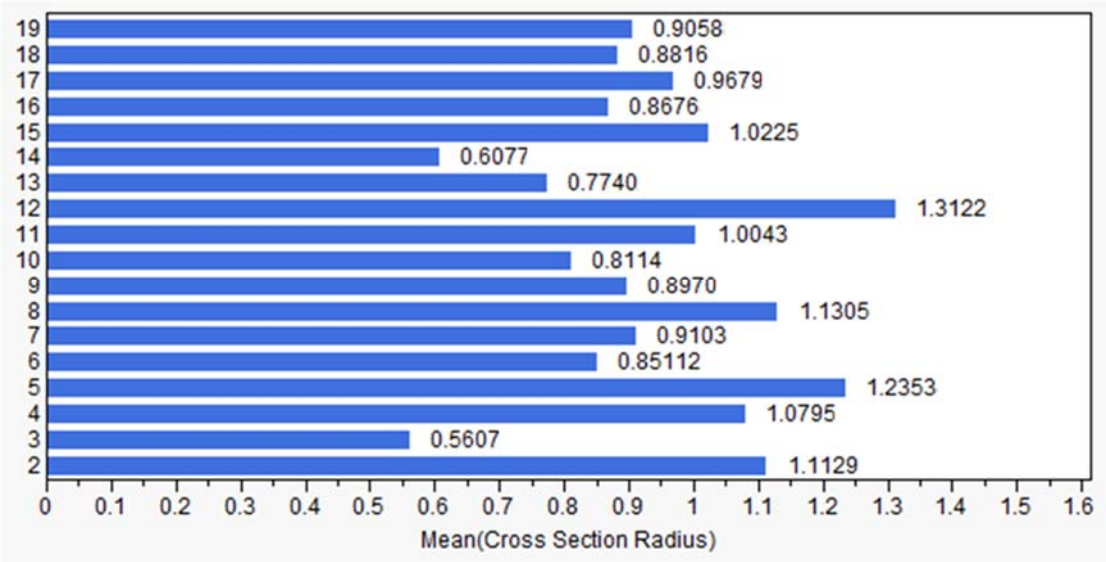

Figure 4.17: Mean Cross Sectional Radius (m) of Intact Objects by EAC Bin

To support the generation of the *z* coefficient for fragment-on-fragment collisions, the MASTER2009 data was decomposed and a size-orbit bin weighted mean was calculated for both the velocity and radius of the fragments. This data is provided in Figures 4.18 and 4.19.

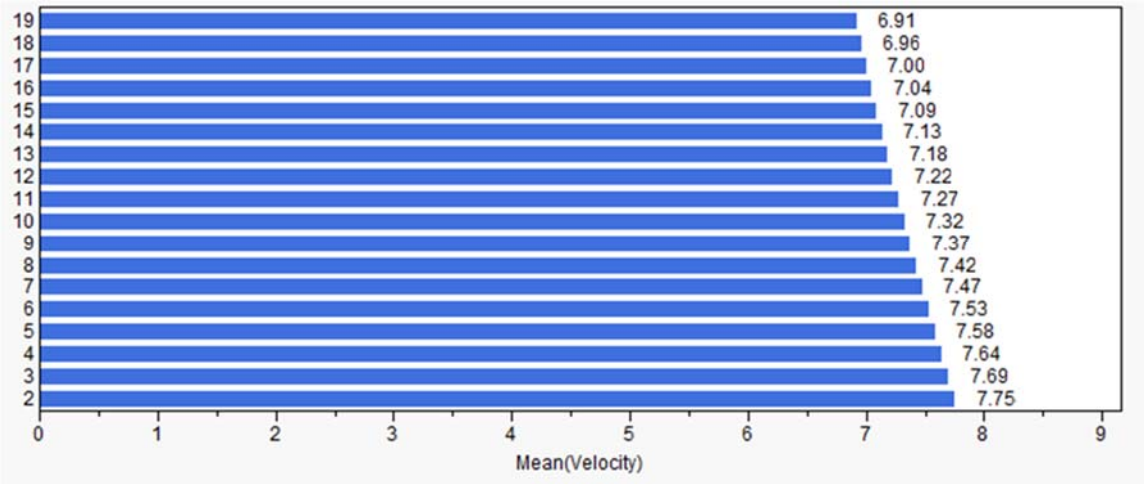

Figure 4.18: Mean Velocity (km/s) of Fragments by EAC Bin

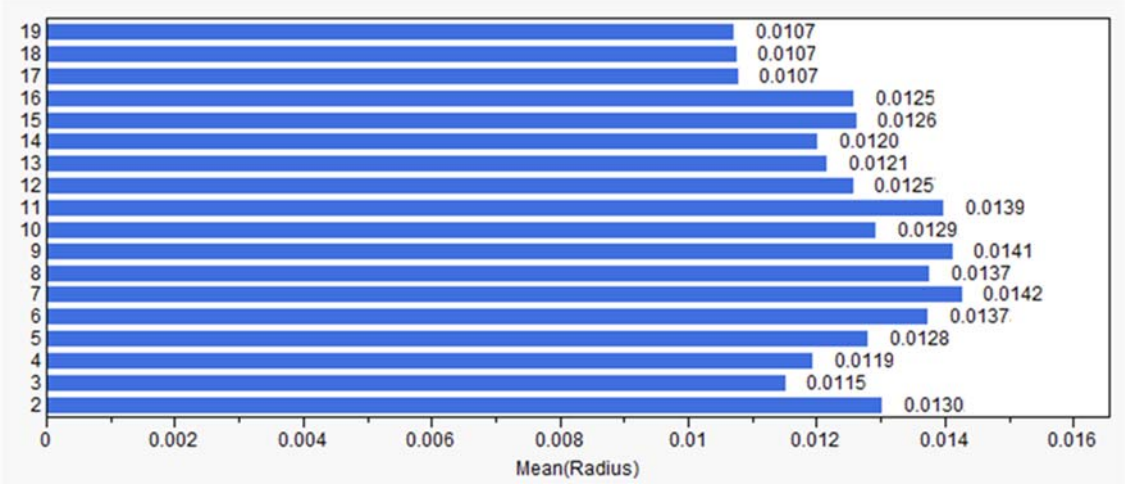

Figure 4.19: Mean Cross Sectional Radius (m) of Fragments by EAC Bin

For both the *y* and *z* coefficients, the radius values for the objects investigated were used for both radius values in Equation 4.16 to calculate the composite collisional cross-section. In the case of the collision coefficient for the intact-fragment collisions, *x*, the mean radius of the intact object and the fragment were summed, using both data sets presented in Figures 4.16 and 4.18. The determination of the velocity value used in the *x* coefficient calculation was achieved by taking a weighted average by orbital shell of the velocity of the fragment and intact object populations. A distribution of this combined velocity value by orbital shell is provided in Figure 4.20.

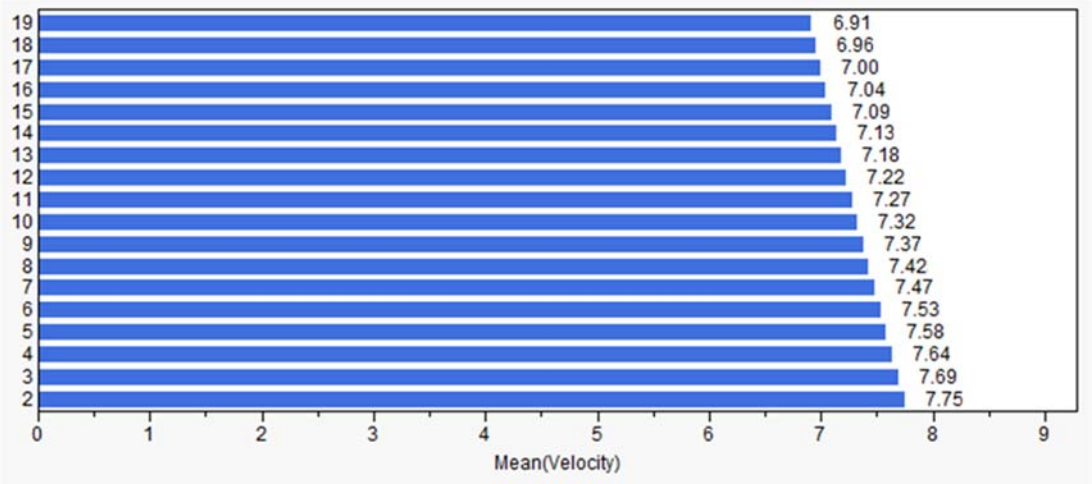

Figure 4.20: Mean Velocity of Fragments and Intact Objects by EAC Bin

The velocity and radius data was then combined using Equations 4.13 – 4.15 to calculate the collision coefficients. Table 4.5 provides the coefficient values for each of the collision coefficients by orbital shell.

Table 4.5: Collision Coefficient Values by EAC Bin

	Coefficient Values		
Orbital Shell	*x*	*y*	*z*
200-300	1.77E-08	3.44E-08	4.72E-12
300-400	4.39E-09	8.42E-09	3.55E-12
400-500	1.54E-08	3.01E-08	3.69E-12
500-600	1.94E-08	3.8E-08	4.09E-12
600-700	9E-09	1.74E-08	4.54E-12
700-800	9.93E-09	1.92E-08	4.73E-12
800-900	1.47E-08	2.87E-08	4.25E-12
900-1000	8.99E-09	1.74E-08	4.32E-12
1000-1100	7.12E-09	1.38E-08	3.5E-12
1100-1200	1.05E-08	2.04E-08	3.96E-12
1200-1300	1.72E-08	3.38E-08	3.1E-12
1300-1400	5.86E-09	1.14E-08	2.81E-12
1400-1500	3.53E-09	6.79E-09	2.66E-12
1500-1600	9.54E-09	1.86E-08	2.83E-12
1600-1700	6.68E-09	1.3E-08	2.73E-12
1700-1800	8.01E-09	1.57E-08	1.95E-12
1800-1900	6.46E-09	1.26E-08	1.86E-12
1900-2000	6.61E-09	1.29E-08	1.81E-12

4.2.3.2 Collision Coefficients: Bulk LEO Representation

The collision coefficients for the bulk representation of LEO were calculated in the same manner as described for the layered representation. The intact objects radius and velocity distributions and summary statistics are provided in Figure 4.21. These mean values were used in the development of the *y* coefficient.

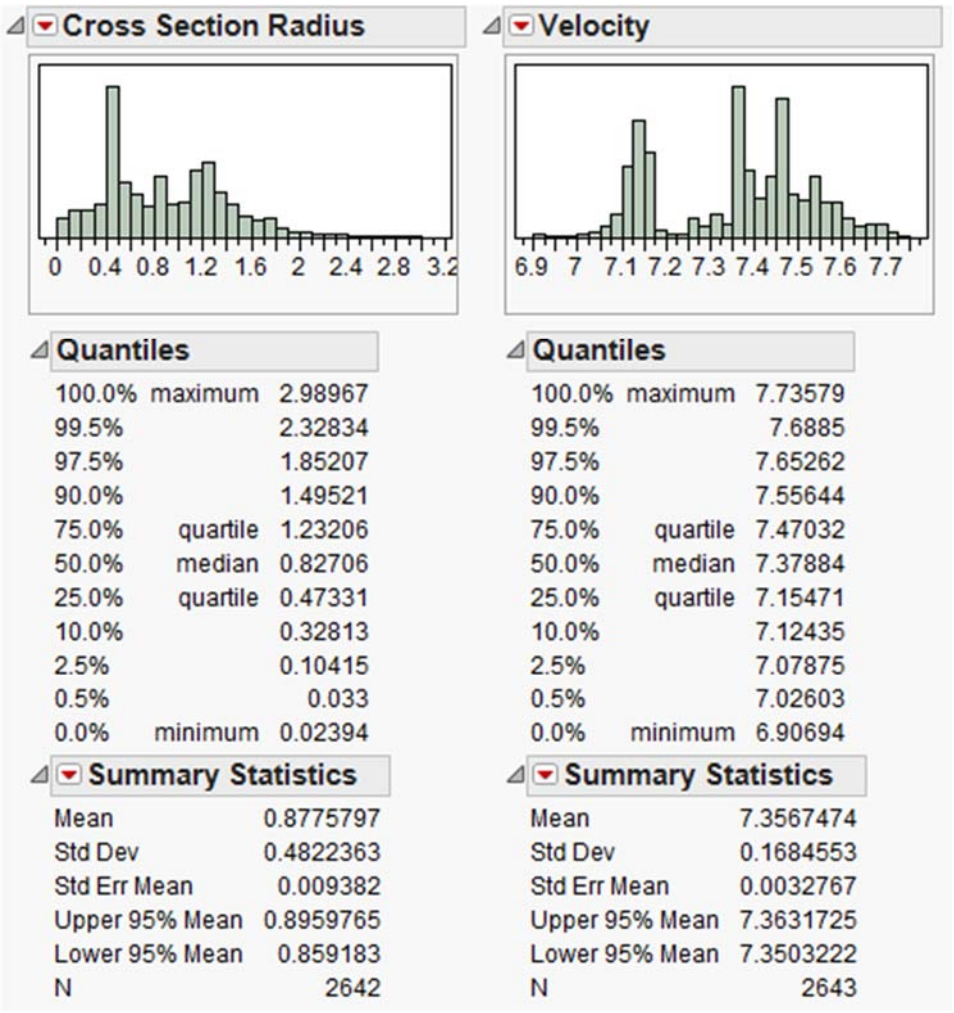

Figure 4.21: Histograms of Cross Sectional Radius (m) and Velocity (km/s) of Intact Objects for Bulk LEO Model

The histograms and summary statistics for the radius and velocity of the fragment population are provided in Figure 4.22. These mean values were used in the development of the *z* coefficient.

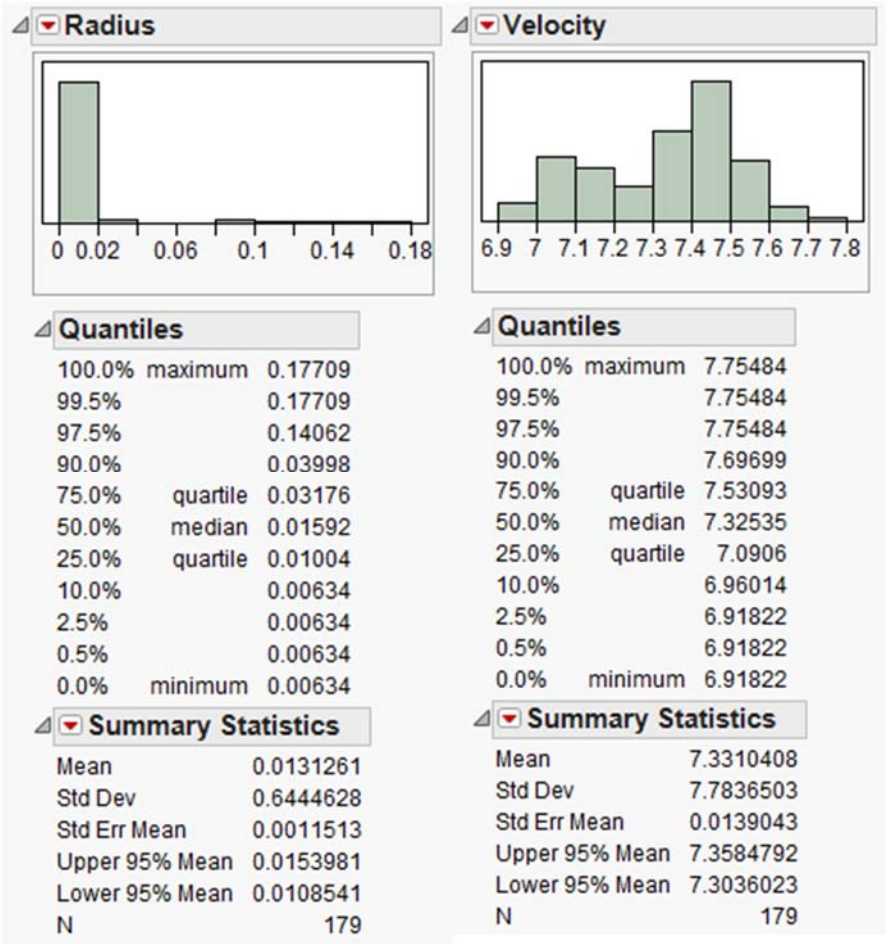

Figure 4.22: Cross Sectional Radius and Velocity of Fragments for Bulk LEO Model

As with the layered coefficients, the mean radius value for the intact objects and fragments were combined to calculate the collisional cross-section for the *x* coefficient. A weighted average value for the combined velocity of fragments and intact objects was calculated to support the calculation of the *x* coefficient. The distribution of this combined velocity is provided in Figure 4.23.

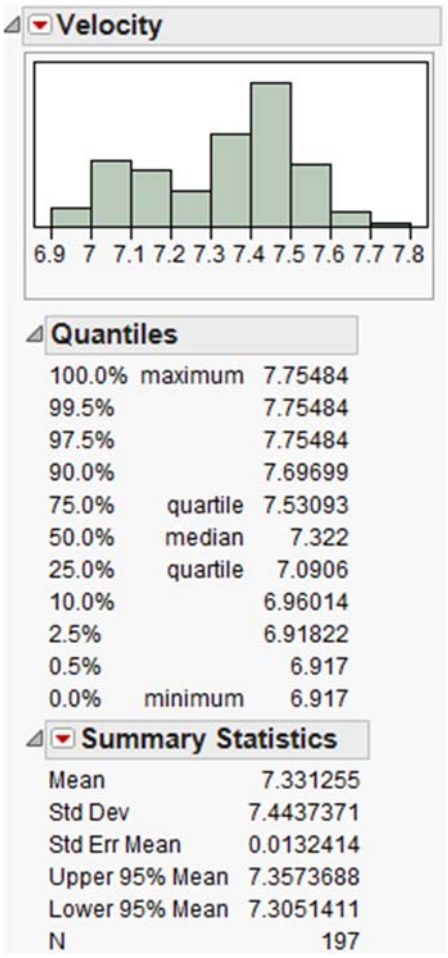

Figure 4.23: Histogram of Velocity for Combined Fragment and Intact Object Populations for Bulk LEO Model

The radius and velocity values for the populations were combined to calculate the collision coefficients using Equations 4.13 – 4.15. The resulting coefficient values for the bulk LEO representation are provided in Table 4.6.

Table 4.6: Collision Coefficients for Bulk LEO Model

Coefficient Values		
x	*y*	*z*
7938.0165	40	7022.742

4.2.4 The Fragmentation Terms

Due to the highly coupled nature of the intact object and fragment populations, it is important to accurately represent the growth of the fragment population. This was seen in the ANOVA performed on the original Lafleur model with the significance of the x, p, and α coefficients, all of which directly relate to the generation of and residence of fragments. In the SLOOP model, collisions are the major source of fragments with a small contribution coming from fragments created on payload deployment. This approach is consistent with findings of several studies that indicate to passivation practices are expected to limit explosions of on orbit objects making collisions the primary fragmentation events.[13]

In Equations 3.3 and 3.4, the SLOOP model captures the likelihood of collisions of various types using the collision terms discussed in section 4.2.3. The fragment population is tracked in Equation 3.5 and it is in this equation that the likelihood of a collision is translated into a number of fragments resulting from that collision. Equations 4.10 and 4.11 quantify the number of collisions experienced by intact objects, both from other intact objects and from fragments. Both of these collision types will produce fragments, many of which will be greater than 1 cm in diameter and thus contribute to the growth of the fragment population. Equation 3.5 uses the coefficients α and γ as multipliers to these collision terms to quantify the number of fragments produced in a collision.

The number of fragments produced is derived from the NASA Breakup Model, most recently revised in a 2001 publication.[33] This breakup model leverages the results of many hypervelocity impact experiments to provide statistical distributions of

the physical characteristics of fragments created in spacecraft collisions. Of specific interest to the SLOOP model is the cumulative number of fragments resulting from different types of collisions. The NASA Breakup model equates collisional energy with the number of fragments produced based on experimental data:

$$N(L_c) = 0.1(M)^{0.75} L_c^{-1.71}. \quad (4.18)$$

The result of the equation is the total number of fragment with a characteristic length greater than or equal to the length value used in the equation. The variable L_c is the characteristic length, taken as the fragment diameter, in meters. The mass variable, M, has a different definition depending on whether the collision is classified as catastrophic or non-catastrophic. According to the NASA Breakup model description, a collision is catastrophic if the relative kinetic energy of the smaller object divided by the mass of the larger object is equal to or greater than 40 J/g. In the event that the collision is catastrophic, M is equal to the mass of the two objects involved in the collision. If the event is non-catastrophic, M is equal to the mass of the smaller object times the collision velocity in km/s.

In all fragment calculations, the fragment characteristic length was set at 1 cm to correspond with the lower end of the size range for fragments being tracked by the SLOOP fragment population equation. In order to apply Equation 4.18 appropriately, it was necessary to determine whether or not a collision was catastrophic. The result of two large objects colliding yields a collision energy ratio well above the 40 J/g limit specified in the breakup model. Therefore, it was decided that all intact-intact collisions would be considered catastrophic. In these cases, the mass value, M, was set to twice the average mass of an intact object to account for two average intact objects colliding.

A quick investigation of the energy ratio for intact-fragment collisions produced the plot provided in Figure 4.24. A range of small object masses was evaluated against a typical range of intact object masses. The kinetic energy of the fragment was calculated using the average collision velocity calculated as part of the collision rate analysis outlined in section 4.2.3. The range of mass values for fragments between 1 cm and 5 cm in diameter is between 0.008 kg and 0.059 kg. This range of fragment sizes represents 99% of the fragments currently in orbit according to the MASTER2009 model. This range of small object masses is highlighted in green in Figure 4.24. The red dashed line highlights the 40 J/g energy limit. It can be seen from this plot that any collision between an intact object and a fragment can be considered non-catastrophic. The result from this collision will most likely be the loss of the intact object or spacecraft, but the energy of the collision will produce significantly fewer fragments than a higher energy, catastrophic collision.

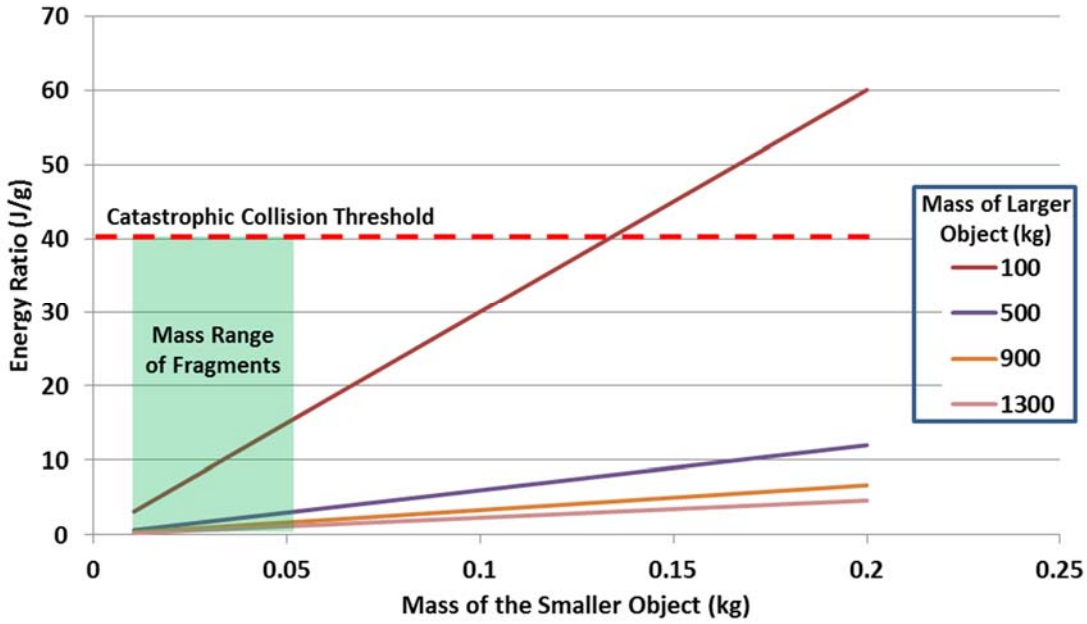

Figure 4.24: Plot of Collisional Energy for Various Size Objects; Green Region Highlights Typical Fragment Mass Range

The third fragmentation coefficient, β in Equation 3.5, is related to the fragments released during payload launch and deployment operations. This number is directly tied to the launch rate term and was originally calculated by Farinella and Cordelli to be 70. This value included fragments released during normal operations as well as a time-averaged number of fragments created by the occasional upper stage failure. Lafleur also used a value of 70 for this coefficient. Using a combination of historical launch data from the SATCAT database and equations from the NASA breakup model, this number was refined for use in the SLOOP model.

A look at historical launch data shows that over the decade from 2002 to 2012, 763 objects were launched into LEO. During this same time period, spacecraft owners and launch providers experienced three failures resulting in fragmentation of either spacecraft or rocket bodies. Two of these events occurred in 2006 [55] with a third occurring in 2012 [56]. Over this same time period, 508 fragments were observed and added to the JSpOC catalog. Of these 508 fragments, 157 were linked through data analysis performed by JSpOC to the three fragmentation events. The NASA breakup model provides the following simple equation for quantifying the number of fragments resulting from a launch fragmentation event:

$$N(L_c) = 6L_c^{-1.6}. \tag{4.19}$$

Based on this equation, it was determined that 28,528 fragments greater than 1 cm in diameter were created by the three fragmentation events over the decade in question. Totaling the number of launched objects and the number of tracked and estimated fragments generated, the β value set for the SLOOP model is 38.06. This value is roughly half the value used by previous models. However, the original value of 70 was

based on the launch record prior to 1991 and the number of launch-related fragmentation incidents has dropped significantly over the past 25 years.

4.2.4.1 Fragmentation Coefficients: Layered LEO Representation

The mean value for the mass of an intact object in each of the orbital shells was used to determine the number of fragments resulting from a catastrophic intact-intact collision. The data was drawn from various sources including the STK spacecraft database and several internet sources.[38,41,42,43] A graph of the mass data for intact objects is provided in Figure 4.25. Similarly, the mean value for the mass of fragments was used to calculate the number of fragments resulting from a non-catastrophic, fragment-intact collision. This data was drawn largely from the MASTER2009 model, as was previously discussed in section 4.2.2. A graph of this data is provided in Figure 4.26. The resulting values for β, α, and γ are provided for each orbital shell in Table 4.7.

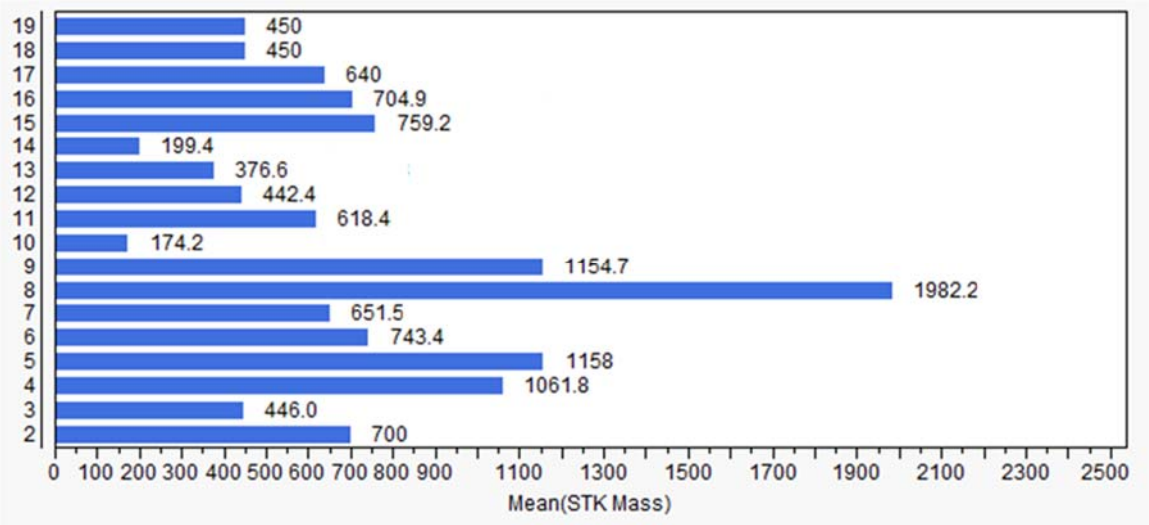

Figure 4.25: Mean Mass of Intact Objects by EAC Bin

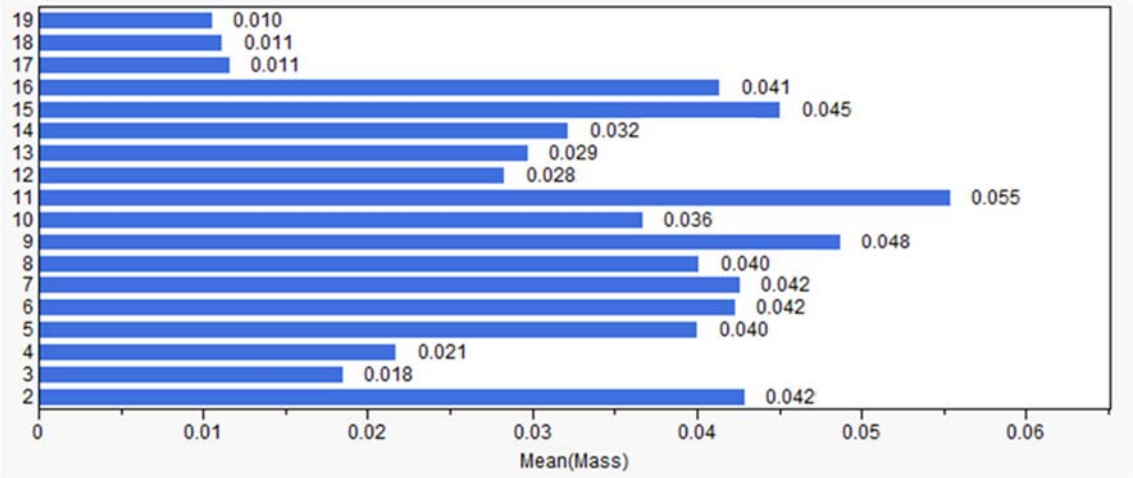

Figure 4.26: Mean Mass of Fragments by EAC Bin

Table 4.7: Fragmentation Coefficients by EAC Bin

	Coefficient Values		
Orbital Shell	β	α	γ
200-300	38.06	193.8	60199.9
300-400	38.06	102.5	42936.3
400-500	38.06	115.1	82284.1
500-600	38.06	180.8	87812.0
600-700	38.06	187.6	62981.1
700-800	38.06	187.6	57045.6
800-900	38.06	182.9	131411.5
900-1000	38.06	205.2	87625.2
1000-1100	38.06	165.1	21212.5
1100-1200	38.06	223.8	54861.9
1200-1300	38.06	134.6	42671.1
1300-1400	38.06	138.8	37822.1
1400-1500	38.06	146.8	23473.9
1500-1600	38.06	188.1	63980.4
1600-1700	38.06	175.6	60517.2
1700-1800	38.06	67.3	56286.9
1800-1900	38.06	65.3	43219.7
1900-2000	38.06	61.9	43219.7

4.2.4.2 Fragmentation Coefficients: Bulk LEO Representation

The fragmentation coefficients for the bulk representation of LEO are based on the overall average mass values for intact objects and fragments within the entire LEO region. The distributions for fragment mass and intact object mass are provided in Figure 4.27. The resulting fragmentation coefficients for the bulk LEO representation are provided in Table 4.8.

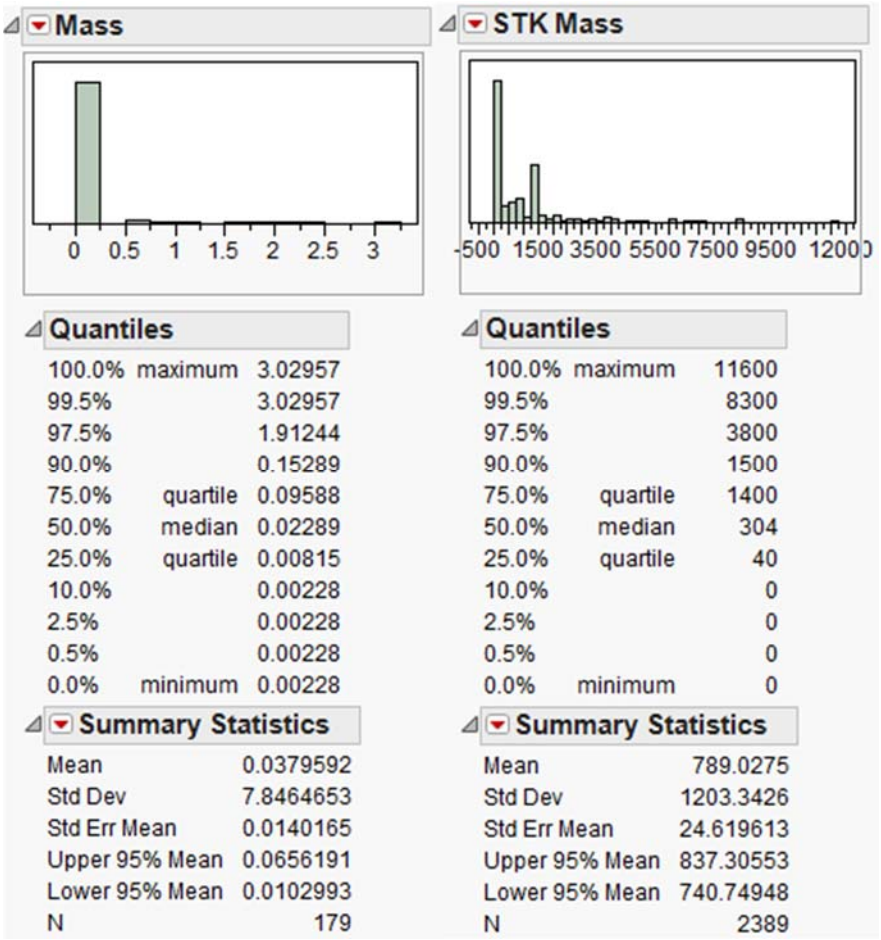

Quantiles		
100.0%	maximum	3.02957
99.5%		3.02957
97.5%		1.91244
90.0%		0.15289
75.0%	quartile	0.09588
50.0%	median	0.02289
25.0%	quartile	0.00815
10.0%		0.00228
2.5%		0.00228
0.5%		0.00228
0.0%	minimum	0.00228

Summary Statistics	
Mean	0.0379592
Std Dev	7.8464653
Std Err Mean	0.0140165
Upper 95% Mean	0.0656191
Lower 95% Mean	0.0102993
N	179

Quantiles		
100.0%	maximum	11600
99.5%		8300
97.5%		3800
90.0%		1500
75.0%	quartile	1400
50.0%	median	304
25.0%	quartile	40
10.0%		0
2.5%		0
0.5%		0
0.0%	minimum	0

Summary Statistics	
Mean	789.0275
Std Dev	1203.3426
Std Err Mean	24.619613
Upper 95% Mean	837.30553
Lower 95% Mean	740.74948
N	2389

Figure 4.27: Histogram of Mass for Fragments and Intact Objects for Bulk LEO Model

Table 4.8: Fragmentation Coefficients for Bulk LEO Model

Coefficient Values		
β	α	γ
38.06	169.5	65855.43

4.2.5 Post-Mission Disposal Rate

The percentage of launched objects compliant with the 25-year guideline for post-mission disposal can be set by the user. The application of this value is found in the deorbit percentage coefficient, *p*, in Equations 3.3 and 3.4. This value splits the number of intact objects into two sub-populations whose totals are tracked by these two equations. The benchmark value for this user input was set at 70% based on results of analysis published in DARPA's 2009 Catcher's Mitt report.[15] Variations on this value can easily be executed by the user to determine model sensitivity.

4.3 Initial Population Data

Initial values are required for the various populations tracked by the SLOOP model. Fragment populations were created through a combination of the MASTER2009 model results and the objects characterized as debris in the JSpOC catalog. The remaining JSpOC catalog items were tallied to develop the intact object initial population values. For the purposes of comparison to the benchmark data set, the populations were established up through 2011. The most recently published results from the LEGEND model were published in 2011 and by excluding the recent years of launch activity, the results from the SLOOP model are not skewed by the CubeSat launches of the recent past. This provides a consistent point of comparison and establishes a pre-CubeSat market "business-as-usual" benchmark from which to evaluate future launch cadence scenarios that may or may not include significant increases in CubeSat launches. The

layered model populations of fragments and intact object are provided in Figures 4.28 and 4.29.

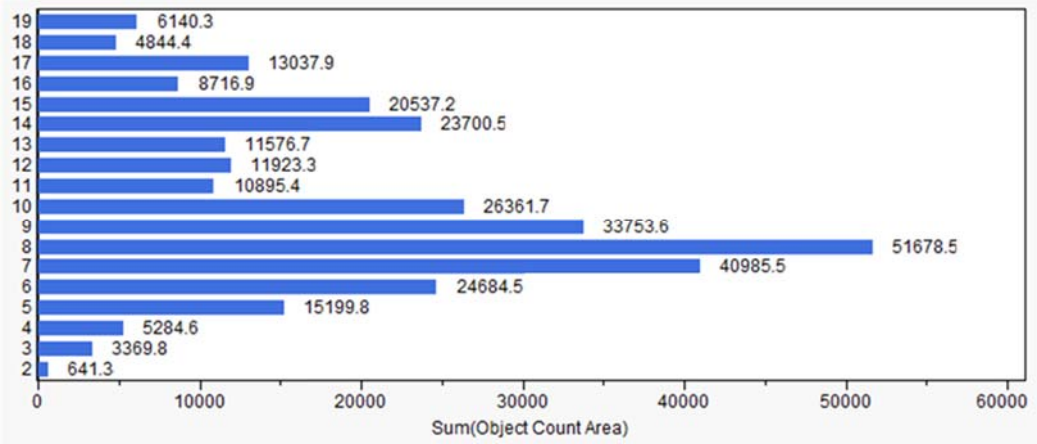

Figure 4.28: Initial Number of Fragments by EAC Bin

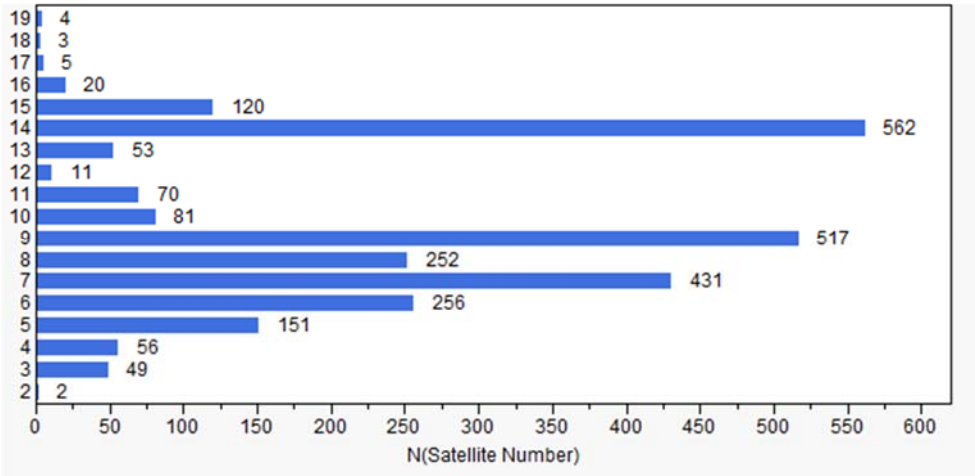

Figure 4.29: Initial Number of Intact Objects by EAC Bin

The initial intact object populations are applied entirely to the naturally decaying intact object sub-population. The initial values for the PMD-compliant intact object sub-population are set to zero meaning that the user-defined PMD percentage is applied to all new launches that occur. For the bulk representation of LEO, the sum total of the layered populations is used as the initial value for the populations. The intact object initial population was taken as 2644 and the initial fragment population was set at 313378.

CHAPTER 5:

BENCHMARKING AND SELECTED ANALYSIS RESULTS

After completing the determination of coefficients, the SLOOP model was compared to the benchmark data described in Chapter 3. A series of sample analyses were performed to compare the functionality and results of the new bulk and layered representations of LEO. Results from both sets of input coefficients were compared to the benchmark data. In addition to population data, the projected number of collisions was also collected and compared. Finally, an evaluation of the sensitivity of the model to user-specified post-mission disposal rate was evaluated and compared to benchmark LEGEND data from recent publications.

5.1 Initial Model Runs

The SLOOP model was run using the coefficient values produced in Chapter 4. The model was first run using the coefficients calculated for the bulk representation of LEO. These coefficients assume that the volume investigated extends continuously from 200 km altitude to 2000 km altitude and that all orbit lifetimes represent the total time to enter Earth's atmosphere. A summary of the input coefficients and initial values is provided in Table 5.1.

Table 5.1: Coefficient and Initial Population Values for the Bulk LEO Model

Symbol	Coefficient	Value
a	Launch Term 1: Vertical Shift	70.9
b	Launch Term 2: Amplitude	22.3
c	Launch Term 3: Period	0.302
d	Launch Term 4: Phase Shift	0.439
f	Intact Object Decay Rate: Vertical Shift	7938.0
g	Intact Object Decay Rate: Amplitude	40
h	Intact & Fragment Decay Rate: Period	7022.7
k	Intact & Fragment Decay Rate: Phase Shift	0
x	Intact-Fragment collision likelihood	4.54E-10
y	Intact-Intact collision likelihood	8.84E-10
β	Fragments produced per satellite deployment	38.06
p	Fragment Decay Rate: Vertical Shift	0.7
q	Fragment Object Decay Rate: Amplitude	0
α	Fragments produced in Intact-Fragment collisions	169.5
γ	Fragments produced in Intact-Intact collisions	65855.4
z	Fragment-Fragment collision likelihood	1.97E-13
NN_0	Initial Intact Object Population	2644
n_0	Initial Fragment Population	313377.8

The SLOOP model was next run using coefficients calculated for the layered representation of LEO. The data collected was evaluated against the benchmark data and then compared to determine the consistency of analysis between the bulk and layered representations. Tables 5.2 – 5.4 contain the full set of layered coefficients and initial population values.

Table 5.2: Coefficient and Initial Population Values for the Layered LEO Model (Table 1 of 3)

	EAC Bin					
Symbol	200 km	300 km	400 km	500 km	600 km	700 km
a	7.00	10.00	3.02	4.43	13.00	20.00
b	6.00	3.00	1.65	-2.87	8.52	14.00
c	-0.19	0.90	0.70	0.23	0.18	0.30
d	1.30	-1.90	-4.45	0.83	-2.57	-0.20
f	10.3	10.7	19.9	37.6	115.1	314.1
g	10.3	10.7	19.9	37.6	40	40
h	0.04	0.41	2.0	6.9	34.7	107.7
k	0	0	0	0	0	0
x	1.765E-08	4.393E-09	1.540E-08	1.942E-08	8.997E-09	9.926E-09
y	3.441E-08	8.423E-09	3.013E-08	3.804E-08	1.743E-08	1.922E-08
β	38.06	38.06	38.06	38.06	38.06	38.06
p	50%	50%	50%	50%	50%	50%
q	0	0	0	0	0	0
α	193.8	102.5	115.1	180.8	187.6	187.6
γ	60199.9	42936.3	82284.1	87812.0	62981.1	57045.6
z	4.724E-12	3.555E-12	3.687E-12	4.087E-12	4.535E-12	4.729E-12
NN_0	2	49	56	151	256	431
n_0	641.3	3369.9	5284.7	15199.9	24684.6	40985.6

Table 5.3: Coefficient and Initial Population Values for the Layered LEO Model (Table 2 of 3)

	EAC Bin					
Symbol	800 km	900 km	1000 km	1100 km	1200 km	1300 km
a	5.70	7.00	0.62	0.62	0.24	0.57
b	2.85	6.00	0.00	0.00	0.00	0.00
c	1.41	-0.19	0.00	0.00	0.00	0.00
d	2.38	1.30	0.00	0.00	0.00	0.00
f	1131.4	2252.9	958.5	3574.4	1975.8	5651.9
g	40	40	40	40	40	40
h	260.3	514.6	893.8	1390.9	2039.8	2876.5
k	0	0	0	0	0	0
x	1.468E-08	8.995E-09	7.117E-09	1.050E-08	1.720E-08	5.864E-09
y	2.868E-08	1.742E-08	1.379E-08	2.042E-08	3.375E-08	1.135E-08
β	38.06	38.06	38.06	38.06	38.06	38.06
p	50%	50%	50%	50%	50%	50%
q	0	0	0	0	0	0
α	183.0	205.2	165.1	223.8	134.6	138.8
γ	131411.5	87625.2	21212.5	54861.8	42671.1	37822.1
z	4.249E-12	4.318E-12	3.504E-12	3.965E-12	3.098E-12	2.807E-12
NN_0	252	517	81	70	11	53
n_0	51678.5	33753.7	26361.8	10895.5	11923.4	11576.8

Table 5.4: Coefficient and Initial Population Values for the Layered LEO Model (Table 3 of 3)

	EAC Bin					
Symbol	1400 km	1500 km	1600 km	1700 km	1800 km	1900 km
a	17.00	0.38	0.33	0.19	0.14	0.19
b	13.30	0.00	0.00	0.00	0.00	0.00
c	-0.16	0.00	0.00	0.00	0.00	0.00
d	0.54	0.00	0.00	0.00	0.00	0.00
f	4850.4	8869.8	15392.9	17779.2	22754.2	26722
g	40	40	40	40	40	40
h	3920.6	5215.5	6855.1	9013.1	11675.9	15052.8
k	0	0	0	0	0	0
x	3.529E-09	9.538E-09	6.683E-09	8.011E-09	6.458E-09	6.611E-09
y	6.789E-09	1.862E-08	1.298E-08	1.568E-08	1.260E-08	1.291E-08
β	38.06	38.06	38.06	38.06	38.06	38.06
p	50%	50%	50%	50%	50%	50%
q	0	0	0	0	0	0
α	146.8	188.1	175.6	67.3	65.3	61.9
γ	23473.9	63980.4	60517.2	56286.9	43219.7	43219.7
z	2.655E-12	2.833E-12	2.730E-12	1.945E-12	1.864E-12	1.806E-12
NN_0	562	120	20	5	3	4
n_0	23700.6	20537.3	8716.9	13037.9	4844.4	6140.3

5.1.1 Benchmark Comparison: Bulk LEO Representation

The bulk LEO model was initially run to provide a prediction of populations and collisions over the next 200 years, consistent with the data derived from published results of the LEGEND tool. Data was collected regarding the population of intact objects and fragments over that time period. Data was also collected for the population of objects greater than 10 cm, a combination of the intact and fragment populations which is consistent with the results published by the LEGEND tool. This population is plotted with the approximated LEGEND population count in Figure 5.1. Figure 5.2 shows a similar comparison between the SLOOP fragment population and the MASTER2009 data approximation.

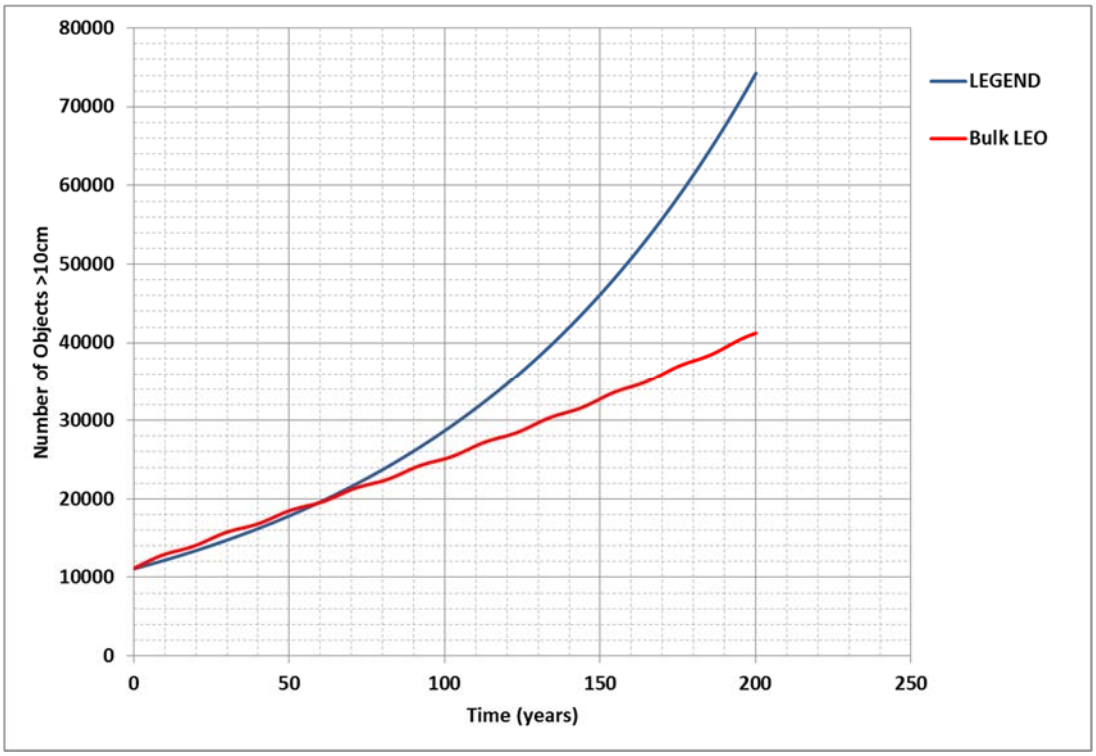

Figure 5.1: Comparison of SLOOP Bulk LEO Model Results to LEGEND for Objects >10cm

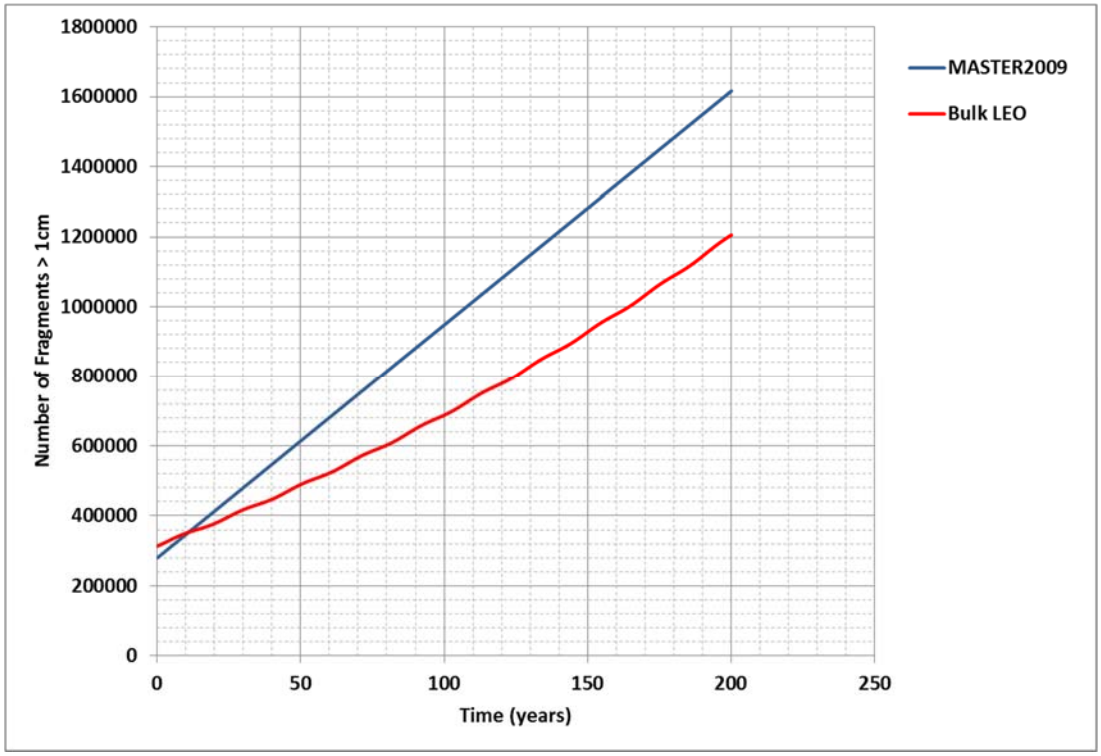

Figure 5.2: Comparison of SLOOP Bulk LEO Model Results to MASTER2009 for Fragments >1cm

There are several items to note from these two plots. First, the SLOOP model appears to under predict the populations of objects greater than 10 cm and fragments when compared to the benchmark data. This is especially true at time steps beyond 100 years. It is important to remember that the number of objects greater than 10 cm contains a portion of the fragment population. Therefore, if the fragment population is underpredicted, the LEGEND comparison data will also be underpredicted. A calculation of the percent error between the SLOOP bulk LEO model and the benchmark data is provided in Figure 5.3.

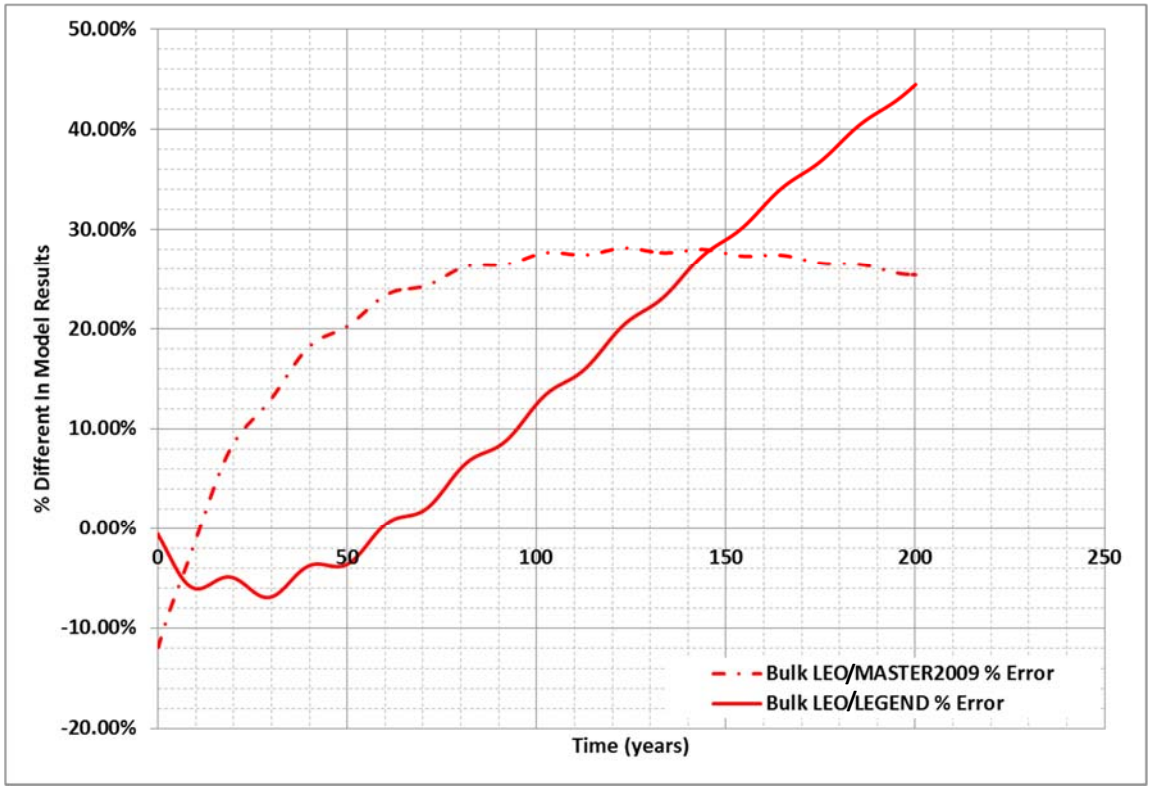

Figure 5.3: Plot of % Difference Between the SLOOP Model and the Benchmark Data

The under prediction observed in the population plots is quantified by the percent error calculation. While the percent error compared to the LEGEND model climbs to 40% over a 200 year time projection, it is also clearly shown that the error remains

between -10% and 10% error for the first 95 years of the simulation. In the original LEGEND data plot used to produce the LEGEND benchmark curve fit, the error bars are provided that resulted from 100 Monte Carlo runs of the LEGEND tool. This percent error is a consistent +/- 23% over the 200 year prediction window. The SLOOP model is well within this percentage of variability through 100 years. This leads to a general guideline that the SLOOP model projection window should be limited to 100 years to ensure relatively consistent results when compared to higher fidelity codes.

In comparing the LEGEND and MASTER2009 benchmark plots above to the 200 year plots of the Lafleur model results, it can also be concluded that the SLOOP model is a significant improvement over previous attempts to produce a simplified modeling approach to predict future populations of orbital objects. The Lafleur model was reasonably consistent with the original Farinella-Cordelli model, both of which significantly over predicted the object populations when compared to current high fidelity tools, as shown in Chapter 3. The SLOOP bulk model is also a simplified approach and, if limited to 100 year projections, provides reasonably close approximations of the high fidelity tool predictions with significant reductions in run times and user interface complexity.

5.1.2 Benchmark Comparison: Layered LEO Representation

The SLOOP model was next run using the layered LEO representation data. By representing LEO as a series of shells of interest rather than one single volume, more accurate information is made available about the interaction of the different population concentrations at various altitudes. When the populations of each layer of the analysis are combined to provide a total population of intact objects and fragments, these numbers

can be compared to the benchmark data sets just as with the bulk LEO representation. The comparison of the layered model with the LEGEND and MATER2009 benchmark data is provided in Figures 5.4 and 5.5. A divergence from the benchmark data similar to that of the bulk LEO representation can be seen in both of the predicted populations.

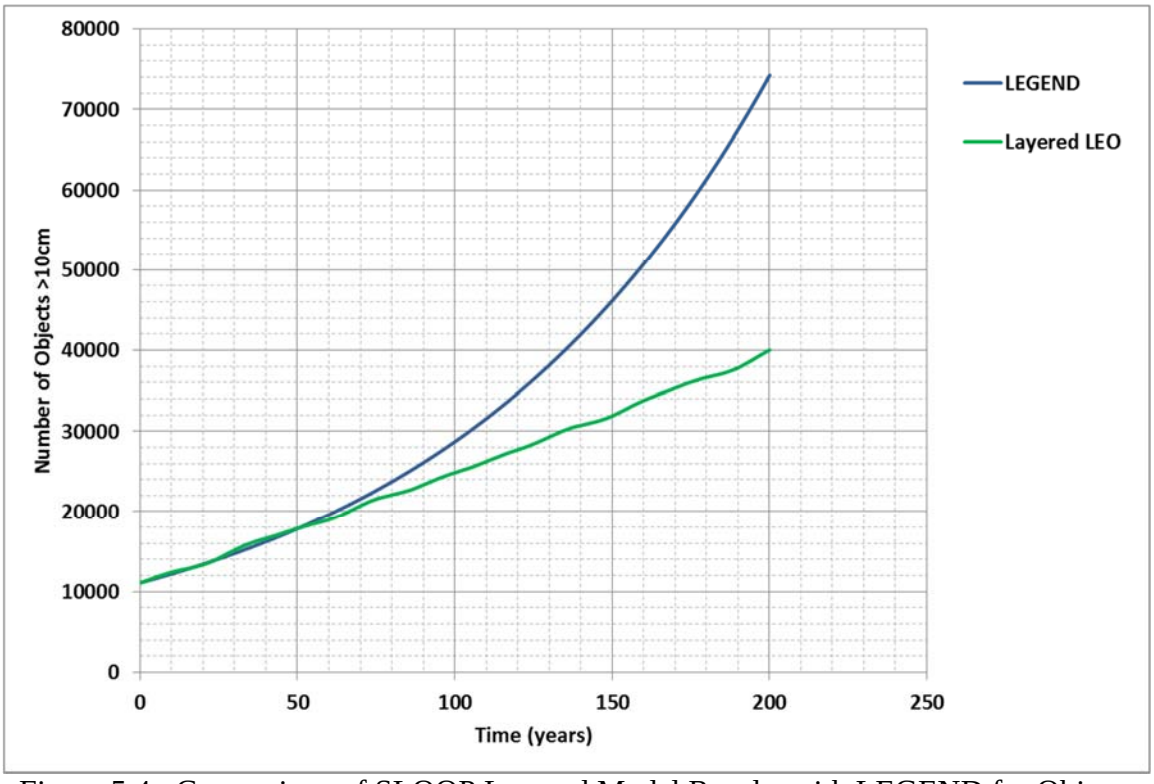

Figure 5.4: Comparison of SLOOP Layered Model Results with LEGEND for Objects >10cm

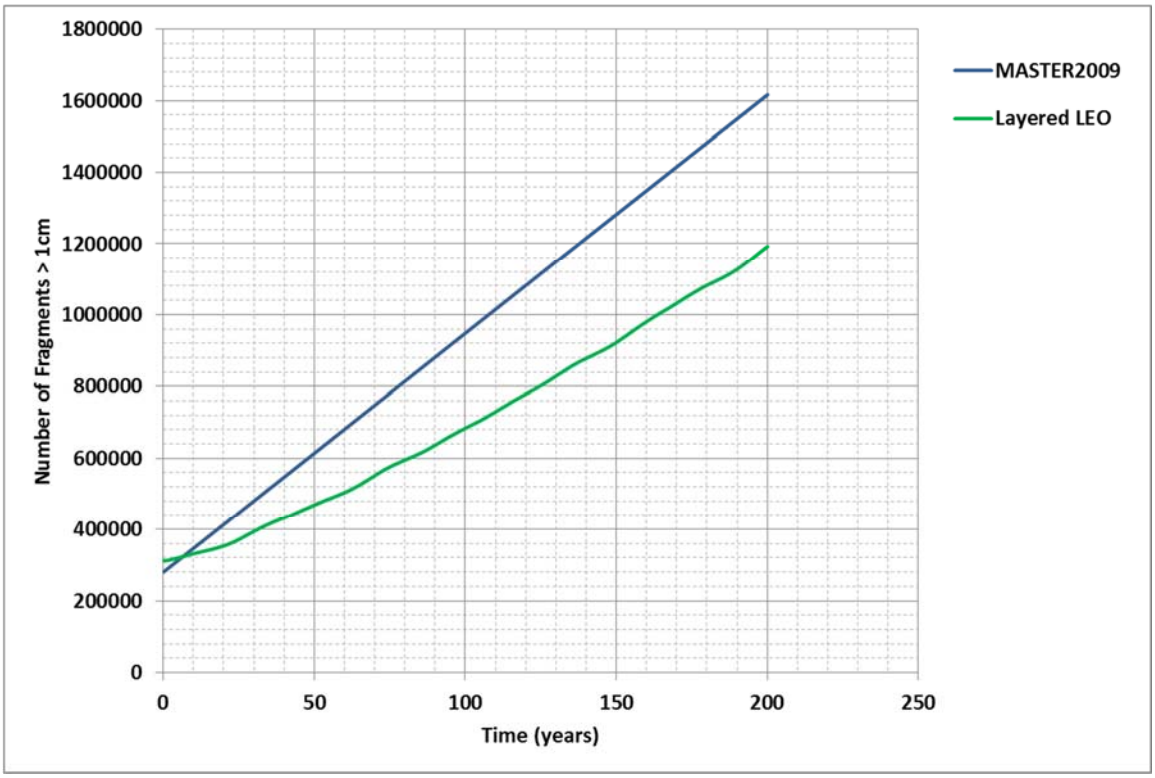

Figure 5.5: Comparison of SLOOP Layered Model Results with MASTER2009 for Fragments >1cm

5.1.3 Comparison: Layered vs. Bulk LEO Representation

The data produced in both the bulk and layered LEO representations is plotted together in Figures 5.6 and 5.7. These plots show how close the predictions are to each other. Both the bulk and the layered representations match the LEGEND data very well over a 100 year projection with a maximum percent error of 12.5% for the bulk model and 13.25% for the layered model. The layered model does appear to under predict the population of objects greater than 10 cm by a slightly larger margin than the bulk model. This small differential in population is expected due to the slightly higher fidelity of the layered model. By tracking the populations at various layers rather than relying on wide reaching averaged values to represent the population of LEO as a whole, the layered model captures some of the more subtle localized population interactions that become lost in a cumulative representation.

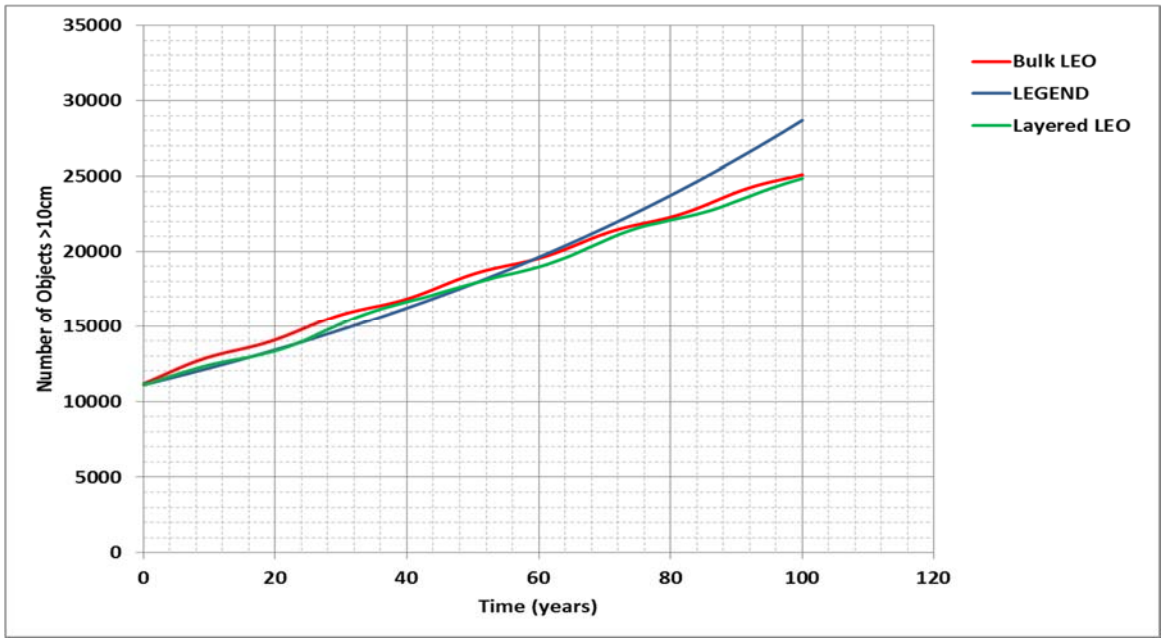

Figure 5.6: Comparison of Bulk and Layered SLOOP Model Results with LEGEND for Objects >10cm over a 100 Year Simulation Period

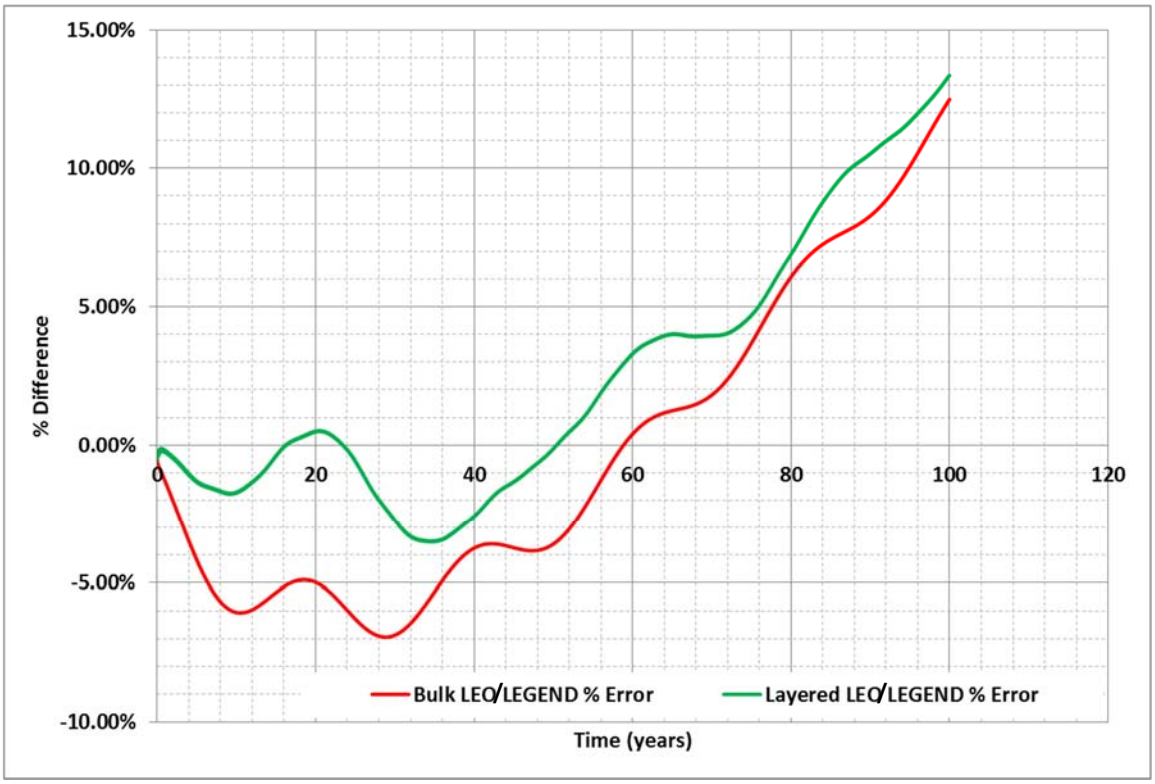

Figure 5.7: Comparison of % Difference Between the Layered and Bulk LEO SLOOP Models and the LEGEND Benchmark Data

This same difference between the bulk and layered representations can be seen in Figure 5.8 which shows the total number of intact objects over time. While the population of tracked objects, represented by the 10 cm threshold set in the data from the LEGEND tool, is a useful benchmark, the true population of interest is the number of intact objects. In previous simplified models of the intact population, the onset of the *Kessler Syndrome* is very obviously indicated in the sharp decline in the population of intact objects. This implies that intact object collisions rates have reached the tipping point after which the population drops over time because the newly launched objects collide almost upon deployment. While previous simplified models show this occurring at or around the 120 year mark (as seen in Figure 2.6) recently published work in this area does not exhibit the same phenomenon.[15,57] Previous data has shown that the Lafleur model significantly overpredicted populations compared to published LEGEND data. While Figure 5.8 shows a slight reduction in the growth of the intact object population, a tipping point is not present. This data is significantly more consistent with recently published data, showing that the SLOOP model exhibits a significant improvement in the representation of high fidelity codes.

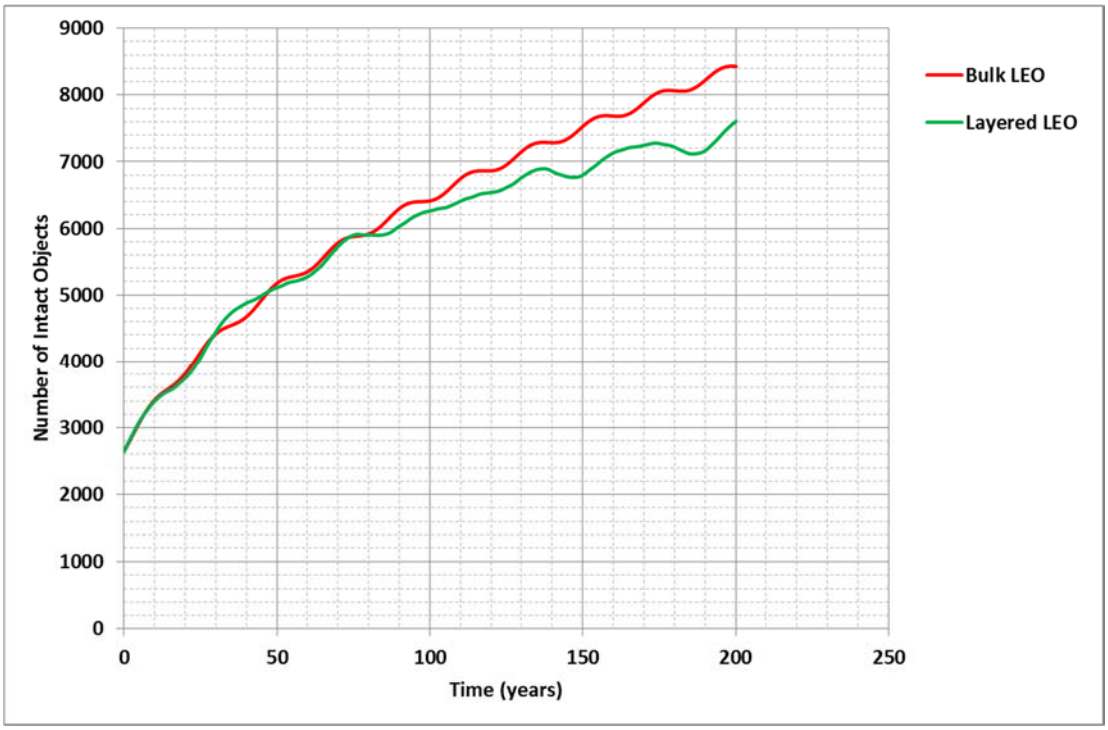

Figure 5.8: Comparison of Intact Object Population Growth Projections using the Bulk and Layered SLOOP Models

It is also important to note that over the first 100 years of the simulation, the bulk and layered representations of LEO present very similar population growth patterns until the simulation nears 100 years. At that point, both models appear to diverge significantly from the LEGEND model but they also exhibit separation between each other, with the layered model showing a lower long term intact object population when compared to the bulk model. Two conclusions can be drawn from this observation. First, the models exhibit very similar behavior which is to be expected when the coefficients for both models have been derived from the same data using similar methods. Second, as will be shown in the next section of this chapter, the layered model is capturing some interactions that are being lost in the mean values of the bulk LEO representation. These subtle, layer-specific interactions are driving the populations lower over time as more collisions are observed in higher population regions of LEO. While the bulk

representation of LEO provides an improved representation of higher fidelity codes than previous simplified model approaches, the SLOOP model appears to be even more accurate when LEO is layered.

5.2 A Deeper Look at the Layered Model

The detail available through the evaluation of LEO as layered region of space can be seen by plotting the data by shells rather than as a cumulative summary value as presented in section 5.1. By quantifying the populations of orbital shells of interest and predicting the behavior of these sub-populations with coefficients specifically derived to capture the unique physical characteristics of these sub-populations, interactions are revealed that would otherwise go unnoticed in the simple bulk representation of LEO. The SLOOP model enables this increased level of fidelity because of its simple algorithms and straightforward coefficient calculation processes.

Figures 5.9 and 5.10 provide the intact object and fragment population projections over the next 100 years with a business-as-usual launch and post-mission disposal rate. This is the same data that was summed and plotted in Figures 5.4 and 5.5 in the previous section. By plotting each individual layer of the model as its own population, the localized trends can be observed. Users can now track the localized trends that result from more populated orbits. Fragment populations, driven by collisions, can reveal which orbital shells are more likely to experience collision events over time. Specifically, observing the fragment population concentrations in Figure 5.10 reveals that there are safer and more collision probable regions of LEO. While most publications tend to represent LEO as a whole region and point to the growing populations as a risk to LEO objects in general, the layered results reveal that this risk is largely localized around

a few key regions of LEO leaving several other “safe zones” in LEO where populations and risks are still relatively low.

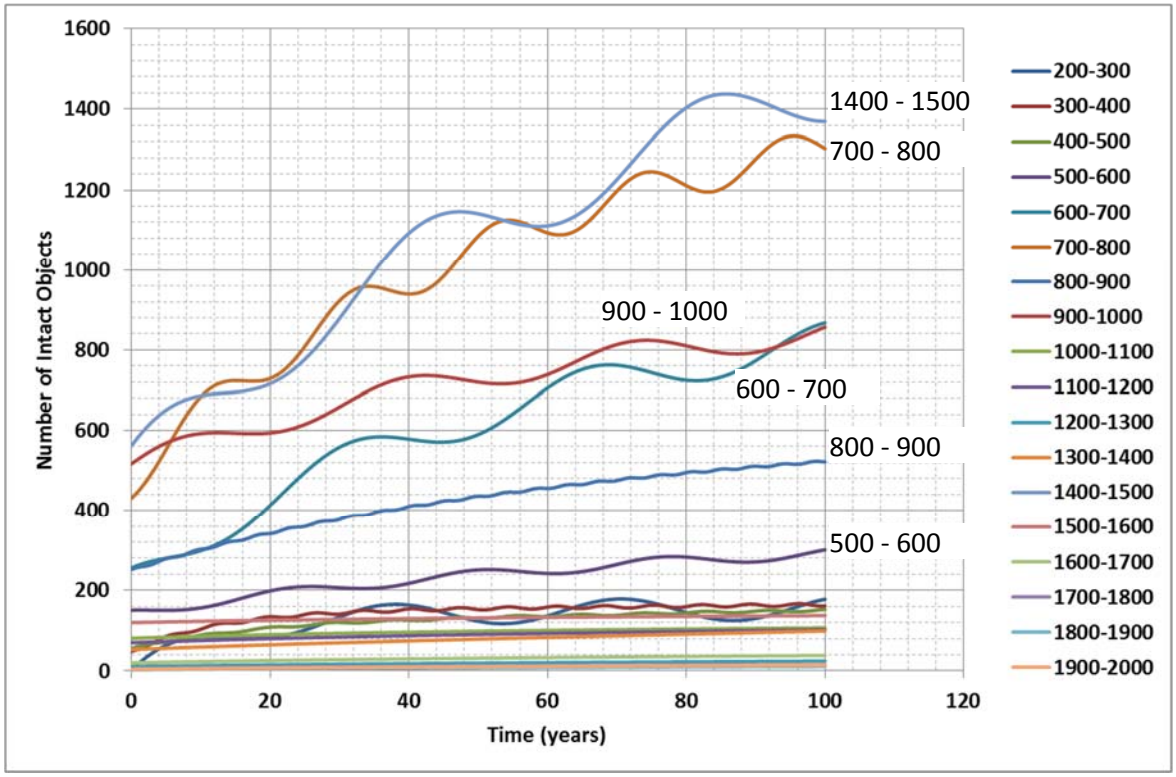

Figure 5.9: Intact Object Population Projections by Altitude Shell

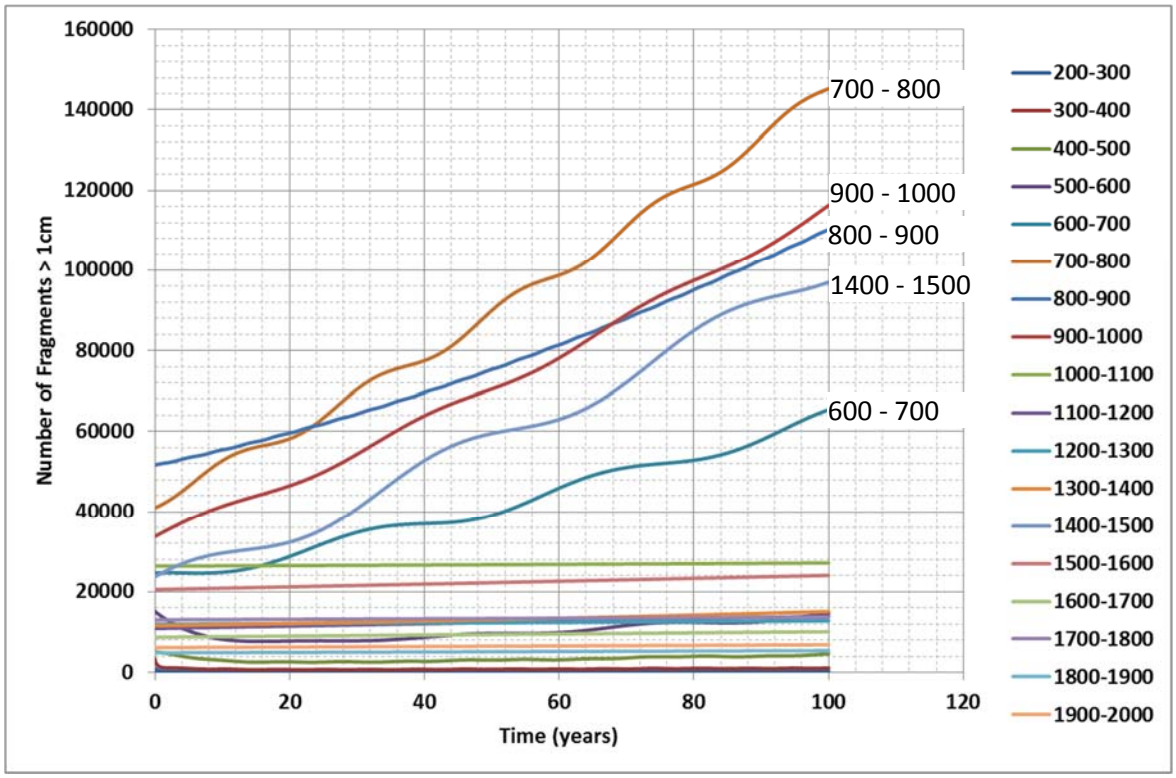

Figure 5.10: Fragment Population Projections by Altitude Shell

The general trends of the intact object populations in different orbital shells can be observed in Figure 5.10. Historical data drives the values of the "*a*" and "*b*" coefficients in Equations 3.3 – 3.5 that combine to form the average launch rate into each shell. By observing the intact object population trends in conjunction with the "*a*" and "*b*" coefficient values from the Tables 5.2 – 5.4, it becomes clear that the orbits that have higher initial intact object populations also show a historical 20 year trend of higher launch rates than other regions of LEO. In the business-as-usual approach to these analysis cases, this trend continues. The launch rate is the only input variable for intact objects. The sinusoidal nature of these launch rates is also observed in the sinusoidal variation over 20 to 40 year periods depending on the historical launch data.

Several of these labeled orbits of high population and subsequent high growth rates are home to several key orbital assets. The shell at 1400 km is home to the Globalstar satellite communications constellation.[14] The shell between 700 and 800 km houses the Iridium and Orbcomm satellite constellations.[14] The A-Train series of Earth observer spacecraft maintained by NASA and NOAA take advantage of the sun-synchronous orbits found at high inclinations between 650 and 700 km.[58] Many rocket bodies and international payloads can be found in the 600 – 800 km region of LEO. It is no surprise that many of these orbits became crowded over the past 20 year, which drives the launch models to project continued growth in these areas.

Also observed from Figure 5.9 is a population trend with a much longer time scale. Although it is most easily observed in the intact object population in the 800-900 km shell, all of the labeled shells in Figure 5.9 show a slight reduction in growth rate exhibited as a concave curvature in the general trend of the data. Since the launch rates are consistently positive on a 20 to 40 year time cycle, a slight concavity in the curvature of these trend lines indicates that over time, the removal rate of the intact objects is beginning to outpace the rate of replenishment. This general trend can be attributed to two phenomena. First, post-mission disposal rates that are sufficiently high will cause population growth to flatten out over time. If satellites and rocket bodies are disposed of when they are replaced, objects will leave orbit at rates close to the rate that they are being added. Many high fidelity models show this trend with post-mission disposal rates of 95% or higher. The baseline business-as-usual post-mission disposal rate is 70%, which is insufficient to cause this trend by itself.

The other potential cause for a slowing of the intact population growth rate is the increase in collision rate. This general trend is the basis for the *Kessler Syndrome*, although the very gradual nature of the growth rate reduction exhibited in these plots suggests that the trend toward a "tipping point" that results in the loss of the use of these regions consistent with the *Kessler Syndrome* is not imminent. However, this trend is a general indicator that more satellites are being lost to collision events as the populations increase. If this is truly the case, a corresponding increase in the fragment population, which is only fed by the collisional generation of fragments, would also be observed.

The plot of fragment population for the individual shells (Figure 5.10) further supports the hypothesis that collisions are occurring in these high population orbits. The orbital shells at 700 km and 1400 km exhibit the highest fragment population growth rate and are also the two orbits with the highest populations of intact objects. The 700-800 km shell only shows a higher fragment population because its initial fragment population is higher than the 1400-1500 km shell. The region of LEO from 700 km to 1000 km has a significant initial fragment population due to the recent Iridium-Cosmos collision and Chinese ASAT tests, both of which occurred in this region of space. Once again, the layered fragment population growth plots show very large regions of space with very little if any growth in the 100 year simulation. This observation further supports the idea that certain LEO "safe zones" exist. Figures 5.9 and 5.10 combined indicate the potential for large numbers of collisions, a trend which is more explicitly discussed in the following section.

5.3 Tracking Collisions with SLOOP

The inclusion of intact-intact and intact-fragment collision terms in the SLOOP model supports the evaluation of population growth trends by tracking the interaction of the orbital object populations. It also supports the tracking of a cumulative number of expected collisions over the duration of a simulation. This value can be tracked for both types of collisions and in both the bulk and layered representations of LEO by isolating the collision terms and incrementally summing their values over time. Figures 5.11 and 5.12 provide these values for the reference business-as-usual case.

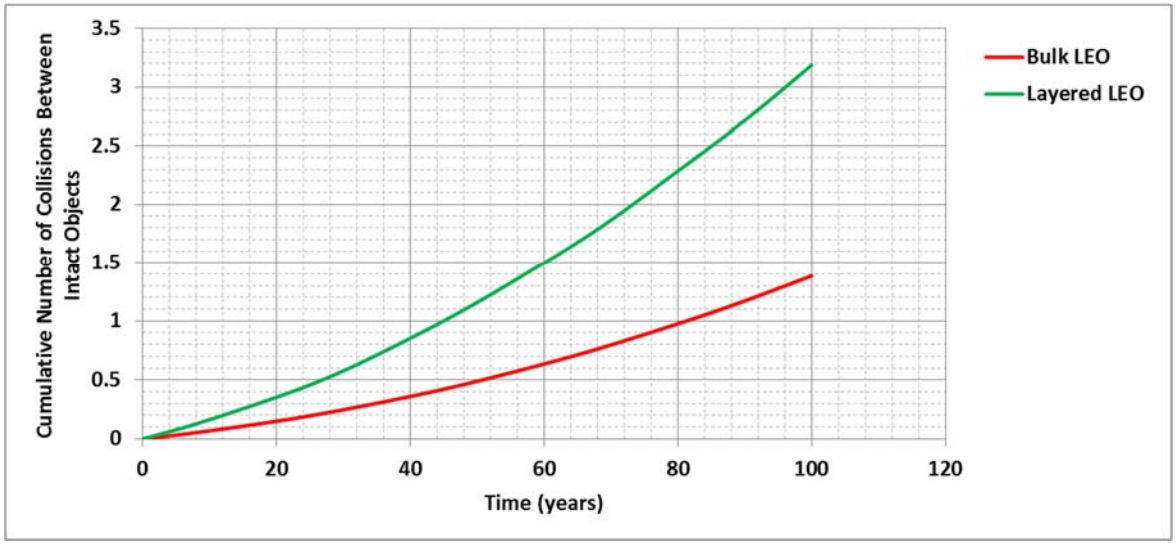

Figure 5.11: Comparison of Predicted Number of Intact Object Collisions

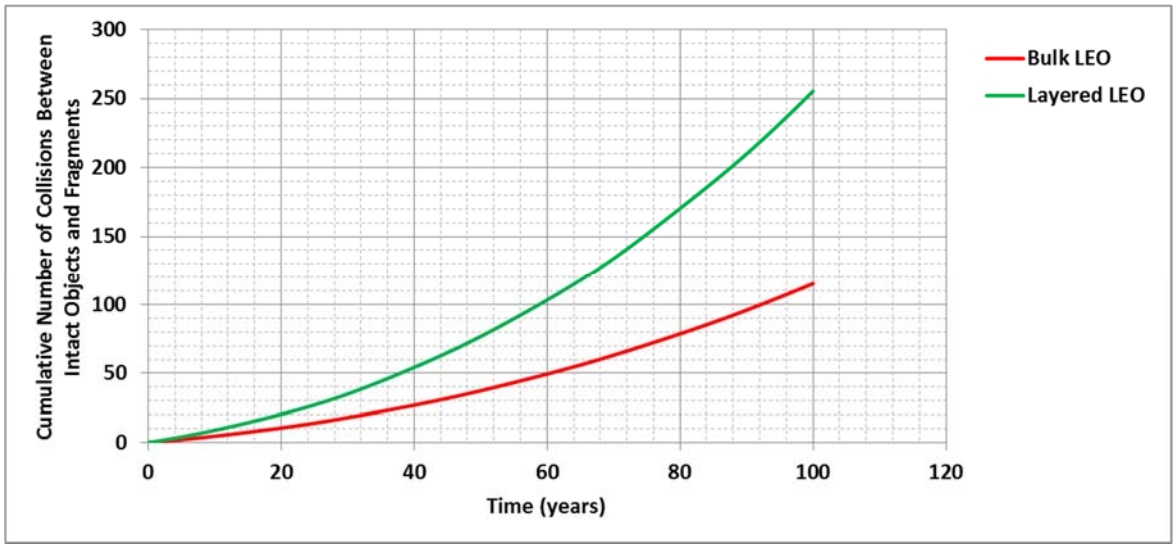

Figure 5.12: Comparison of Projected Number of Collisions Between Fragments and Intact Objects

While the total population values for both fragments and intact objects appear to be consistent between the bulk and layered representations of LEO, it was noted that there was a slightly lower intact object population observed in the layered representation. Looking at the collision plots above, it is noted that the layered version of the SLOOP model records significantly more collisions when compared to the bulk model. The SLOOP model projects between 1 and 3.5 collisions between intact objects over the next 100 years in a business-as-usual scenario. It also predicts as many as 250 collisions between intact objects and fragments over the same time period. When compared to published data, the layered model appears to be a more accurate representation of the expected collisions than the bulk model, further supporting the idea that the simplified model should be executed in layered mode to increase the fidelity of the analysis.

The reason for the discrepancy between the bulk and layered model collision numbers can be shown by looking at the spatial density of the fragments in the two representations of LEO. Figure 5.13 shows the spatial density of fragments in each of the

orbital shells in the layered representation of LEO and the assumed general fragment spatial density that results from the averaged values used in the bulk model, shown as the thick red line. This graph shows that the globally average values used in the bulk model do not account for the concentrated populations of some of the more crowded orbital shells in LEO. These concentrated shells will experience higher rates of collisions but that higher incident rate is lost by treating LEO as one region and using mean values for the coefficients. These results also suggest the preferred mode of operation for the SLOOP model is the layered representation. While the bulk and layered models are fairly close in their overall representation of population increases, when tracking the expected number of collisions, the higher fidelity of the layered model presents a more complete picture of the interactions happening in LEO.

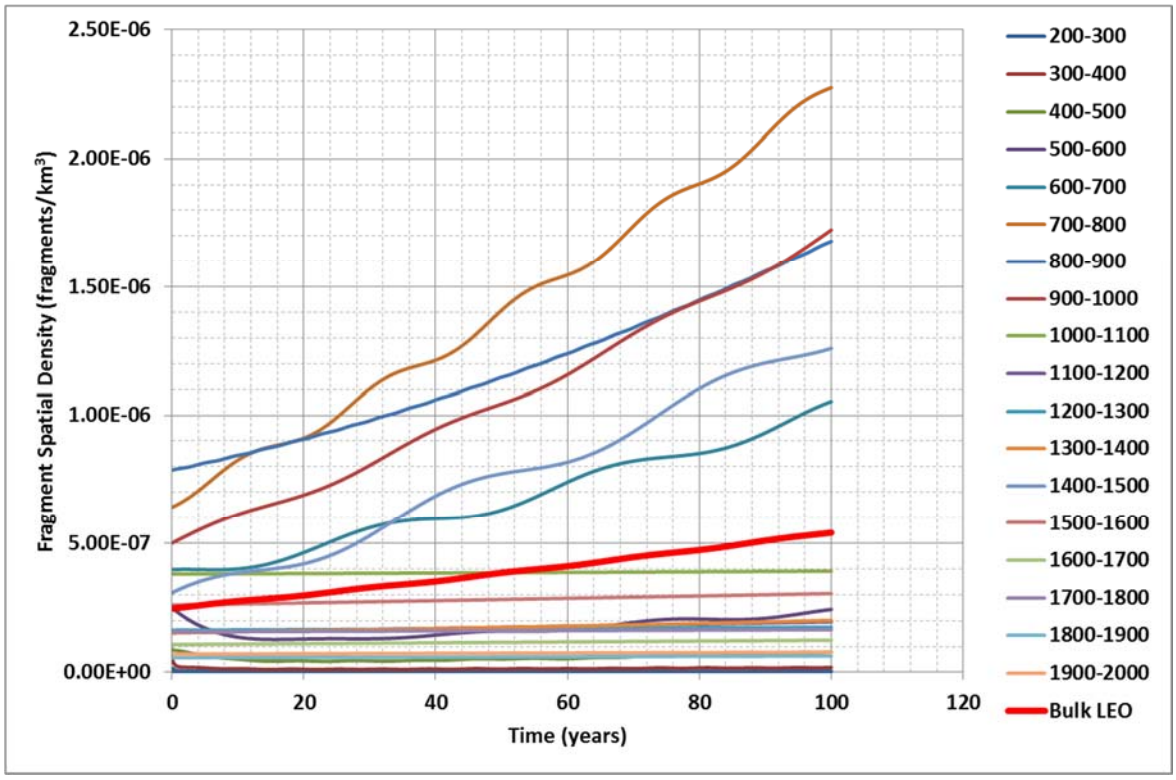

Figure 5.13: Spatial Density of Fragments by Altitude Shell

Using the layered model, the high-risk orbits can be identified and a projected number of collisions can be captured for each orbital shell. This data is provided in Figures 5.14 and 5.15. As was originally suspected based on the projected fragment populations and the general concave shape of the intact object population curves noted in section 5.2, the predicted collision data reveals that the orbital shell between 700 km and 800 km will see the most collisions over the next 100 years in a business-as-usual scenario. High collision rates are also expected in the 900-1000 km shell and the 1400-1500 km shell. Likewise, the cumulative intact-on-intact collision rate shows that one of the 3.5 collisions expected between two intact objects will most likely happen in the 700-800 km shell. These charts also reveal a host of alternative orbits where the collision rates are significantly lower and, therefore, significantly safer than the current high-traffic regions of LEO.

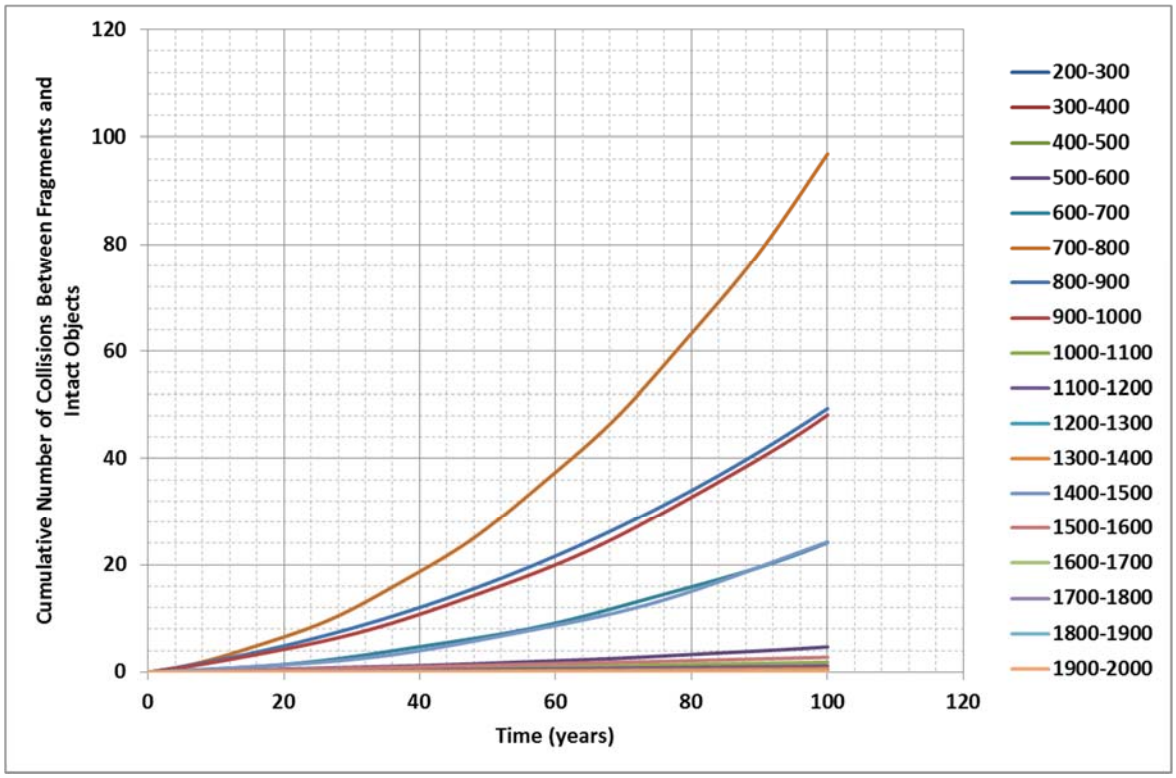

Figure 5.14: Number of Projected Fragment-Intact Collisions by Altitude Shell

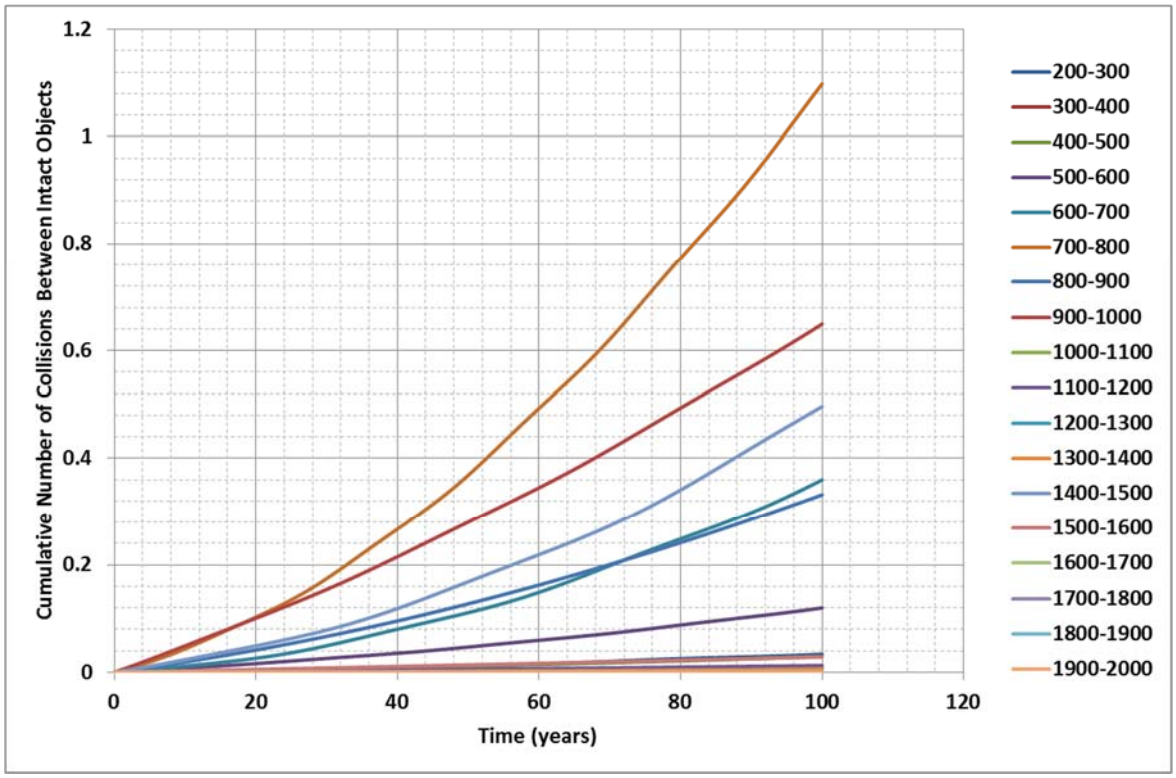

Figure 5.15: Number of Projected Intact Object Collisions by Altitude Shell

5.4 Sensitivities to Major User Inputs

The SLOOP model was next evaluated for sensitivities to the more significant user inputs and assumptions. These sensitivity analyses focused on the number of launches and post-mission disposal rate which are the two major user inputs that drive the types of investigations that the SLOOP model is designed to support. In the baseline model, the launch rates were developed based on historical data while the PMD rate was set to 70% based on an excerpt from DARPA's Catcher's Mitt report.[15] This is the only explicit mention of the post-mission disposal rate found in the current literature and it was not supported by data within the report which calls into question the accuracy of the statement. Therefore, the PMD rate sensitivity analysis is important to establishing the true baseline coefficient set.

5.4.1 PMD Sensitivity

To investigate the sensitivity to PMD rate, four cases were run through the layered representation of LEO in the SLOOP model. The baseline case modeled a 70% PMD compliance rate. Also evaluated were 90%, 50%, and 30% compliance rates. These four cases are compared to the LEGEND benchmark in Figure 5.16. As expected, the higher the PMD compliance rate, the lower the number of projected collisions and the lower the population of intact objects and objects greater than 10 cm. As the PMD rate is decreased, more collisions occur and the populations increase.

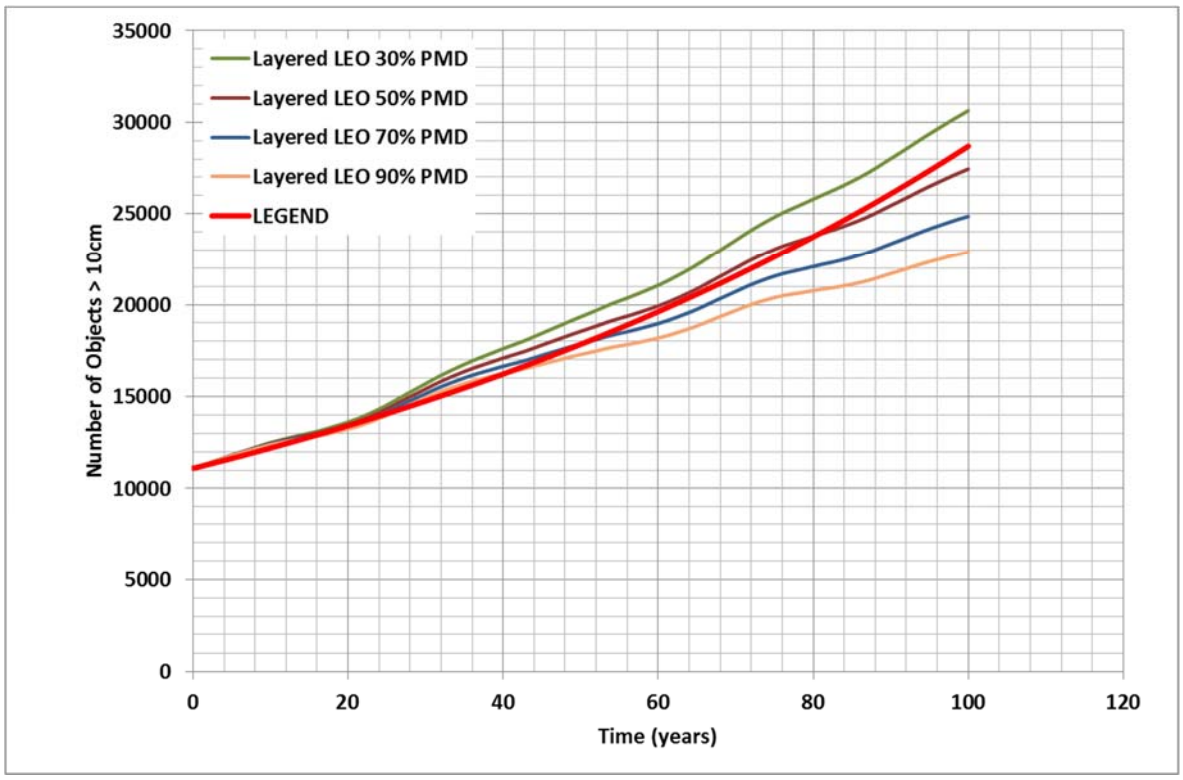

Figure 5.16: Sensitivity of the SLOOP Model Population Projections to Assumed Post-Mission Disposal (PMD) Rate

This plot shows the general trend relating populations and PMD compliance rates. It also shows that the 50% PMD rate generally has the closest correlation with the LEGEND 100 year data. The plot of percent error between these cases and the LEGEND

data is provided in Figure 5.17. The 50% PMD compliance rate shows an error of plus or minus 5% over a 100 year simulation where the baseline 70% PMD rate tends to underpredict populations up to 13% relative to the LEGEND benchmark data. Given this improved fit and the lack of published data relating to the real post-mission disposal rate, the recommended baseline PMD rate for use in the SLOOP model is 50%.

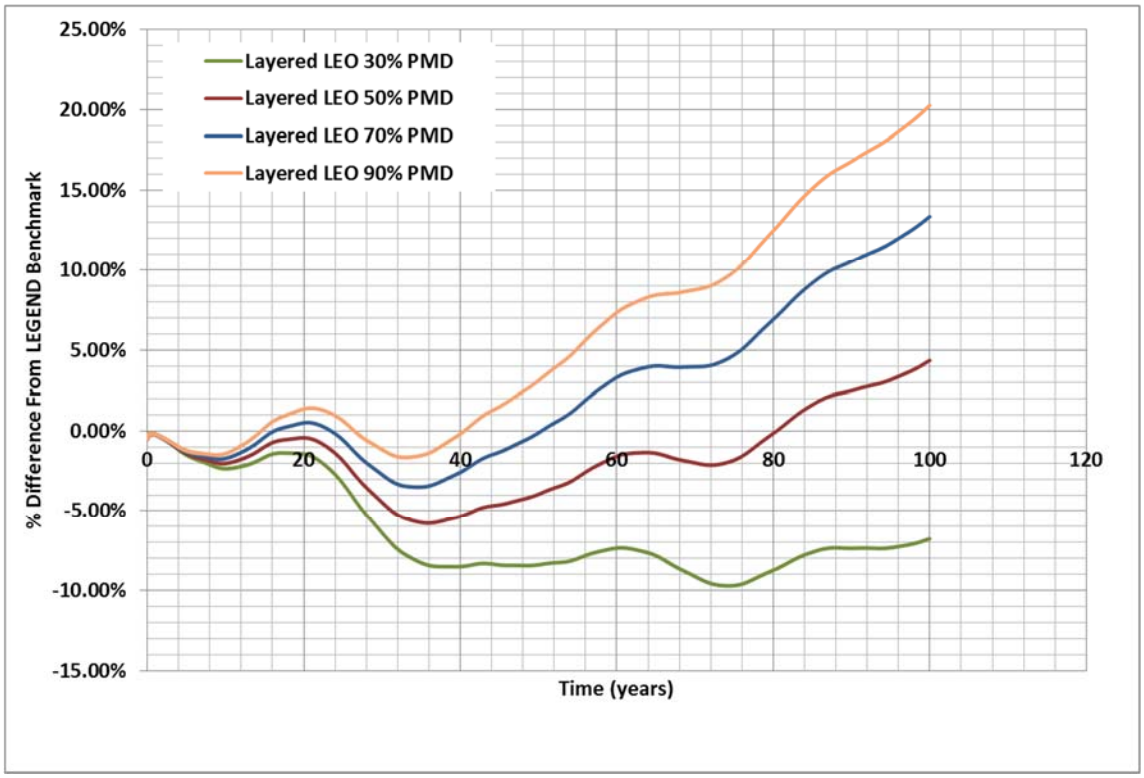

Figure 5.17: Sensitivity of % Difference Between the SLOOP Model and the LEGEND Benchmark Data to Assume PMD Rate

The number of predicted collisions was also capture in this sensitivity analysis. These data are shown in Figures 5.18 and 5.19. This confirms that as PMD rate drops, more collisions will take place. The rate of collisions also increases with time in these plots. This means that as more objects are allowed to remain resident in LEO for longer periods of time, the number of collisions will increase, driving up the fragment population, and further increase the number of potential future collisions. This is more

evidence of the emergence of the *Kessler Syndrome* in LEO, although as was stated previously, this appears to be a more gradual onset than previous simplified models have predicted.

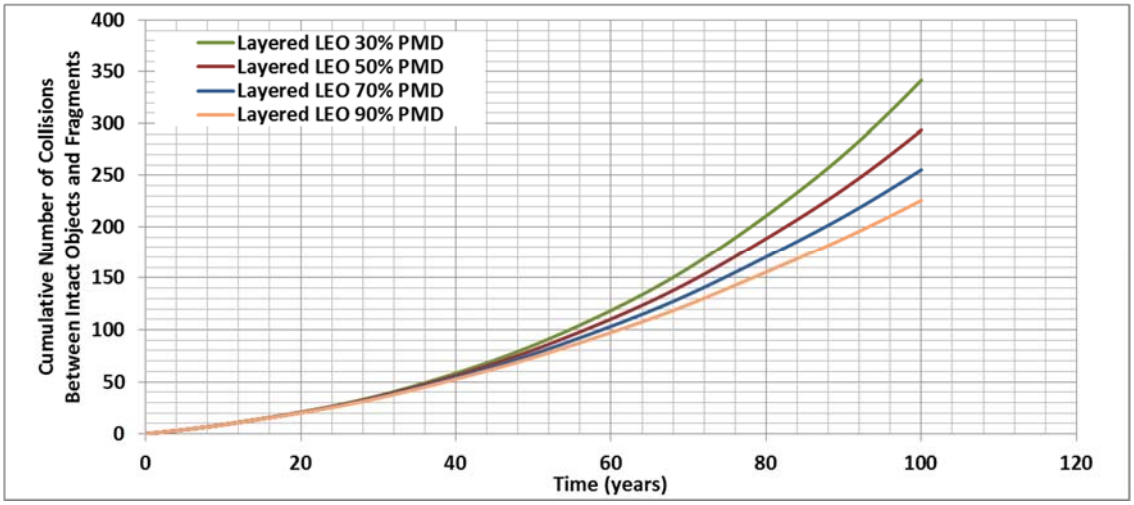

Figure 5.18: Sensitivity of Projected Number of Fragment-Intact Collisions to Assumed PMD Rate

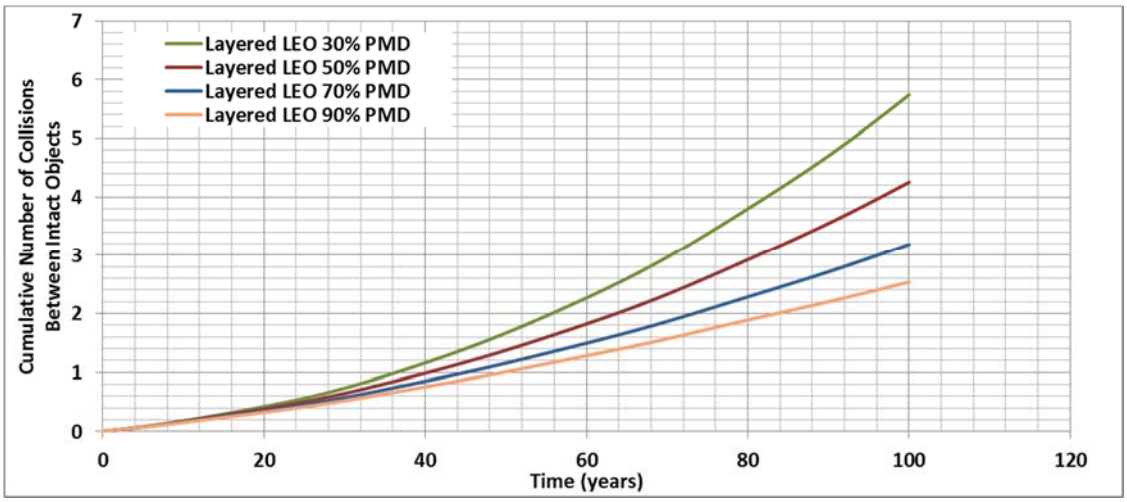

Figure 5.19: Sensitivity of Projected Number of Intact Object Collisions to Assumed PMD Rate

5.4.2 Launch Rate Sensitivities

To investigate the sensitivity to launch rate, an artificial change in the launch rate terms "*a*" and "*b*" was evaluated. Capturing a wholesale change in the launch and

satellite market, these variations show how the number of fragments and intact objects will be affected by launch rate variation. The plots provided in Figures 5.20 and 5.21 track both the intact object and fragment populations as the launch rate is varied in increments of 10% from a 10% reduction in launches to a 20% increase in launches. This results in a 6.65% variation in the populations for every 10% change in the launch rate for both populations at the end of the 100 year simulation.

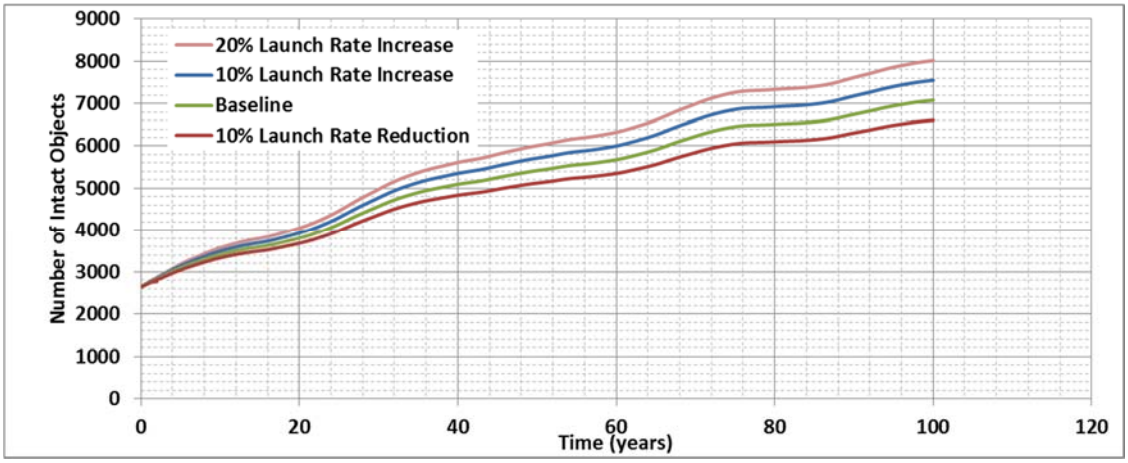

Figure 5.20: Intact Object Population Projection Sensitivity to Launch Rate

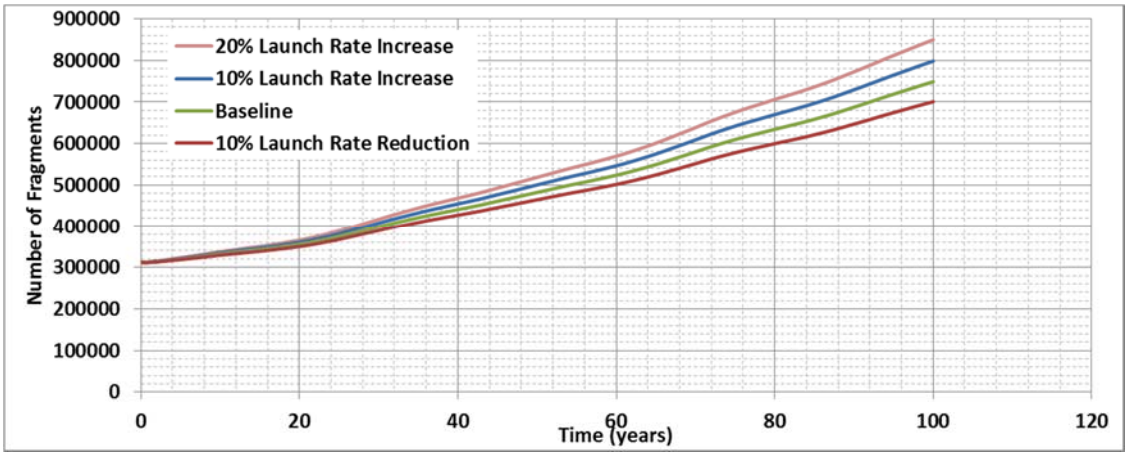

Figure 5.21: Fragment Population Projection Sensitivity to Launch Rate

Another interesting launch rate sensitivity that is often investigated in these analyses is the case of no new launches. This represents the absolute minimum impact to

the future population. Figures 5.22, 5.23, and 5.24 show the number of fragment-intact object collisions, the number of intact objects and the number of fragments over a 100 year period for three different scenarios. The baseline scenario is a business-as-usual scenario with the baseline historical data-based launch rates and 50% post-mission disposal compliance. The second scenario is the same launch rate but a 90% PMD compliance. The third scenario is 50% post mission disposal but no new launches.

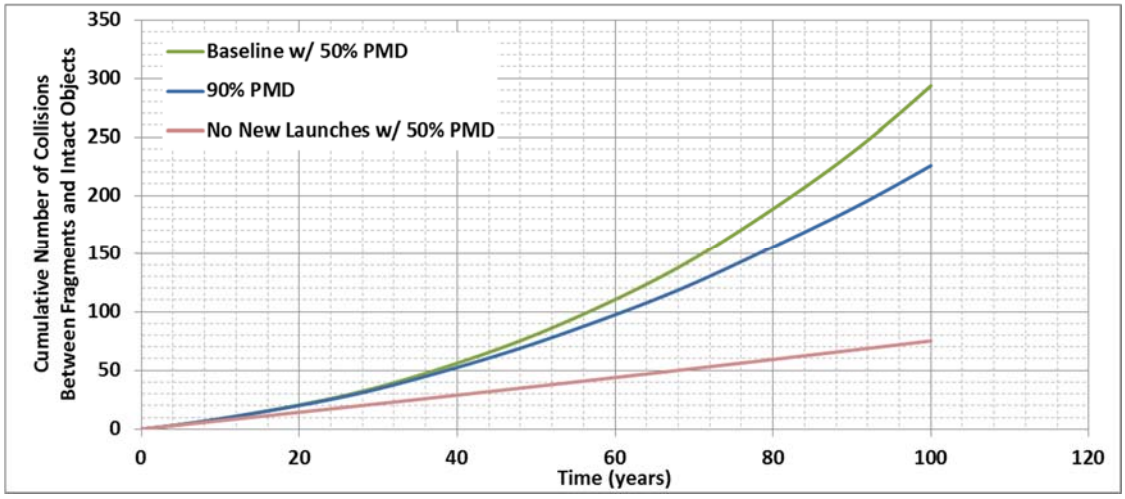

Figure 5.22: Sensitivity of Number of Fragment-Intact Collisions to Future Operational Scenarios

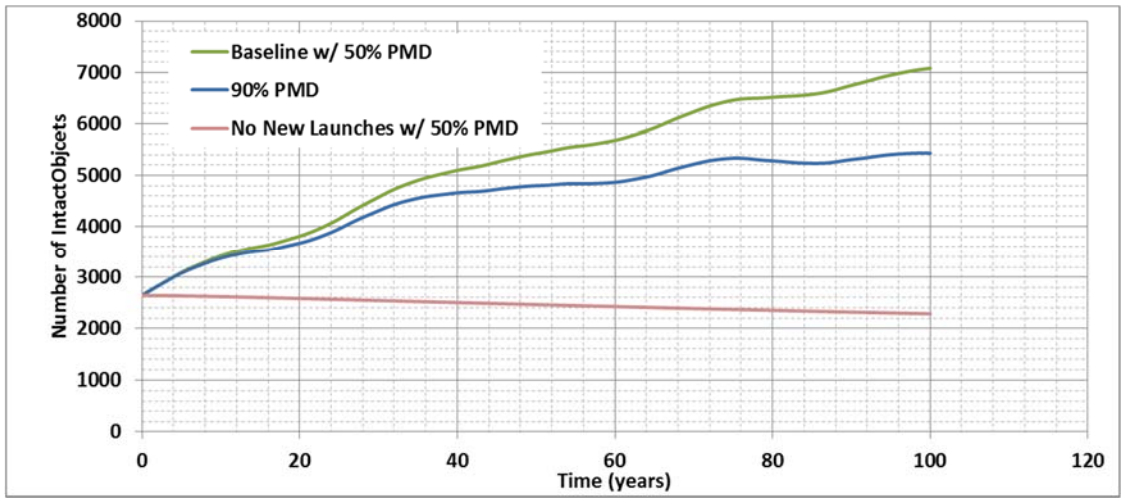

Figure 5.23: Sensitivity of Number of Intact Objects to Future Operational Scenarios

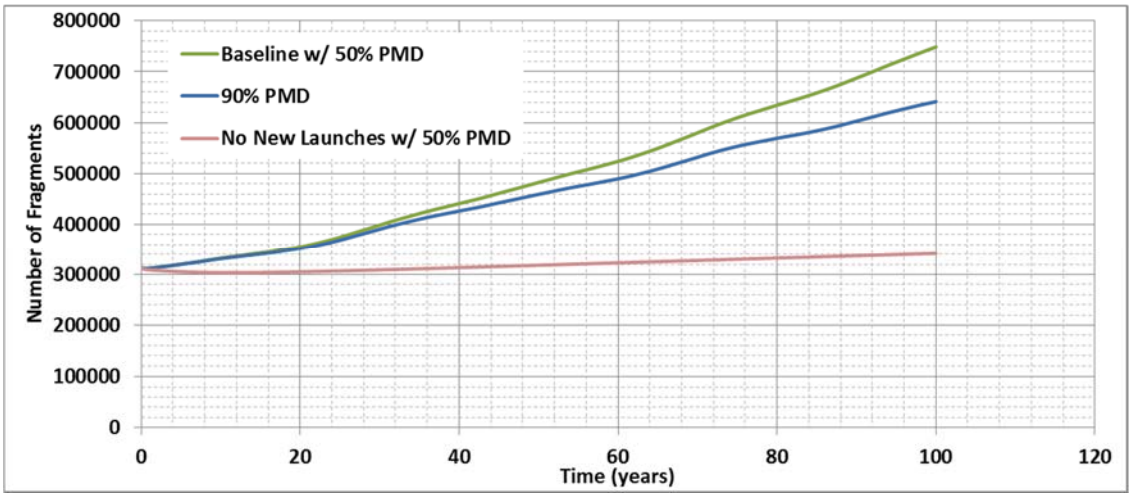

Figure 5.24: Sensitivity of Number of Fragments to Future Operational Scenarios

Two main trends can be seen from these plots that are consistent with other high-fidelity analyses. They confirm the previously observed trend that higher PMD compliance rates result in reduced numbers of collisions. Combined with the fact that more objects are being deorbited within 40 years of launch, this results in lower populations of both fragments and intact objects. The second trend of note is that, even with no new objects being launches into LEO for the next 100 years, there are still 75 fragment-intact object collisions expected. While the no new launches scenario does result in a gradual decrease in the intact object population, this results in only a reduction of a few hundred objects over a 100 year time period. In that time, the fragment population continues to grow due to collisions. This result indicates that even halting all launches will not solve the over-population issues. This finding is consistent with other published analysis results.

5.4.3 Launch Sensitivity: Specific Orbits

The layered approach to modeling the LEO environment has already been shown to increase the fidelity of population projections in a simplified modeling approach.

Another powerful example of this is the investigation of an increase in launch rate to a specific orbit. Through the use of a layered representation of LEO, the SLOOP model can track the impact of launch rate increases to specific regions of LEO. For example, recent announcements by Virgin Galactic indicate that they plan to launch a new constellation of internet satellites within the next 5 years.[21] This constellation of 650 satellites is to be deployed into two separate orbits between 800 km and 950 km. Assuming the satellites are deployed over a 20 year period at 32 satellites per year, that they have an operational life of 20 years, and that they are replaced on a 20 year cycle, this deployment can be approximated by increasing the average number of launched objects per year to the 800 km orbital shell by 32 per year.

In the bulk representation of LEO, this is simply modeled as a 32 object increase in the launch rate. In the layered model, this 32 object per year increase can be specifically targeted to the 800 km orbital shell, which is one of the more populated shells in LEO. The expectation is that an increase in the population at that particular shell will have more impact than average. The SLOOP model can also be used to investigate alternatives where the constellation is launched to a less populated region, such as the 500 km orbital shell. Figures 5.25, 5.26 and 5.27 show the expected collision rate and population increases from three scenarios: launching into the 800 km shell, launching into the 500 km shell, and the associated bulk mode prediction.

There is a clear difference between launching this constellation into the 800 km shell and launching it into the 500 km shell. By adding 650 satellites to the congested 800 km shell, a significant increase in the number of fragment-intact object collisions is observed. The total number of collisions expected over the 100 year simulation is nearly

3 times higher with the constellation in 800 km versus 500 km. The bulk representation of LEO fails to distinguish between the two alternatives. The bulk representation over predicts the fragments compared to the 500 km orbit option and significantly under predicts the fragments compared to the 800 km case. The bulk mode also under predicts the number of collisions expected. By leveraging the layered analysis capability of the SLOOP model, these orbit-specific deployment trades can also be investigated, providing another layer of analysis capability using the simplified modeling approach.

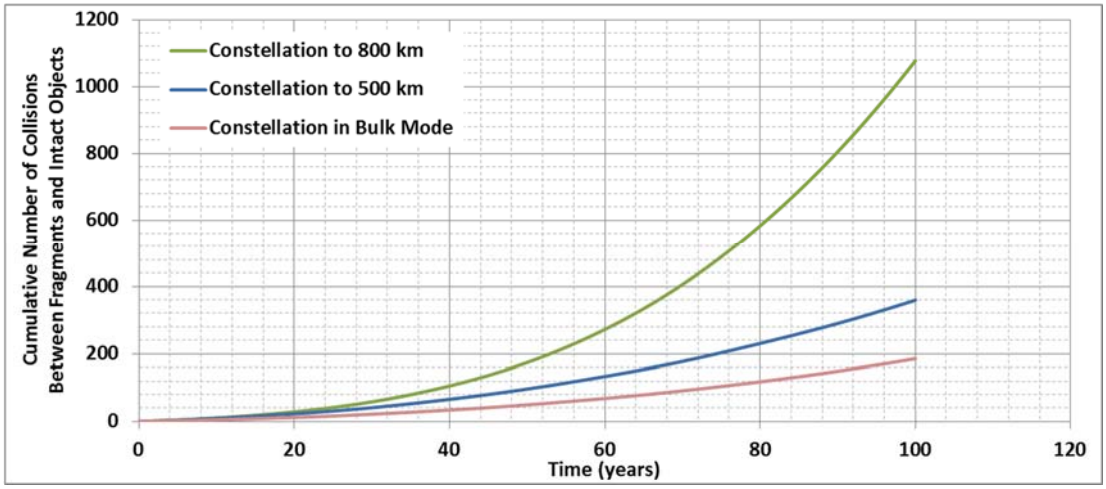

Figure 5.25: Number of Projected Fragment-Intact Collisions When Adding a New Constellation of Satellites in Various Locations

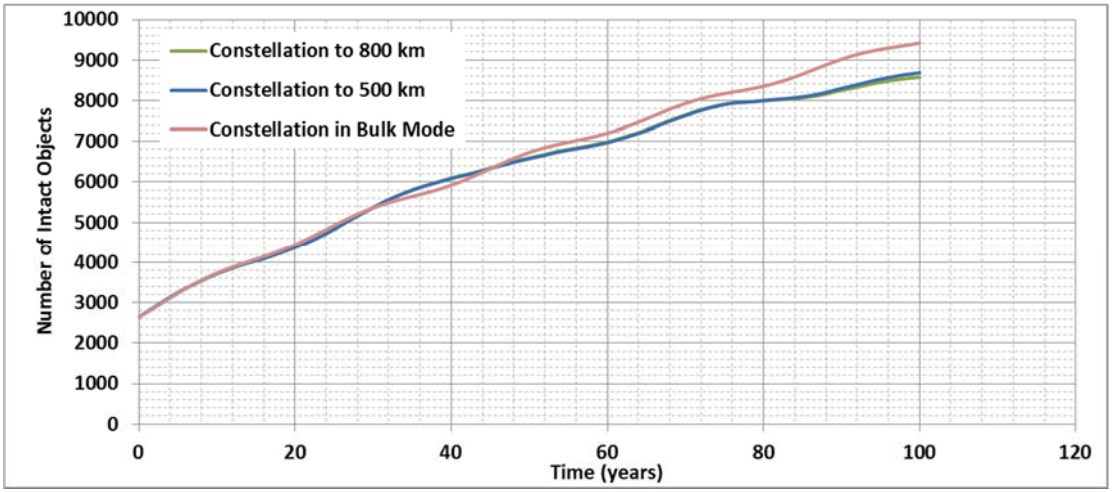

Figure 5.26: Number of Projected Intact Objects When Adding a New Constellation of Satellites in Various Locations

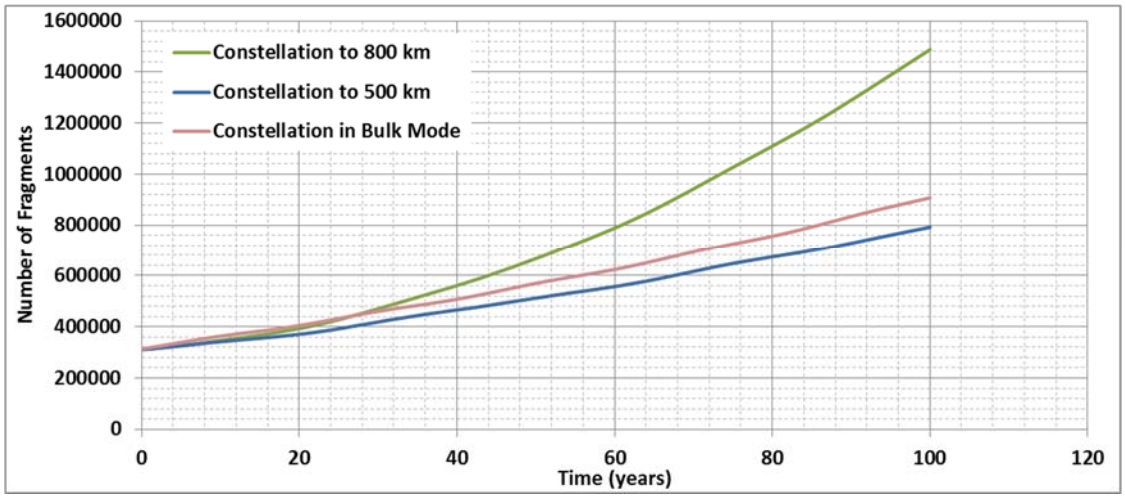

Figure 5.27: Number of Projected Fragments When Adding a New Constellation of Satellites in Various Locations

The results presented in this chapter highlight the advanced capability of the new SLOOP model approach to simplified population modeling. The sensitivities have also provided new benchmark values for the PMD rate and shown that the true power of the SLOOP model lies in its ability to model LEO in layers rather than relying on mean values to represent the entire region of LEO at once. Runs using SLOOP should be limited to 100 year simulations to maintain closer relationship to the high fidelity LEGEND tool. A 50% PMD rate brings the benchmark results to within 5% of the LEGEND tool over the 100 year simulation. In the next chapter, the SLOOP model will be used in a sample analysis to show how these new capabilities can be leveraged in real world scenarios.

CHAPTER 6:

A SAMPLE SLOOP ANALYSIS: CUBESATS AND DATA DRIVEN POLICY MAKING

Policy making surrounding the use of satellites in LEO is a challenging, multi-faceted problem. Domestic policy in the United States is enacted not by one central body but by six semi-independent government agencies. Although the United Nations sets international guidelines, the operators of satellites are free to fly as they choose. The data presented so far shows that overcrowding in certain regions of LEO can increase risk to operational satellites. As markets open to more satellite operators, the *space* in space will continue to dwindle and risk will continue to climb. Due to its significant reduction in cost, the CubeSat represents a newly emerging forcing function in the LEO satellite market and stands poised to drastically increase the growth rate of the satellite population. While CubeSat launches to date have been to low orbits that are naturally compliant with post-mission disposal guidelines, as the market matures and secondary payload launch opportunities become more popular, these CubeSats will begin to fly in higher orbits with longer decay times and larger satellite populations. With many potential future scenarios involving the growth of the CubeSat market, the SLOOP model is uniquely positioned to support data-driven policy analyses that will allow the LEO

satellite community to get out in front of this potential issue rather than enacting corrections after the fact.

Thus far, national and international guidelines for responsible operation of satellites have guided, but not regulated, the industry. However, recent data showing the effects of lower than desired post-mission disposal compliance is beginning to call those approaches into question. Some agencies are calling for more strict operating rules for LEO to help enforce a more responsible use of space. Those calling for stricter regulation sometimes find themselves at odds with the operators themselves. The satellite industry and the people it serves are constantly trying to make the industry more affordable and improve the services that they provide. Stricter regulation typically brings with it higher operating costs.

In the case of LEO satellites, the burden to comply with post-mission disposal guidelines requires additional sub-systems which increase the complexity and cost of satellites. CubeSats further complicate the balance between regulation and operation because their small size makes it difficult to integrate the de-orbit technologies that will be required for CubeSats to comply with PMD guidelines as their operational altitude increases. Finding the right balance between regulators and operators requires a thoughtful process with access to reliable data that can help weigh the pros and cons of various alternatives while supporting the long term financial and physical viability of the industry.

6.1 The U.S. Satellite Regulatory System

The discussion of data driven policy making in the satellite industry will focus on the industry in the United States. The general policies of the U.S. with regards to satellite

operations are similar to those found in satellite industries around the world so the policies discussed in this context will provide a sense of the global industry as well. Internationally, it is recognized that objects in space are the responsibility of the nation that launched them. Therefore, the United States government is responsible for all objects launched from the United States just as other nations are responsible for their own launches. By examining the U.S. regulatory system, we can begin to understand the challenges of balancing regulation with competitiveness in a global market.

6.1.1 The Structure of U.S. Satellite Regulation

Under the guidance of the Office of Science and Technology Policy, each presidential administration crafts their vision for the use of space and publishes it as the National Space Policy of the United States. The inclusion of orbital debris in the national space policy has been the norm since 1988. However, the U.S. government has recently placed increased emphasis on addressing space debris and has given it an even more prominent standing in the current National Space Policy. One of the six main goals identified in the 2010 National Space Policy is:

> "Strengthen stability in space through: domestic and international measures to promote safe and responsible operations in space; improved information collection and sharing for space object collision avoidance; protection of critical space systems and supporting infrastructures, with special attention to the critical interdependence of space and information systems; and strengthening measures to mitigate orbital debris."[59]

Additionally, the National Space Policy identifies "Preserving the Space Environment and the Responsible Use of Space" as one of seven *Intersector Guidelines*. In this guideline, the policy discusses improving data sharing for space situational awareness, including collision avoidance data, and continued adherence to the U.S. Government Orbital Debris Mitigation Standard Practices. The policy also advocates for research and development in the area of mitigation and removal of on-orbit debris.

The Department of Defense, in conjunction with the Director of National Intelligence, drafts the National Security Space Strategy to describe the plan to implementing those aspects of the President's space policy that are related to national security matters. The most recent National Security Space Strategy has included space sustainability as one of the major items addressed. The strategy details the current state of the space environment calling it "congested, contested and competitive".[19] This reference to the congestion of space refers specifically to the current state of space debris and the need for national assets to be capable of protecting against and responding to increases in the congestion.

Both of these instances of national policy declarations make reference to the U.S. Government Orbital Debris Mitigation Standard Practices.[3] First established in 1997, the latest version of this document was released in 2002 and outlines four major debris mitigation objectives:

- Control of Debris Released During Normal Operations,
- Minimizing Debris Generated By Accidental Explosions,
- Selection of Safe Flight Profile and Operational Configuration, and
- Post-mission Disposal of Space Structures

Within each of these four areas, major themes are outlined. These include the 25-year rule for decommissioned spacecraft in LEO, acceptable parking orbits for decommissioned spacecraft in MEO and GEO, passivation of space objects to minimize the probability of explosion, and size thresholds for debris released through nominal operations. The guidelines, policies, and regulations of each licensing agency within the federal government echo some or all of these standard practices.

An overview of the current policy structure for space debris in the United States is provided in Figure 6.1. While the mitigation standard practices provide a good framework for the orbital debris discussion, the current system of oversight in the United States is fragmented, with six different agencies overseeing space assets. Each government agency identified has its own individual orbital debris policy and guidance. While many follow the general principals laid out in the National Debris Mitigation Standard Practices, they vary in their level of application and regulation.

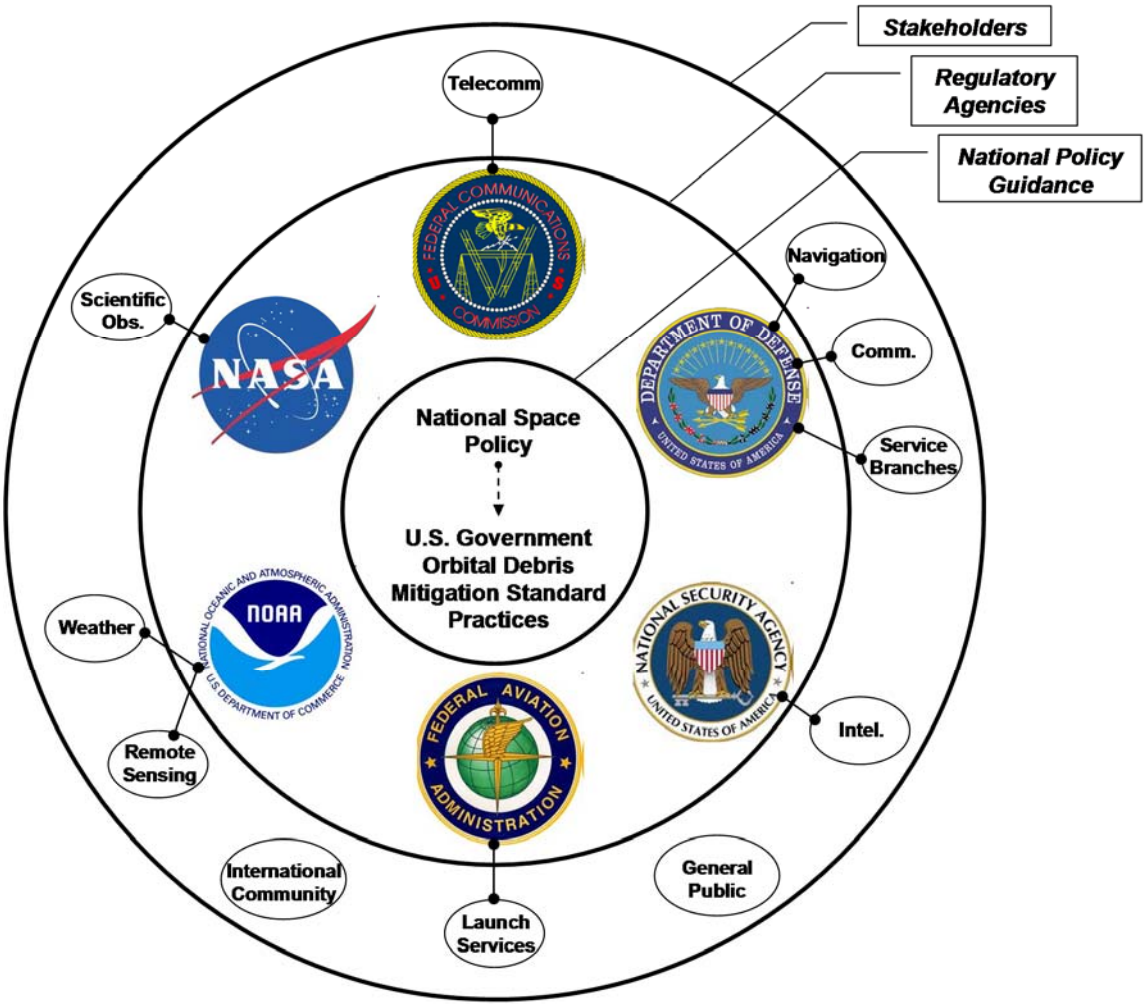

Figure 6.1: Diagram of Stakeholders in the United States Satellite Regulatory System

NASA's Procedural Requirement for Limiting Orbital Debris (NPR 8715.6A) [60], for example, requires all missions involving NASA to comply with NASA-STD 8719.14 Process for Limiting Orbital Debris.[61] The companion NASA-HDBK 8719.14 Handbook for Limiting Orbital Debris [62] provides additional insight into debris analysis and mitigation methods. These documents outline NASA's guidance on operational debris and spacecraft disposal as well as potential mitigation practices. They also highlight the 25-year rule.[61] Ultimately, NASA requires Orbital Debris Assessment Reports throughout the design process with updates during the spacecraft's

operational life. NASA also requires End of Mission Plans (EOMP), the final one to be delivered 3 months prior to the spacecraft's end of life. The EOMP outlines the manner in which the spacecraft will transition from operational to non-operational status while still complying with all guidelines provided with respect to passivation, control, and public safety during final re-entry.[61]

The Department of Defense maintains an orbital debris standard directive very similar to NASA's. This is not surprising given that the two agencies were the primary authors of the mitigation standard practices. The National Oceanic and Atmospheric Administration (NOAA) oversees the licensure of commercial remote sensing satellite systems and is governed by the Land Remote Sensing Policy Act of 1992. This act declares that spacecraft must be disposed of in a manner approved by the U.S. government but no specifics are noted and NOAA policy is to evaluate each mission on a case by case basis.[63]

The Federal Communications Commission (FCC) oversees commercial communications satellites. The FCC announced in 2005 that they will require an orbital debris mitigation plan that includes post-mission disposal.[64] While many of the assets licensed by the FCC are in GEO, an increasing number of communication satellite constellations are being deployed in LEO, specifically in the altitude band between 700 km and 900 km. Thus, post-mission disposal of FCC-licensed satellites has significant impact on the LEO debris environment and this update in licensing policy is a big step in the right direction.

The Federal Aviation Administration (FAA) within the Department of Transportation approves all launch vehicle assets for flight. The debris mitigation stance

of this agency applies mostly to spent rocket stages and only addresses the passivation of these stages to avoid accidental explosion. Current FAA licensing requirements do not discuss the deorbit of stages after delivery of their payloads. However, upper stage disposal is covered in the NASA orbital debris regulations.

6.1.2 The stakeholders

As seen in Figure 6.1, many stakeholders are affected by the space debris policy of the United States. These stakeholders can be grouped into three categories. The members of the first group are satellite owners and mission operators. These operators tie directly to regulating agencies. Some are commercial entities operating within the jurisdiction of the Unites States and are, per international treaty, the responsibility of the United States. Some are program and project offices within the regulating agency, such as specific scientific missions run by NASA or weather satellites operated by NOAA.

The stakes that the operator entities hold are twofold. First, the operators are affected financially and operationally by the nature of the space debris policy and resulting regulations and guidelines. Requirements for the reduction of operational debris and post-mission disposal impact the design of the spacecraft. In some cases, they even serve to limit the effective life of the satellite by requiring propellant reserves for end of mission disposal. Any additional de-orbit systems will add mass and complexity to satellite designs potentially driving up costs and increasing the potential for mission failure. These requirements can impact design costs as well as return on investment and revenue streams.

The second operator stake is one of a sustained space environment for continued operations. In this arena, the operators are dependent on their own actions and the

actions of other operators in their community just as much as they are on the efficacy of national policy recommendations. While regulations and policy can promote a clean environment, ultimately, only responsible operations from these stakeholders can ensure long-term sustainability of the space environment. If certain orbits are subject to the chain reaction collisions hypothesized as the *Kessler Syndrome*, everyone stands to lose. With space currently a $16 billion per year industry, these stakeholders must ask themselves if they are willing to sacrifice long term capability for near term profits.

The issue of long term sustainability of the space environment leads us to the second group of stakeholders. In Figure 6.1, two stakeholders that are not tied to a particular regulating agency were identified as international operators and the general public. These stakeholders are just as dependent on the long term sustainment of the space environment as the operators. These two entities are referred to as the beneficiaries of domestic space debris policy. International operators, like their American counterparts, require debris-free space in which to operate their own space assets. Indeed, the national space policy highlights the use of space as a right for all nations. The general public, as a receiver of benefits from the operation of space assets, is also an important stakeholder because of our growing dependence on space products. Global communications, weather observations, and even national security through increased transparency are all major benefits to our daily lives. In developing a comprehensive space policy, we must not forget about these beneficiaries who rely on all nations to act responsibly so that they may continue to enjoy the benefits that space assets offer.

Finally, the third group of stakeholders is the regulating agencies within the federal government (NASA, NOAA, NSA, DoD, FAA, and FCC). These agencies are

impacted by changes made to domestic space debris policy. It is their job to regulate the operators and ensure the safety of and quality of product received by the beneficiaries. Any change in space debris policy must account for the regulator's ability to effectively manage new regulations, track compliance, and maintain efficient internal operations. Striking a balance between the needs of these three key stakeholder groups requires consideration of all aspects and impacts of space policy. The SLOOP model is ideally suited for quick evaluations of potential regulatory strategies for impacts to the operators and the beneficiaries of satellite operations.

Identification and understanding of the stakeholders is an important first step in enacting effective policy. In systems engineering, the identification of the stakeholders help to frame the requirements of a design. A similar approach to data-driven policy allows decision makers to consider all aspects of the policy they are trying to establish. Fully understanding the landscape of the LEO satellite industry helps decision-makers craft metrics that are used to evaluate the effectiveness of policy at all levels of the industry. For example, CubeSat operators rely on the same low risk of collisions as many traditional satellite operators to ensure the continued success of their endeavors. Policy can help protect those satellites by promoting responsible use of LEO but those policies must balance risk reduction with cost, implementation, and the ability of the regulators to effectively regulate. By understanding the layers and interactions of the stakeholders, policy makers can better apply the data generated by models like the SLOOP model to craft broadly effective policy maximizes risk reduction while minimizing economic impact.

6.2 CubeSats: The Perturbing Force in the Satellite Industry

Over the past few years the satellite industry has seen the emergence of a new sector of market of operators. This sector has been enabled by the development of a new satellite concept; the CubeSat. As discussed in Chapter 4, the CubeSats present a unique opportunity to open LEO up to a completely new set of operators. A 1U CubeSat (10 cm on a side weighing less than 1 kg) can be purchased for as little as $13,000 and is a fully functional satellite once built and deployed. CubeSats can be made in any multiple of U-units and, because of their low mass and small physical size, can be launched from any number of platforms and flown as secondary payloads at a drastically reduced price compared to traditional means of accessing space. While current deployer designs can only accommodate up to 3U satellites, a design for a 6U satellite deployer is in the works and satellite designers are considering satellites comprised of as many as 27 units or more.[65]

The combination of low satellite costs with low launch costs has the CubeSat market poised for a major surge. Industry startups, like the company Planet Labs mentioned in Chapter 4, as well as universities and government agencies on tight budgets, view the CubeSat concept as a way to break into a market that has traditionally required significant startup capital. The United Launch Alliance and other launch providers are also finding a windfall in the emergence of this new sector of satellite operations. Launch providers have unused lift capability remaining on virtually all of their launches because the primary payload for the launch is typically lighter than what the launch vehicle can lift into space. For decades, that excess capability has been left on the table. With the development of CubeSats and other smaller classes of satellites, the

launch providers are finding ways to maximize their lift capability and their profits by providing flight opportunities to secondary payloads. Launch providers have found that, with a few modifications to the structure that holds the primary payload, they can charge other customers a small fee to use the left over capacity of the launch vehicle thus capitalizing on resources once left as the price of doing business. Configurations like the SpaceX configuration shown in Figure 4.4 exist for several launch providers.

6.2.1 The Potential to Flood the Market

Because of their affordability and appeal to both operators who want to fly in space and launch providers who want to find a way to sell their excess capability, there is tremendous potential for CubeSats to flood the market of LEO spacecraft. Startups like Planet Labs are beginning to build entire business models around large constellations of CubeSats. Their plan to launch 131 satellites by the end of 2015 will make them the first commercial operator of a constellation of CubeSats. Universities are leveraging programs like NASA's CubeSat Launch Initiative [46] to give students hands-on experience with satellite design, manufacturing, and operations.

To date, these CubeSat initiatives have remained in relatively low orbits. The Flock constellation planned by Planet Labs will fly at 400 km altitude.[47] The CubeSat Launch Initiative program provides dedicated launches for CubeSats and other small satellites and targets a region between 400 km and 550 km. In 2013, two dedicated CubeSat/small sat launches occurred within 2 days of each other. These two launches flew to 480 km and 580 km altitude and deployed a total 62 satellites between them.

With their small size and low cost, it is easy to see how CubeSats have the potential to flood the satellite market. However, to date, these CubeSats are residing in

lower population orbits with short orbital decay times. That may change as the secondary payload market grows. The launch provider's responsibility is first and foremost to the primary payload for any launch. That primary payload has paid the premium price for a launch to a specific destination and launch providers will ensure that obligation is met above all else. When a CubeSat secures a ride as a secondary payload with a launch provider such as ULA, that secondary payload is typically flying to whatever orbit the primary payload is being launched to. Historical launch trends show that populated orbits will continue to be popular destinations. This indicates that, as the secondary payload market begins to grow, launches to populated orbits will no longer contain one payload but many and the CubeSat will no longer be relegated to low orbits. Table 6.1 shows potential launch opportunities for secondary payloads available through the United Launch Alliance (ULA). We can see that there are opportunities for significant secondary payload presence on several launches over the next three years. All of these launches are to higher orbits, between 600 and 800 km, with larger populations.

Table 6.1: ULA Rideshare Opportunities Over the Next Three Years [66]

Mission	Customer	Vehicle	Site	Orbit	Margin, Excluding Disposal (kg)	FY15	FY16	FY17	Notes
GPS-IIF	USAF	401	ER	MEO - Direct	~600	IIF-4, IIF-6	IIF-7, IIF-8		Transfer orbits missions
GPS-III	USAF	411	ER	MTO	[~1100]		IIIA-2	IIIA-5	
SBIRS	USAF	401	ER	GTO	~100		GEO-3	GEO-4	
AFSPC	USAF	401	ER	GTO	TBD	AFSPC-8			
NRO	NRO	411	ER	GTO	TBD			L-61	
AEHF	USAF	531	ER	GTO	Performance Limited			AEHF-4	
MUOS	USAF	551	ER	GTO	Performance Limited	MUOS-4	MUOS-5		
GOES	NASA	541	ER	GTO	Performance Limited		GOES-R	GOES-S	
TDRS	NASA	401	ER	GTO	Performance Limited		TDRS-M	TDRS-N	
MMS	NASA	421	ER	GTO	Performance Limited	MMS			
Discovery	NASA	401	ER	Hyperbolic	TBD	D-12			Earth escape trajectories
ExoMars	NASA	421	ER	Hyperbolic	Performance Limited		EM		
Osiris Rex	NASA	401	ER	Hyperbolic	Performance Limited			OR	
Europa	NASA	551	ER	Hyperbolic	Performance Limited			EO	
Solar Orbiter	NASA	551	ER	Hyperbolic	Performance Limited			SO	
NRO	NRO	401	WR	TBD	TBD			L-79	LEO Missions Disposal TBD
NRO	NRO	541	WR	TBD	Performance Limited	L-67		L-42	
NRO	NRO	401	WR	TBD	TBD	L-55			
STP	USAF	401	WR	~700km 98 deg	**>5,000**			STP-3	
CLARREO	NASA	[Delta II]	WR	~600 km Polar	TBD			CLARREO	
ICESat	NOAA	[Delta II]	WR	Polar	TBD		ICESat-2		
DMSP	USAF	401	WR	~800km 99 deg	**>4,000**	DMSP-19/DSX	DMSP-20		
JPSS	NOAA	[Delta II]	WR	~800km 98deg	~900		JPSS-1		
GeoEye	GeoEye	401	WR	~700km 98 deg	**>4,000**			GEOEYE-2	
WorldView	Digital Globe	401	WR	~700km 98 deg	**>4,000**		WV-4		
Comm I-9	CLS	401	WR	TBD	**>4,000**		Comm I-9		

6.2.2 The Challenge of the CubeSat Market

The challenge of an expanding CubeSat market is twofold. First, the simple increase in number of satellites launched. Whether it is through dedicated launches or as secondary payloads, the satellite launch market will see a shift in the coming years where many satellites, not just one or two, will be launched in a single launch. This will lead to a population explosion where the annual object launch rate could increase significantly with no real impact to the launch market itself. The second challenge is the final destination for these CubeSats. Previous data has shown that orbit lifetime and population concentrations have a significant impact on the potential for collisions in any region of LEO. While the volume of objects launched presents a challenge in all orbits, higher orbits and more populated orbits will be more adversely impacted by a population explosion. The CubeSats will reside longer in higher orbits and the orbits that they will most likely end up in as secondary payloads have higher initial populations to begin with.

Figure 6.2 shows the typical orbital life of several different size classes of CubeSats as a function of altitude. This assumes a 10 year operational life followed by natural decay of the orbit. The PMD guideline is shown as a dashed red line and is adjusted to 35 years to account for the 10 year operational life plus the 25 year post-mission duration guideline. The plot shows that CubeSats in lower altitudes, where most are today, have relatively short natural lives. The natural decay of most CubeSat orbits below 500 km is less than 5 years. In fact, the altitude must exceed 550 km for small CubeSats and 500 km for larger CubeSats before the natural life of the CubeSat exceeds the current 25-year guideline for post-mission disposal. However, the plot also shows that at the higher orbits, the life significantly exceeds the 25-year guideline. In the 700

km to 900 km region where most CubeSats will end up when taking a ride share opportunity, the natural life can easily exceed 1000 years or more. Coupling this with the increased population density at these altitudes, one can expect to see a significant increase in projected collisions in those higher regions.

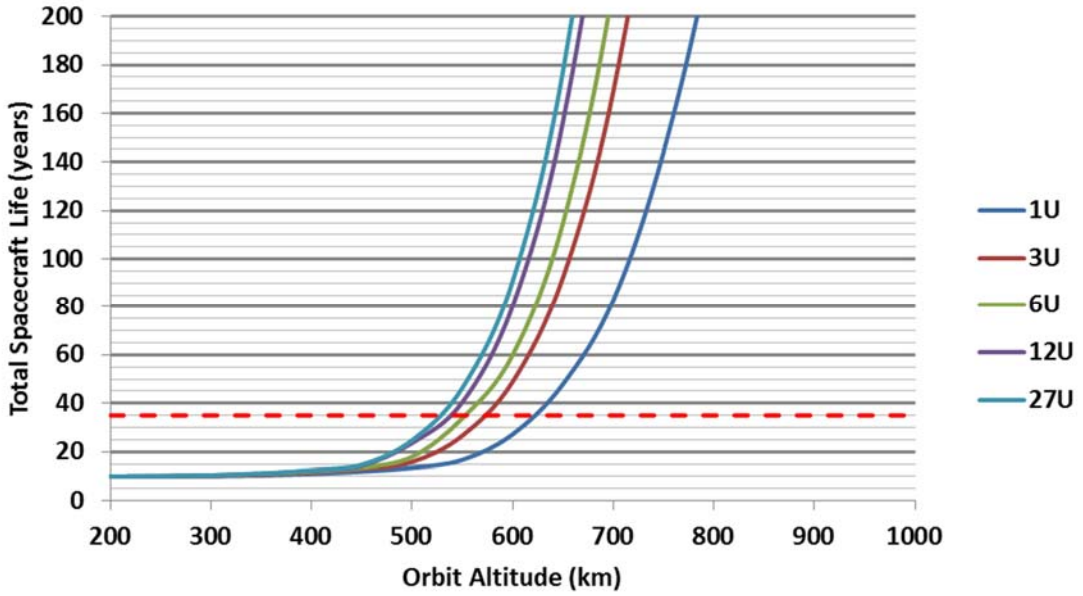

Figure 6.2: CubeSat Orbital Life as a Function of Configuration and Initial Orbit Altitude

Policy makers will no doubt engage in discussion about the potential rise in risk to orbiting assets presented by CubeSats. Already, the topic of orbital debris and orbital asset management has increased in profile over the last decade. Satellite operators are growing more concerned with the potential risk to their expensive assets and government agencies in the U.S. are equally concerned about risk to national security and scientific investigations. The challenge with managing LEO satellite risk through policy is that the risk reduction is tightly coupled with the physics of flying in space and the effectiveness of any proposed policy to mitigate satellite risk can only be evaluated by modeling the satellites and their environment. Once a policy option has been evaluated to show that it

will reduce satellite operational risk, the impact of that policy to the satellites and operators themselves must also be factored in.

Three proposed policies for reducing the risk of flying more satellites in LEO have included restricting the orbits to which the satellites can fly, mandating post-mission disposal to increase the compliance rate, or reducing the post-mission life from 25 years to some lower number. Each of these restrictions or regulations carries an impact to the commercial viability of the satellites to be flown. Orbit restrictions will change the design of instruments and communications systems and will impact the secondary payload market of the large launch vehicle providers. Mandated PMD compliance will require new sub-systems on some satellites and enhanced sub-systems on others in order to support the maneuvers required to facilitate a timely deorbit. Reducing the time it takes to deorbit can further exacerbate that problem by requiring larger, more complex systems. These additional de-orbit systems may not be viable for many of the small CubeSat designs simply due to a lack of space available in the satellite for the systems required.

These tightly coupled considerations require a robust data source to help inform the policy making process. The data-driven policy making can ensure that new policies are put in place that balance impact to the market with responsible use of LEO and can ensure that the policies enacted will actually have the intended positive impacts. There are many alternatives to be evaluated and their impacts can be evaluated based on a spectrum of potential levels of application of the changes. We need to understand how sensitive the system is to the inputs so that we can understand the degree to which we can implement a policy or regulation that is affective but minimally impactful to the market.

Even within the three options mentioned above there are sensitivities to be driven out and combinations of policies that can be implemented at varying degrees.

The SLOOP model is ideally suited to perform broad evaluations of potential policy shifts. The short calculation time enabled by the simplified modeling algorithms supports the relatively quick evaluation of many potential options. The user inputs are already in place to support evaluation of the more impactful policy options, such as enhanced PMD compliance and reduced post mission life. The SLOOP model provides a reasonably accurate representation of detailed analysis tools making it ideal for rapidly evaluating a broad trade space to provide guidance for the more detailed analysis tools to explore certain regions of that trade space with higher fidelity analyses. Essentially, the SLOOP model can be used as a screening process to find promising alternatives for more detailed study. Unlike previous attempts to simplify the modeling process, the layered approach to modeling the LEO environment enables the nuanced evaluation of specific regions of LEO and how they impact the region globally. The next section will provide an example of how data driven policy making can be supported by the SLOOP model.

6.3 Data Driven Policy Evaluation: Regulating to Lower Risk

As discussed in earlier sections, the CubeSat market has the potential to greatly increase the populations of intact objects in space by enabling multi-manifested launches. The impact of this potential surge in launch rate can be evaluated by running the SLOOP model with increased launch rates to various orbits. First, the impact of increased CubeSat activity is quantified and compared to the current business-as-usual scenario. Three cases are compared to the baseline. First, an increase of 45 launched objects per year to 500 km altitude is evaluated to capture the potential for future dedicated CubeSat

launches. Second, an increase of 25 launched objects per year to 800 km altitude is evaluated to account for growth in the secondary payload market. Finally, the two scenarios are combined. All cases are evaluated with 50% PMD compliance rate.

The plots of intact object population and projected intact-fragment collisions are shown in Figures 6.3 and 6.4 for each of the three scenarios and the "business-as-usual" scenario. The plots clearly show a significantly higher risk of collisions when introducing a significant increase in population to the already congested 800 km region of LEO. In fact, over the next 100 year, the SLOOP model shows an increase in the number of fragment-intact collisions of 500, or a 167% increase, over the business-as-usual scenario. If CubeSat flights are restricted to lower orbits, even if more CubeSats are launched, the resulting risk of collisions only increases by 33% over the same 100 year period. This initial data would suggest that restricting CubeSat flights to lower orbits is the safer course of action. However, this all but eliminates the possibility of leveraging ride-share options on larger launches.

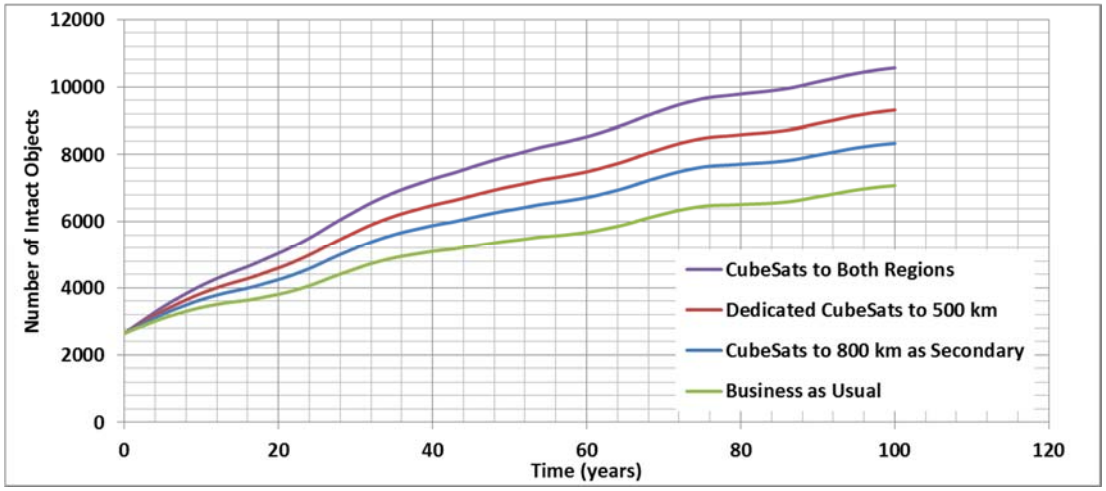

Figure 6.3: Change in Intact Object Population Projection with Increase in CubeSat Flight Rate to Various Regions of LEO

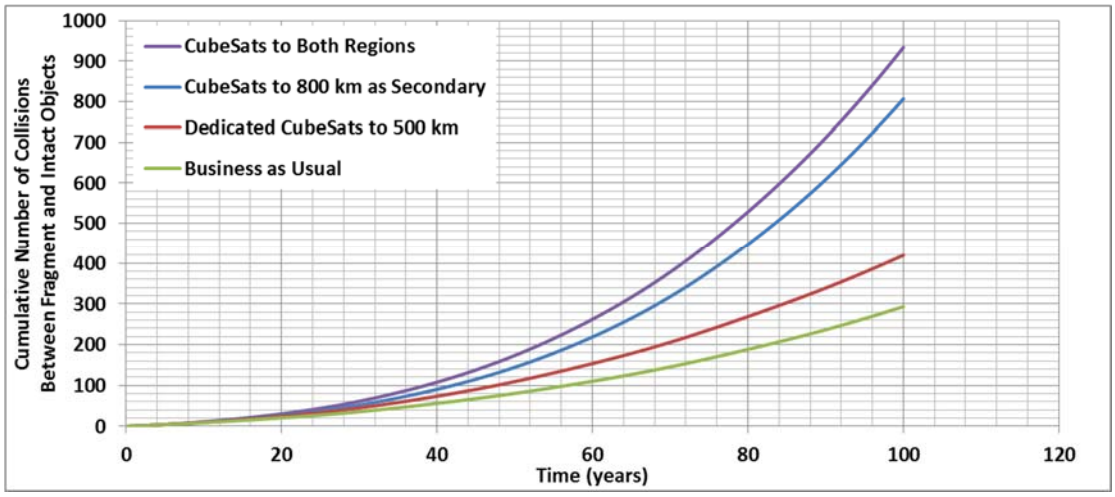

Figure 6.4: Change in Projected Fragment-Intact Collisions with Increase in CubeSat Flight Rate to Various Regions of LEO

Other courses of action are also possible. One potential solution for combating the increased risk of collision is to mandate compliance with the current PMD guidelines. By requiring all objects to comply with the 25-year rule for post-mission disposal, the residence time of newly launched objects will be greatly reduced. A high rate of compliance will result from this regulation. While spacecraft anomalies and premature failures will prevent the PMD compliance rate from reaching 100%, a 90% compliance rate is believed by many within the orbital debris community to be a reasonable assumption for standard satellites. This compliance rate represents a significant challenge for CubeSats. Constraints on mass, power, and physical space limit the potential systems that can be added to a CubeSat to assist in its deorbit. Assuming a PMD compliance rate of 90% represents the best case scenario for populations that include a significant percentage of CubeSats and further design studies are required to evaluate the feasibility of implementing this type of regulation with CubeSats through system design.

The previous three scenarios were evaluated using the SLOOP model with a PMD compliance rate of 90%. The plots comparing the original results to those with the increased PMD compliance rates are shown in Figures 6.5 and 6.6. The plot of intact object count shows that with increased PMD compliance, in two of the cases where significantly more objects are launched, the cumulative number of intact objects is the same or lower than in the business-as-usual case. This plot shows the power of increased PMD compliance, similar to the plots shown in Chapter 5. This same result is not seen in the cumulative number of collisions. While the 90% PMD compliance shows a significant reduction in the number of projected fragment-intact collisions over the 100 year simulation, the number of collisions does not drop below the business-as-usual case. The projected number of collisions is still significantly higher than the business-as-usual case when launching a significantly higher number of objects into crowded orbits such as the 800 km shell investigated here. The natural life of CubeSats in the 500 km shell is already less than the PMD compliant 25 year life, so the reduction in collision count is minimal for the case of launching CubeSats exclusively to 500 km orbits.

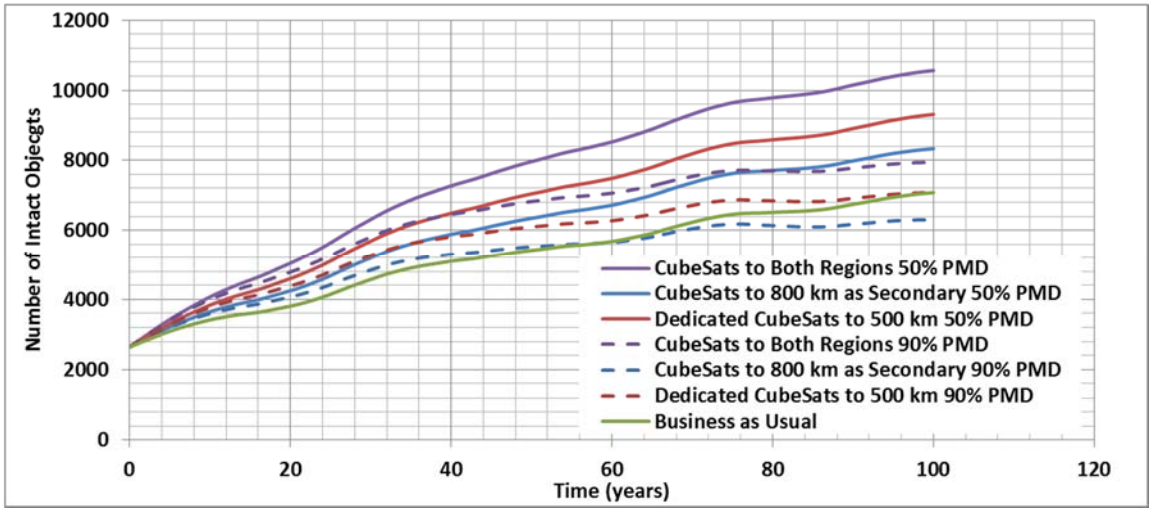

Figure 6.5: Impact of Enhanced Post-Mission Disposal Rates on Projected Intact Object Populations under Various CubeSat Flight Rate Scenarios

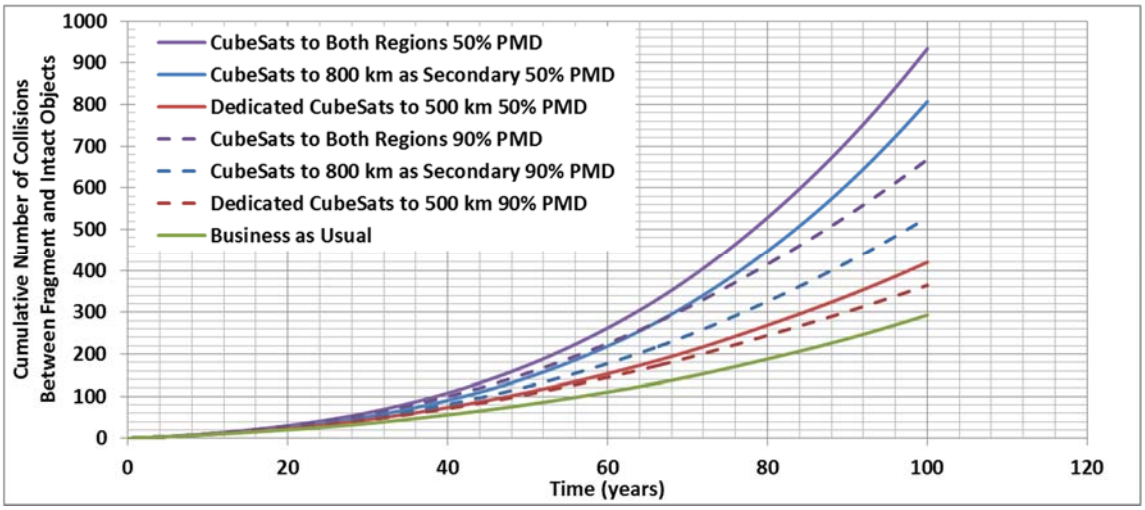

Figure 6.6: Impact of Enhanced Post-Mission Disposal Rates on Projected Fragment-Intact Collisions under Various CubeSat Flight Rate Scenarios

The power of higher PMD compliance is still evident in the figures above. A 90% PMD compliance rate will result in fewer overall resident objects over time. The increase to 90% compliance also results in a 32% reduction in the expected number of collisions over the 100 year simulation. While the risk to operational satellites is increased in the crowded orbits with the increase in CubeSat launches, one potential policy solution may be to require compliance with the 25-year rule rather than suggest it, as is currently the case. While this higher compliance rate does not eliminate the increased risk, it can significantly reduce the risk.

Another potential policy solution is to reduce the post-mission life of the objects in orbit. The original 25-year rule was developed to strike a balance between spacecraft design requirements (and associated, spacecraft cost) and the positive impact of reducing residence time of orbital objects. The 25-year post-mission life resulted in significant reductions in the risk of collisions while resulting in minimal spacecraft design impacts by requiring only modest propellant loads to enable the propulsive reduction of the orbit altitude to make the spacecraft compliant. The analyses that supported this duration were

performed over 20 years ago and do not account for the advances in spacecraft propulsion that have occurred in that time. Thrusters are more efficient and propellantless propulsion options such as deployable drag devices and electro-dynamic tethers have been developed. These new technologies may enable a reduction in the 25 year post-mission life while continuing to minimize impacts to spacecraft design.

The plots in Figures 6.7 and 6.8 show the sensitivity of the 800 km CubeSat ride-share case to PMD duration. The scenario where 25 extra satellites were launched to 800 km orbits every year is representative of the increase in ride-share opportunities for CubeSats. Previously discussed results show that this scenario resulted in a significant increase in both population and projected collisions when compared to the business-as-usual approach. Assuming a 50% PMD compliance rate but reducing the post-mission life in increments of 5 years, Figures 6.7 and 6.8 show that there is very little added benefit for accelerated post-mission life. In fact, a 5 year reduction in post-mission life corresponds to a reduction of approximately 20 fragment-intact objects collisions over the 100 year simulation. This is a 2.5% reduction in projected collisions. These initial results indicate that reducing post-mission life does not result in a significant reduction in collision risk.

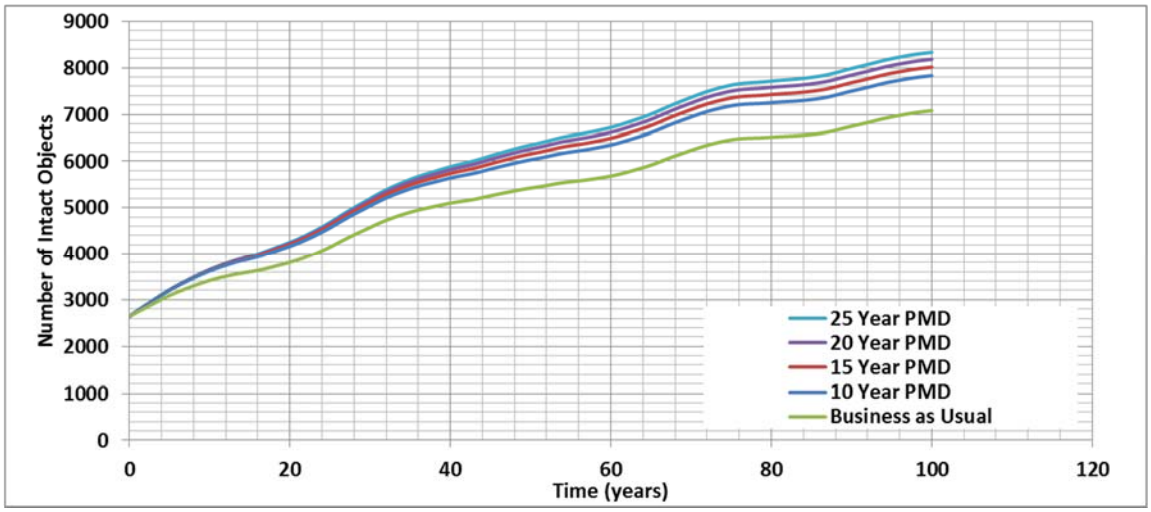

Figure 6.7: Sensitivity of Projected Intact Object Populations to Post-Mission Lifetime

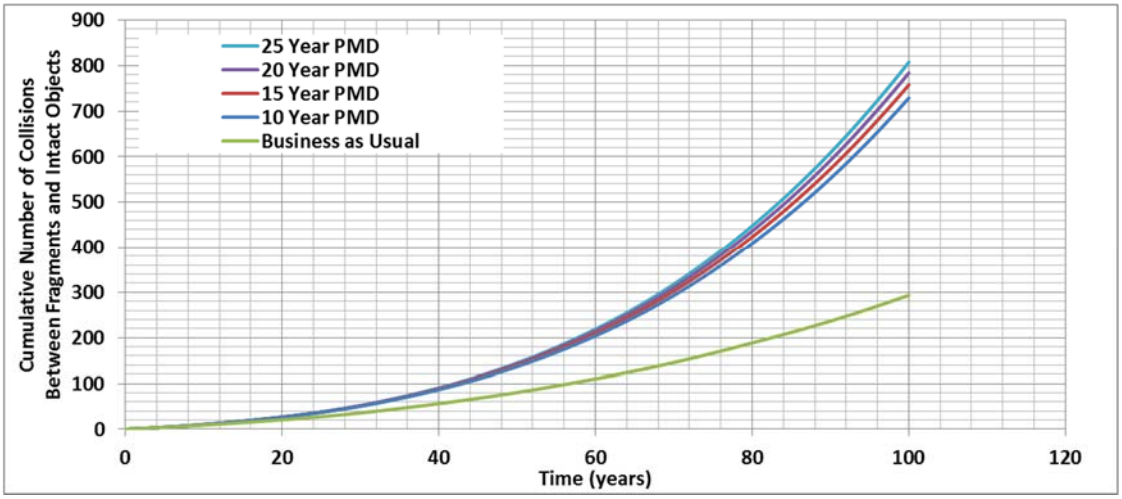

Figure 6.8: Sensitivity of Projected Fragment-Intact Collisions to Post-Mission Lifetime

The sample data provided in this chapter shows a clear and relevant application of the SLOOP model to support data-driven policy making. The emergence of the CubeSat market has the potential to cause a significant shift in LEO satellite risk. This market is so new that the full breadth and depth of its impact is not fully understood and many potential futures may result. The SLOOP model, which is capable of rapidly evaluating a broad trade space of operational scenarios and policy options, can have wide-reaching applications in evaluating the impacts of CubeSats to the LEO environment. A policy

maker can use the survey results presented above to focus higher-fidelity tools on the areas of the policy trade space that appear to provide the highest potential impact to the problem.

The results presented in this chapter show very little impact from reducing post-mission life but potentially significant reductions in risk to operational spacecraft through an increase in the general PMD compliance rate. The data also shows that a significant number of CubeSats can be launched if the altitude of their orbits is restricted to regions below 500 km where their natural orbit life is short and the populations are lower. The CubeSat market is very new and these results further highlight the need to address the potential impacts of this market early because of the potential for rapid population growth.

This policy impact data only tells part of the story. The design impacts to these satellites must also be evaluated. The small size of the CubeSat design limits the potential solutions for post-mission disposal. While new technologies are currently under development to address this issue, the feasibility of requiring post-mission disposal of CubeSats must also be taken into consideration when evaluating potential policy alternatives. Impacts to the market must also be considered. A solution that restricts CubeSat flights to lower altitudes eliminates a significant portion of the secondary payload market for large launch providers. Design changes required to bring satellites into compliance with new regulations my increase satellite costs and reduce the number of potential operators, thus shrinking the CubeSat market as a whole. It is also important to consider the global nature of the satellite and launch markets. If the U.S. were to set policy unilaterally that adversely affected U.S. corporate standings in the global market,

it may force investors and satellite manufacturers to find regions of the market that are less restrictive. Not only would this hurt the U.S. market share, but it would also reduce the effectiveness of the policies by driving more of the market into regions where the same regulations do not apply.

CHAPTER 7:

SUMMARY AND CONCLUSIONS

There is universal agreement among the space agencies of the world that the concentration of orbital debris in LEO presents an increasing threat to satellite operations. Although guidelines are in place to help steer the world's satellite operators into sustainable practices, voluntary compliance rates are falling short and populations continue to climb. With the 2009 Iridium-Cosmos collision, the community can no longer operate under the "big sky" theory and assume that collisions between large objects are not going to happen.

Studies completed by NASA and other space agencies all point to a growth in collision incidents over the next several hundred years. Predictions using the NASA LEGEND tool presented in Chapter 2 show that populations will continue to rise unless mitigation strategies are implemented. Compliance with post-mission disposal guidelines such as the 25-year rule can have a significant impact if the compliance rates are high enough. Studies have also shown that actively removing the source of debris fragments, large intact objects, can also help slow the collision rates. Studies performed by ESA add a layer of spatial fidelity by examining LEO as a series of discrete orbital shells. Results show that not all regions of LEO are created equal and that some higher population

regions are expected to experience significant debris growth while others remain relatively unpopulated.

Regardless of the eventual solutions recommended to support risk reduction for operational spacecraft in LEO, the path to determining appropriate policy must be guided with data. The cornerstone of any analysis of policy effectiveness in the space debris community is the ability to effectively model the future populations in LEO. Many space agencies have high fidelity codes to perform these analyses but they are computationally expensive and difficult to learn. The idea of a simplified analysis approach for orbital object population prediction was born out of necessity due to limited computing resources. Farinella and Cordelli first introduced the idea of coupled differential equations as a simplified means to perform population projections in the early 1990s. The fidelity of these methods was expanded over time, but typically in ways that increased their complexity. Increasing computing power has somewhat improved the utility of the higher fidelity, deterministic evaluation methods. However, an improved, well-defined simplified modeling approach has the power to quickly evaluate broad trade spaces. Such a code can serve as a screening function for the higher fidelity codes, quickly identifying promising areas of the trade space for further study.

The SLOOP model presented in this dissertation is a computationally rapid, simplified modeling approach to orbital object population projection that provides a new layer of spatial fidelity while remaining simple enough for a broad user community. Building on the two-equation models of Farinella, Cordelli, and Lafleur, the SLOOP model expands the differential equation set, adding a third equation to distinguish between naturally decaying intact objects and PMD-compliant intact objects. The

SLOOP model further simplifies the more complex and less effective portions of the Lafleur model. Differential equation coefficients and functions that represent the various contributors to the orbital object populations were investigated and modified as appropriate to both simplify and increase accuracy. Another improvement is the layered treatment of LEO that provides the ability to capture region-specific impacts to the bulk LEO environment.

The coefficients that classify the various characteristics of the LEO populations have been built on an extensive information base. A new Space Asset Management Database was created to compile information from several sources and provide the one-stop shop for orbital object information for users throughout the community. This data was leveraged to quantify collision probabilities, launch rates, and the physical characteristics of intact objects and fragments that drive their orbital life.

A new model was also created to quantify orbital life using a response surface model for atmospheric density based on high fidelity environment codes maintained by NASA. Currently available atmospheric models such as the COSPAR Standard Reference Atmosphere only provide atmospheric density values up to 900 km altitude. By using a neural net response surface fit to develop a surrogate model of the NASA's MET 2.0 model, a more accurate representation of atmospheric density at high altitudes is achieved. This response surface fit avoids extrapolation of the COSPAR data to higher altitudes of LEO and captures the temporal variations that are lost with the currently available summary data. This new density model was incorporated into an orbit life model that was then used to refine the estimates of orbital decay time in the SLOOP model and provide a more accurate value than used in the Lafleur model.

Comparison of the SLOOP model predictions to the benchmark data gathered from LEGEND shows that the SLOOP model is significantly more accurate than its predecessors. Using a 50% post-mission disposal compliance rate, the percent error between the LEGEND benchmark data and the data produced by the SLOOP model is within +/- 5% over a 100 year simulation. The layered representation of LEO provides higher spatial fidelity which supports more accurate "what if" analyses. Data presented shows that orbit selection for new assets has a significant impact on projected collisions. Launch rate increases to more populated orbits produce more potential collisions than increases to orbits with lower populations. This stands to reason given that the higher population orbits also have higher concentrations of fragments. Using the typical bulk representation of LEO, this aspect of the projection is lost as all orbital objects are combined in a global average. With the layered representation of LEO in the SLOOP model, these discrete impacts can be evaluated and understood.

While active debris removal is a potential solution to the LEO debris problem, policy and technical challenges will continue to make this a difficult solution to fully realize. Post-mission disposal guidelines such as the 25-year rule have the potential to significantly reduce the likelihood of collisions if higher compliance rates can be achieved. The SLOOP model is capable of evaluating both the compliance rate and the post-mission duration to support impact analyses for enacting policies related to post-mission disposal. Preliminary analysis using the SLOOP model agrees with general published findings on this subject. Comparing a 90% compliance rate to the current baseline of 50% shows a significant reduction in collision risk. A sensitivity study predicts a small reduction in collision risk for shorter post-mission durations. These

findings are consistent with recently published NASA and ESA studies that show a reduction in collision rates with higher compliance with post-mission disposal guidelines regardless of the prescribed post-mission duration.

The other major accomplishment of this dissertation is an example of data-driven policy analysis using the SLOOP model to probe aspects of the policy trade space regarding the emergence of CubeSats. The population of operational satellites in LEO is on the verge of an explosion as CubeSats greatly reduce the costs for access to space. Their small size facilitates launching many CubeSats in a single launch, shifting the paradigm of satellite launches from one or two spacecraft per launch to tens of satellites per launch. In addition, these secondary payloads are being deposited in higher orbits with much longer lifetimes. This sharp increase in satellites launched on an annual basis will lead to a significant shift from the current business-as-usual object flight rate. The SLOOP model was used to evaluate several future scenarios for CubeSat launches and their impacts to satellite collision rates. By evaluating these impacts and the efficacy of various policy options to help mitigate the increased risk, policy makers can make informed decisions based on data. It was shown that orbit selection plays a major role with launches to lower altitudes and lower population regions being significantly safer than launches of multiple CubeSats to higher, more populated regions. Also, compliance with PMD guidelines can significantly reduce the impacts of CubeSat launches. However, this will require the implementation of new technologies to support de-orbit of these platforms.

The multi-faceted nature of satellite operations policy requires a multi-faceted analysis approach. The SLOOP model greatly simplifies one important aspect of that

analysis. By reducing model run time and complexity, the SLOOP model can help define and explore the trade space of potential policy alternatives. A broad survey of policy options can be evaluated for efficacy in a much shorter period of time. The resultant data is also available to help guide more detailed and time consuming analyses. The simplified SLOOP user interface opens the tool up to a broader user community where more ideas can be evaluated. The layered approach to modeling LEO provides an important level of spatial fidelity that was not present in previous simplified modeling approaches. Comparisons to benchmark results show that the SLOOP model is a reasonable approximation to the longer running, higher fidelity codes, giving the user confidence. Overall, these results and examples simulations show that the SLOOP model fills an important niche in the world of orbital debris analysis.

APPENDICIES

APPENDIX A

MATLAB Code for Lafleur Model

```
clc

time(1)=0.0;       % time at i=1
tf = 200;          % duration of simulation
h=0.1;             % time step in years

i = 1;
j = 1;

while j < 2
   while time(i) < tf;
      i = i+1;
      time(i) = time(i-1) + h;

      L = c(j,1)+(c(j,2)*sin((c(j,3)*time(i))+c(j,4)));  %Launch Term
      RN = N(j,i-1)/(c(j,5)+(c(j,6)*sin((c(j,7)*time(i))+c(j,8))));  %Deorbit of Large
      CnN = c(j,9)*n(j,i-1)*N(j,i-1);  %Collision of Large on Small
      CNN = 2*c(j,10)*N(j,i-1)*N(j,i-1);   %Collision of Large on Large

      Rn = n(j,i-1)/(c(j,12)+(c(j,13)*sin((c(j,7)*time(i))+c(j,8)))); %Deorbit of Small
      nL = c(j,11)*L; %Small Objects from Launch & Deployment
      nCnN = (c(j,14)*CnN);   %Small Created from Collision of Large on Small
      nCNN = (c(j,15)*0.5*CNN);  %Small Created from Collision of Large on Large
      Cnn = 2*c(j,16)*n(j,i-1)*n(j,i-1);   %Collision of Small on Small

      N(j,i) = N(j,i-1) + (h*(L-RN-CnN-CNN));   %Number of Large Objects at time t
      n(j,i) = n(j,i-1) + (h*(nL-Rn+nCnN+nCNN-Cnn));  %Number of Small Objects at time t
   end
   j = j+1;
   i = 1;
end
```

APPENDIX B

MATLAB Code for SLOOP

```
%SLOOP (Simplified LEO Orbiting Object Population) Model
%Created January, 2015
%Created by Thomas Percy, PhD Candidate
  %University of Alabama in Huntsville
  %Department of Mechanical and Aerospace Engineering

clc

tf = 200;          % duration of simulation in years
h=0.1;             % time step in years
i = 1;
j = 1;
k = size(c,2)+1;  %number of shells is this value minus 1
RNN(j,k) = 0;
RND(j,k) = 0;
Rn(j,k) = 0;
time(1,1) = 0;

while i < k
  RNN(1,i) = 0;
  RND(1,i) = 0;
  Rn(1,i) = 0;
  i = i+1;
end

i = 1;

while time(j,i) < tf
  j = j+1;
  i = 1;
  time(j,i) = time(j-1,i)+h;
  while i < k
    L(j,i) = c(1,i)+(c(2,i)*sin((c(3,i)*time(j,i))+c(4,i)));  %Launch Term

    %Natural Decay Terms (NN)
    LN(j,i) = (1-c(12,i))*L(j,i);
    RNN(j,i) = NN(j-1,i)*(1/c(5,i));  %Removal of Large Natural Decay Objects from Shell
    CnNN(j,i) = c(9,i)*n(j-1,i)*NN(j-1,i);  %Collision of Large Natural Decay on Small
    CNNN(j,i) = 2*c(10,i)*NN(j-1,i)*NN(j-1,i);   %Collision of Large Natural Decay on Large Natural Decay

    %Deorbited Terms  (ND)
    LD(j,i) = (c(12,i))*L(j,i);
    RND(j,i) = ND(j-1,i)*(1/c(6,i));  %Removal of Large PMD Objects from Shell
    CnND(j,i) = c(9,i)*n(j-1,i)*ND(j-1,i);  %Collision of Large PMD on Small
    CNND(j,i) = 2*c(10,i)*ND(j-1,i)*ND(j-1,i);   %Collision of Large PMD on Large Natural Decay

    %Small Debris Terms (n)
    nL(j,i) = c(11,i)*L(j,i); %Small Objects from Launch & Deployment
    Rn(j,i) = n(j-1,i)/c(7,i);  %Fragment Deorbit Rate
    nCnNN(j,i) = (c(14,i)*CnNN(j,i));   %Small Created from Collision of Large Natural Decay on Small
    nCnND(j,i) = (c(14,i)*CnND(j,i));   %Small Created from Collision of Large PMD on Small
```

```
    nCNNN(j,i) = (c(15,i)*0.5*CNNN(j,i));  %Small Created from Collision of Large Natural Decay on Large Natural
Decay
    nCNND(j,i) = (c(15,i)*0.5*CNND(j,i));  %Small Created from Collision of Large PMD on Large PMD
    Cnn(j,i) = 2*c(16,i)*n(j-1,i)*n(j-1,i);   %Collision of Small on Small

    if j > 1
      Nin(j,i) = RNN(j-1,i+1);
      nin(j,i) = Rn(j-1,i+1);
    else
       Nin = 0;
       nin = 0;
    end

    NN(j,i) = NN(j-1,i) + (h*(LN(j,i)+Nin(j,i)-RNN(j,i)-CnNN(j,i)-CNNN(j,i)));   %Number of Large Natural Decay Objects at
time t
      if NN(j,i)<0
         NN(j,i) = 0;
      else
         NN(j,i) = NN(j,i);
      end
    ND(j,i) = ND(j-1,i) + (h*(LD(j,i)-RND(j,i)-CnND(j,i)-CNND(j,i)));   %Number of Large PMD Objects at time t
      if ND(j,i)<0
         ND(j,i) = 0;
      else
         ND(j,i) = ND(j,i);
      end
    n(j,i) = n(j-1,i) + (h*(nL(j,i)+nin(j,i)-Rn(j,i)+nCnNN(j,i)+nCNNN(j,i)+nCnND(j,i)+nCNND(j,i)-Cnn(j,i)));  %Number of
Small Objects at time t
      if n(j,i)<0
         n(j,i) = 0;
      else
         n(j,i) = n(j,i);
      end
    N(j,i) = NN(j,i) + ND(j,i);  %Number of Large Objects at time t
    Pn(j,i) = c(9,i)*n(j,i);   %Probability of Small on Large Collision
    PN(j,i) = 2*c(10,i)*N(j,i);    %Probability of Large on Large Collision
    N_10(j,i) = N(j,i)+0.0272*n(j,i);     %Number of objects greater than 10 cm
    SumCNN(j,i) = 0;
    SumCNN(j,i) = SumCNN(j-1,i)+(h*CNNN(j,i)/2)+(h*CNND(j,i)/2);
    SumCnN(j,i) = 0;
    SumCnN(j,i) = SumCnN(j-1,i)+(h*CnNN(j,i))+(h*CnND(j,i));
    Ntot(j,i) = N(j,i)+n(j,i);
    i = i+1;
    time(j,i) = time(j,i-1);
  end
  SumN_10 = sum(N_10,2);
  SumCNNall = sum(SumCNN,2);
  SumCnNall = sum(SumCnN,2);
  SumRN = sum(RNN,2)+sum(RND,2);
  SumN = sum(N,2);
  Sumn = sum(n,2);
  SumL = sum(L,2);
  RealTime(j,1) = time(j,1);
  Legend(j,1) = 11096*exp(0.0095*time(j,1));   %Curvefit of Legend predicted population
  Master(j,1) = (6681*time(j,1))+279652;       %Curvefit of Master2009 predicted population
  Err1(j,1) = (Legend(j,1)-SumN_10(j,1))/Legend(j,1);
  Err2(j,1) = (Master(j,1)-(Sumn(j,1)))/Master(j,1);
end
```

APPENDIX C

MATLAB Code for Orbit Life Model

```
clc

i = 1;
j = 1;
k = size(Q,1);

while i < k+1

%SATELLITE ORBITAL DECAY
M = Q(i,j); %Satellite mass (kg)
A = Q(i,j+1); %Satellite area (m^2)
H = Q(i,j+2); %Starting height (km)



%define constants
Cd = 2.2;  %Drag Coefficient
Re = 6378000; %'Earth radius (m)
Me = 5.98E+24;  %Earth mass (kg)
G = 6.67E-11; %Universal constant of gravitation
T = 0; %time (days)
dT = 1; %time increment (days)
D9 = dT * 3600 * 24; %'put time increment into seconds
AM = A/M; %area to mass ratio

%calculate initial orbit values
R = Re + H * 1000; %'R is orbital radius in meters
H0 = H;
P = 2 * pi * (R * R * R / Me / G)^0.5; %'P is period in seconds

if M*A*H > 0
   while H > 180 % if H>180, loop until alt drops below 180 km if H>H0-100, loop until altitude drops 100 km
      DenTime = 4018*((T/4018)-(floor(T/4018)));  %Time on 0 to 4018 day timescale for use in repeating density cycle
      T1 = tanh(0.5*(0.4658+(0.000065*DenTime)-(0.004212*H))); %First Term in Response Surface Fit
      T2 = tanh(0.5*(3.3367-(0.001422*DenTime)+(0.0000548*H)));  %Second Term in Response Surface Fit
      T3 = tanh(0.5*(-0.26232-(0.0004975*DenTime)+(0.000722*H)));  %Third Term in Response Surface Fit
      DN = exp(-24.960481+(11.76373*T1)+(3.81465*T2)-(7.667977*T3));  %Density response surface fit from MET2.0
model


      dP = 3 * pi * (A*Cd) / M * R * DN * D9; %decrement in orbital period
      P = P - dP;
      T = T + dT;
      R = (G * Me * P * P / 4 / pi / pi) ^ .33333; %new orbital radius
      H = (R - Re) / 1000; %new altitude (semimajor axis)
   end
   Life(i,j) = T / 365.25; %orbit life in years
else
   Life(i,j) = -100; %dummy orbit life value if inputs include a 0
end

i=i+1;
end
```

REFERENCES

[1] D. Kessler and B Cour-Palais, "Collision Frequency of Artificial Satellites: The Creation of a Debris Belt," *Journal of Geophysical Research*, vol. 83, NO. A6, pp 2637-2646, Jun. 1978.

[2] D. Kessler, N. Johnson, J. Liou and M. Matney, "The Kessler Syndrome: Implications to Future Space operations", presented at the 33rd Annual AAS Guidance and Control Conference, Breckenridge, CO, Feb 6-10, 2010.

[3] "U.S. Government Orbital Debris Mitigation Standard Practices," Available: orbitaldebris.jsc.nasa.gov/library/USG_OD_Standard_Practices.pdf

[4] "IADC Space Debris Mitigation Guidelines," IADC-02-01, Sep. 2007.

[5] "Space Debris Mitigation Guidelines of the Committee on the Peaceful Use of Outer Space", V.09-88517, Jan. 2010.

[6] J. Liou, "Engineering and Technology Challenges for Active Debris Removal," presented at the 4th European Conference for Aerospace Sciences, 2011.

[7] J. Lafleur, "Extension of a Simple Mathematical Model for Orbital Debris Proliferation and Mitigation", AAS 11-173, presented at the 21st AAS/AIAA Space Flight Mechanics Meeting, New Orleans, LA, Feb. 2011.

[8] N. Johnson, "The Disposal of Spacecraft and Launch Vehicle Stages in Low Earth Orbit", presented at the 2nd International Association for Advancement of Space Safety, Chicago, IL, May 14-16, 2007

[9] "Limiting Future Collision Risk to Spacecraft: An Assessment of NASA's Meteoroid and Orbital Debris Programs", National Research Council, 2011, pp 65.

[10] B. Wheeden, "2009 Iridium-Cosmos Collision Fact Sheet", Secure World Foundation, Nov 10, 2010.

[11] N. Johnson, "History of On-Orbit Satellite Fragmentations", 14th ed., NASA TM-2008-214779, June 2008, pp 9-11.

[12] D. Wright, "Space Debris", *Physics Today*, American Institute of Physics, October, 2007.

[13] J. Liou, "An active debris removal parametric study for LEO environment remediation", *Advances in Space Research*, vol 38, 2006, pp 2102-2106.

[14] Joint Space Operations Center Catalog, Available: www.space-track.org

[15] W. Pulliam, et al, "Catcher's Mitt Final Report", DARPA publication, 2011.

[16] B. Weeden, "Overview of the Legal and Policy Challenges with Orbital Debris Removal", presented at the 61st International Astronautical Congress, Prague, Czech Republic, 2010.

[17] R. Walker, et al, "Update of the ESA Space Debris Mitigation Handbook: Executive Summary", ESA Contract 14471/00/D/HK, July, 2002.

[18] A. Bradley and L. Wein, "Space Debris: Assessing Risk and Responsibility", *Advances in Space Research*, Vol 43., 2009, pp 1372-1390.

[19] "National Security Space Strategy", Department of Defense & National Intelligence joint publication, January, 2011.

[20] "State of the Satellite Industry Report", Satellite Industry Association, Sep. 2014, Available: http://www.sia.org/wp-content/uploads/2014/09/SSIR-September-2014-Update.pdf

[21] A.Svitak, "SpaceX, OneWeb Unveil Rival Broadband Constellation Plans," *Aviation Week & Space Technology*, Jan 21, 2015, Available: http://aviationweek.com/space/spacex-oneweb-unveil-rival-broadband-constellation-plans

[22] "Falcon 9 Launch Vehicle Payload User's Guide", Space Exploration Technologies Corporation, Hawthorne, CA, 2009.

[23] "Antares OSP-3 User's Guide", Orbital Sciences Corporation, Dulles, VA, Jul. 2013.

[24] T. Kelso, "Satellite Catalog (SATCAT)", Celestrak, Available: http://www.celestrak.com/satcat/search.asp

[25] "CubeSat ELaNa IV Launch on ORS-3", NASA Fact Sheet NF-2013-11-573-HQ, Nov. 2013.

[26] W. Graham, "Russian Dnepr conducts record breaking 32 satellite haul," Available: http://www.nasaspaceflight.com/2013/11/russian-dnepr-record-breaking-32-satellite-haul/

[27] D. Kessler, "Derivation of the Collision Probability between Orbiting Objects: The Lifetimes of Jupiter's Outer Moons," *Icarus*, Vol 48, 1981, pp 39-48.

[28] W. Vincenti and C. Kruger, Jr., *Introduction to Physical Gas Dynamics*, Krieger, Malabar, 1965.

[29] J. Liou, "LEGEND – a three-dimensional LEO-to-GEO debris evolutionary model", *Advances is Space Research*, Vol 34, Feb. 2003, pp 981-986.

[30] P. Farinella and A. Cordelli, "The Proliferation of Orbiting Fragments: a Simple Mathematical Model," *Science & Global Security*, Vol 2, 1991, pp 365-378.

[31] A. Cordelli, et al, "Future collisional evolution of Earth-orbiting debris," *Advances in Space Research*, Vol. 13, Aug. 1993, pp 215-219.

[32] "Stability of the Future LEO Environment," Inter-Agency Space Debris Coordination Committee Report, IADC-12-08, Jan. 2013, pp 3-8.

[33] N. Johnson, et al, "NASA's New Breakup Model of EVOLVE 4.0", Advances in Space Research, Vol. 28, 2001, pp 1377-1384.

[34] S. Flegel, et al, "Final Report: Maintenance of the ESA MASTER Model," European Space Agency Report, Jun. 2011.

[35] J. Liou, "A Parametric Study on Using Active Debris Removal for LEO Environment Remediation," presented at the 61st International Astronautical Congress, Prague, Czech Republic, 2010. Available: http://ntrs.nasa.gov/archive/nasa/casi.ntrs.nasa.gov/20100033207.pdf

[36] "JMP® 10 Discovering JMP," SAS Institute Inc., Cary, NC, 2012.

[37] F. Brauer and C. Castillo-Chavez, "Mathematical Models in Population Biology and Epidemiology," Springer Science & Business Media, 2001.

[38] "Satellite Took Kit (STK)," Analytical Graphic Incorporated, Exton, PA, Available: http://www.agi.com/downloads/products/product-literature/120213_STK_Free_Flyer_Missiles.pdf

[39] Z. Slepian, "The Average Projected Are Theorem – Generalization to Higher Dimensions," eprint arXiv:1109.0595, Cornell University Library, 2011.

[40] "Union of Concerned Scientists (UCS) Satellite Database," Available: http://www.ucsusa.org/nuclear_weapons_and_global_security/solutions/space-weapons/ucs-satellite-database.html

[41] "Gunter's Space Page," Available: http://space.skyrocket.de/.

[42] "Encyclopedia Astronautica," Available: http://www.astronautix.com/.

[43] "NASA Space Science Data Center (NSSDC)," Available: http://nssdc.gsfc.nasa.gov/.

[44] "Iridium NEXT Satellite Constellation," Iridium Communications, Inc. Data Sheet, 2010, Available: https://www.iridium.com/about/IridiumNEXT.aspx

[45] "CubeSat Kit," Available: http://www.cubesatkit.com/content/design.html

[46] "CubeSat Launch Initiative," Available: http://www.nasa.gov/directorates/heo/home/CubeSats_initiative.html

[47] "Planet Labs Story," Planet Labs Inc., San Francisco, CA, Available: https://www.planet.com/story/

[48] "ESPA: The EELV Secondary Payload Adapter," CSA Engineering MOOG Data Sheet, Mountain View, CA, Available: http://www.moog.com/literature/Space_Defense/Vibration_Control/MCSA_ESPA.pdf

[49] "Secondary Payload Planner's Guide For Use On The EELV Secondary Payload Adapter," U.S. Department of Defense Space Test Program, Jun 2001.

[50] "Spaceflight Inc. Secondary Payload Users Guide," SF-2100-PUG-00001 Rev D, Spaceflight Inc., Tukwila, WA, 2013

[51] "Debris Assessment Software (DAS) User's Guide," NASA Technical Document, JSC 64047, Jan. 2012.

[52] "Satellite Orbital Decay Calculations," Australian Space Weather Agency, Bureua of Meteorology, Haymarket, New South Wales, Available: http://www.ips.gov.au/Category/Educational/Space%20Weather/Space%20Weather%20Effects/SatelliteOrbitalDecayCalculations.pdf

[53] "COSPAR International Reference Atmosphere – 2012," Committee on Space Research, 2012, Available: http://sol.spacenvironment.net/CIRA-2012

[54] J. Owens, "NASA Marshall Engineering Thermosphere Model – Version 2.0," NASA Technical Memorandum, TM-2002-211786, Jun. 2002.

[55] "Significant Increase in Satellite Breakups During 2006," NASA Orbital Debris Quarterly News, Vol 11, Issue 1, Jan. 2007, p. 2.

[56] "New Russian Launch Failure Raises Breakup Concern," NASA Orbital Debris Quarterly News, Vol. 16, Issue 4, Oct. 2012, pp 2-3.

[57] J. Liou, “Collision activities in the future orbital debris environment,” *Advances in Space Research*, Vol 38, 2006, pp 2102-2106.

[58] “Formation Flying: The Afternoon “A-Train” Satellite Constellation,” NASA Fact Sheet, FS-2003-1-053-GSFC, Mar. 2003.

[59] “National Space Policy of the United States of America,” White House publication, June, 28, 2010.

[60] “NASA Procedural Requirements for Limiting Orbital Debris,” NASA Report, NPR 8715.6A, May 2009.

[61] “Process for Limiting Orbital Debris,” NASA Report, NASA-STD 8719.14, Aug. 2007.

[62] “Handbook for Limiting Orbital Debris,” NASA Report, NASA-HBK 8719.14, Jul. 2008.

[63] M. Taylor, “Orbital Debris: Technical and Legal Issues and Solutions”, Master of Law Thesis Submission, Institute of Air and Space Law, McGill University, Aug. 2006.

[64] “Orbital Debris Mitigation: Regulatory Challenges and Market Opportunities”, Futron Corporation, Mar. 2006.

[65] R. Hevner, et al, “An Advanced Standard for CubeSats,” presented at the 25th Annual AIAA/USU Conference on Small Satellites, SSC11-II-3, Jun. 2011.

[66] J. Szatkowski, “ULA Rideshare with CubeSat Missions for Lunar & Inter-Planetary Exploration,” presented at the 2nd Interplanetary Cubesat Workshop, Cornell, NY, May 2013.